

REGULATION OF POTASSIUM CHANNEL IN VENTRICULAR MYOCYTES
OF RAT FOLLOWING VOLUME OVERLOAD

Except where reference is made to the work of others, the work described in this dissertation is my own or was done in collaboration with my advisory committee. This dissertation does not include proprietary or classified information

Hui Gao

Certificate of Approval:

Robert L. Judd
Associate Professor
Anatomy, Physiology and
Pharmacology

Juming Zhong, Chair
Associate Professor
Anatomy, Physiology and
Pharmacology

Dean D. Schwartz
Associate Professor
Anatomy, Physiology and
Pharmacology

Vishnu Suppiramaniam
Associate Professor
Pharmacal Sciences

Ya-Xiong Tao
Assistant Professor
Anatomy, Physiology and
Pharmacology

George T. Flowers
Dean
Graduate School

REGULATION OF POTASSIUM CHANNEL IN VENTRICULAR MYOCYTES
OF RAT FOLLOWING VOLUME OVERLOAD

Hui Gao

A Dissertation

Submitted to

the Graduate Faculty of

Auburn University

in Partial Fulfillment of the

Requirement for the

Degree of

Doctor of Philosophy

Auburn, Alabama
May 9, 2009

REGULATION OF POTASSIUM CHANNEL IN VENTRICULAR MYOCYTES
OF RAT FOLLOWING VOLUME OVERLOAD

Hui Gao

Permission is granted to Auburn University to make copies of this dissertation, upon request of individuals or institutions and at their expense. The author reserves all publication rights.

Signature of Author

Date of Graduation

VITA

Hui Gao, son of Wenting Gao and Zongying Zhang, was born May 1, 1972, in Beijing, China. He graduated from Nanjing Agricultural University, Nanjing, Jiangsu, China in July, 1996. After working as a research assistant scientist for six years at Beijing Academy of Agriculture and Forestry Sciences, he entered the Graduate School, Tuskegee University in August, 2003 and graduated with a Master of Science degree in Plant and Soil Sciences. In fall 2005 he joined the Department of Anatomy, Physiology and Pharmacology in the College of Veterinary Medicine as a graduate research assistant. He married Ronghua Meng and has a son, Yi (Kevin M.) Gao and a daughter, Sophia K. Gao.

DISSERTATION ABSTRACT
REGULATION OF POTASSIUM CHANNEL IN VENTRICULAR MYOCYTES
OF RAT FOLLOWING VOLUME OVERLOAD

Hui Gao

Doctor of Philosophy, Biomedical Sciences, May 9, 2009
(M.S., Tuskegee University, 2005)

132 Typed Pages

Directed by Juming Zhong

Heart failure (HF) is a leading cause of death in the US. Among the deaths of patients with HF, up to 50% are sudden and unexpected. The sudden deaths have been related to the lethal ventricular arrhythmias such as ventricular tachycardia or ventricular fibrillation. However, the mechanisms underlying arrhythmias in HF patients are unknown. Previous studies supported that the abnormal repolarizations may play an important role in arrhythmogenesis in patients with HF. In human and animal failing hearts, the most consistent electrophysiological change is prolonged action potential (AP), whereas downregulation of transient outward potassium current (I_{to}) is also a consistent change in ion currents. So far, the cellular and molecular mechanisms involving AP prolongation and I_{to} downregulation in HF patients is still incompletely understood. Recently growing evidence for the alteration of the ubiquitin-proteasome

system (UPS) have been reported in various heart diseases. In addition, some ion channels have been reported to be degraded by the UPS. In the present study, using a rat model of volume overload induced by aortocaval fistula, we examined the electrophysiological characteristics in ventricular myocytes and possible molecular mechanisms underlying the electrophysiological alterations following ventricular remodeling. We found that AP duration was prolonged in fistula myocytes compared with control myocytes at 10- and 13-week post-fistula. Consistently, I_{to} densities were significantly decreased in fistula myocytes. In addition, depressed Kv4 α subunits were detected in protein level, but not in mRNA level, suggesting that posttranscriptional modification occurred on the Kv4 α subunits in fistula myocytes. Furthermore, elevated ubiquitinated Kv4 α subunits were detected in fistula myocytes compared with control. To determine whether the Kv4 α subunits are degraded by the proteasome, we employed MG-132, a proteasomal inhibitor, and chloroquine, a lysosomal inhibitor, respectively. Incubation with MG-132, but not chloroquine, for 24 hours led to increased I_{to} densities and protein expression of Kv4 α subunits in fistula myocytes, whereas neither MG-132 nor chloroquine altered I_{to} density and Kv4 α subunits expression in control myocytes. Accordingly, we conclude that the Kv4 α subunits are degraded by the proteasome and that the accelerated degradation of Kv4 α subunits results in the downregulation of transient outward potassium current therefore lengthening APD in rat ventricular myocytes following volume overload.

ACKNOWLEDGMENTS

I would like to express my deepest appreciation to my major advisor, Dr. Juming Zhong, for his support, guidance, advice, patience, and encouragement all these years. Without him, none of this work would have been possible. I would also thank the members of my committee, Dr. Robert L. Judd, Dr. Dean D. Schwartz, Dr. Ya-Xiong Tao, Dr. Vishnu Suppiramaniam, and outside reader Dr. Wei Zhan, for all their help and advice on executing this project. I would also like to thank Dr. Janicki, Dr. Pinkert, and Dr. Morrison, for the financial support. My deep appreciation goes to Dr. Dean D. Schwartz for some results from his laboratory. I would thank Dr. Yanfeng Ding, Qiao Zhong, Dr. Elaine S. Coleman, Dr. Tim D. Braden, Dr. Eric P. Plaisance, Dr. Shuxiu Wang, Dr. John Dennis, and Kathy O'Donnell, for their kind help on the project. I would also like thank Colin Rogers, Dr. Heather Gray-Edwards, Dr. Xueyou Hu, and Dr. Zhenchuan Fan, for their friendship during this process. Many thanks go to Debbie Allgood, Hattie Alvis, Dorothy Span, Diane Smith, Mary Lolyd, and Dot Dunn for their help and kindness. I would like to present my profound appreciation to my wife Ronghua Meng, my son Kevin, and other family members for the continue love, joys, understanding, and support they give me all the time.

Style manual or journal used: American Journal of Physiology

Computer software used: Microsoft Word, Lotus 1-2-3, SigmaPlot, SigmaStat, Adobe Photoshop, UN-SCAN-IT Gel & Graph Digitizing Software, Reference Manager

TABLE OF CONTENTS

LIST OF TABLES	xiii
LIST OF FIGURES	xiv
LIST OF ABBREVIATIONS.....	xvi
CHAPTER I. INTRODUCTION	1
CHAPTER II. LITERATURE REVIEW	5
Heart failure	5
Sudden death in HF.....	8
Arrhythmias	9
Electrophysiology	12
Action potential (AP).....	12
Prolonged action potential and altered ion currents.....	14
Potassium channel.....	18
Transient outward currents I_{to}	19
Molecular basis of I_{to} downregulation in HF.....	20
Ubiquitin-proteasome system	22
Discovery of ubiquitin	22
The ubiquitin-proteasome system.....	22
The UPS alteration in the heart.....	24
Animal model for HF.....	26

CHAPTER III. EXPERIMENTAL DESIGN	30
CHAPTER IV. ELECTROPHYSIOLOGICAL REMODELING IN RAT VENTRICULAR MYOCYTES DURING VENTRICULAR REMODELING FOLLOWING CHRONIC VOLUME OVERLOAD.....	32
ABSTRACT.....	32
INTRODUCTION	33
MATERIALS AND METHODS.....	34
Animal model of heart failure.....	34
Preparation of isolated ventricular myocytes.....	35
Action potential and current measurement	36
Solutions for electrophysiological experiments.....	37
Cell membrane preparation.....	38
Western blot.....	38
mRNA level of outward K ⁺ channel α subunits	39
Statistical analysis.....	40
RESULTS	41
General characteristics of control and fistula rats.....	41
Action potential durations.....	41
L-type Ca ²⁺ current density.....	42
Outward K ⁺ currents	42
Voltage dependent activation and inactivation of I _{t0}	42
Expression of Kv α subunits	43

mRNA of Kv α subunits	44
DISCUSSION	44
CHAPTER V. MEDIATION OF TRANSIENT OUTWARD POTASSIUM CHANNEL BY PROTEASOME IN RAT VENTRICULAR MYOCYTES DURING VOLUME OVERLOAD-INDUCED VENTRICULAR REMODELING	69
ABSTRACT	69
INTRODUCTION	70
MATERIALS AND METHODS	72
Animal model of heart failure	72
Isolation of ventricular myocytes	72
Cell culture and incubation with inhibitors	73
Transient outward potassium current measurement	73
Western blot	74
Immunoprecipitation	75
Statistical analysis	76
RESULTS	76
Effects of inhibitors on I_{to}	76
Presence of ubiquitinated Kv4 α subunits	77
Effect of inhibitors on the expression of Kv4 α subunits	78
Ubiquitinated proteins in fistula ventricular myocytes	79
DISCUSSION	79
CHAPTER VI. SUMMARY	92

REFERENCES	94
------------------	----

LIST OF TABLES

Table 2.1.	New York Heart Association functional classification.....	8
Table 4.1.	The resting membrane potential (E_m) and the action potential amplitude in control and fistula group at 5-, 10-, and 13-week.....	50

LIST OF FIGURES

Figure 2.1.	Action potential waveform and underlying ionic currents in adult human ventricular myocytes	14
Figure 2.2.	Structure and assembly of voltage-gated potassium channel (Kv) α subunits	18
Figure 4.1.	General characteristics in control and aortocaval (AV) fistula rats at 5-, 10-, and 13-week after the AV fistula was induced	52
Figure 4.2.	Membrane action potential (AP) in ventricular myocytes.....	54
Figure 4.3.	Calcium currents (I_{CaL}) and Cav1.2 expression in ventricular myocytes	56
Figure 4.4.	Transient outward K^+ currents (I_{to}) in ventricular myocytes	58
Figure 4.5.	Delayed rectifier K^+ currents (I_K) in ventricular myocytes.....	60
Figure 4.6.	Voltage dependent I_{to} activation and inactivation.....	62
Figure 4.7.	Protein expression of Kv4 α subunits of ventricular myocytes	64
Figure 4.8.	Protein expression of Kv4 α subunits in sarcolemma of ventricular myocytes	66
Figure 4.9.	mRNA level of Kv4.2 and Kv4.3 in ventricular myocytes.....	68
Figure 5.1.	Transient outward K^+ current (I_{to}) density in ventricular myocytes treated with chloroquine and MG-132, respectively, at 13-week post-fistula.....	85

Figure 5.2.	Ubiquitinated Kv4 α subunits in ventricular myocytes at 13-week post-fistula.....	87
Figure 5.3.	Expression of Kv4 α subunits in lysates from myocytes with treatment of inhibitors at 13-week after fistula	89
Figure 5.4.	Accumulation of ubiquitinated proteins in protein lysates of ventricular myocytes.....	91

LIST OF ABBREVIATIONS

ACE	Angiotensin converting enzyme
AP	Action potential
APD	Action potential duration
AV	Aortocaval
CO	Cardiac output
DAD	Delayed afterdepolarization
DCM	Dilated cardiomyopathy
E1	Ubiquitin activating enzyme
E2	Ubiquitin conjugating enzyme
E3	Ubiquitin ligase
EAD	Early afterdepolarization
E_m	resting membrane
ENaC	Epithelial sodium channel
ERG	Ether-a-go-go related gene
HF	Heart failure
I_{CaL}	L-type calcium current
ICM	Ischemia cardiomyopathy
I_K	Delayed rectifier current
I_{K1}	Inward rectifier potassium current

I _{to}	Transient outward potassium current
KChIP	Potassium channel interaction protein
Kv	Voltage-gated potassium channel
LQTS	Long QT syndrome
LV	Left ventricle
MI	Myocardium infarction
NCX	Sodium-Calcium exchange
NYHA	New York Heart Association
PO	Pressure overload
SD	Sudden death
TAC	Thoracic aortic constriction
UPS	The ubiquitin-proteasome system
VF	Ventricular fibrillation
VO	Volume overload
VT	Ventricular tachycardia

CHAPTER I. INTRODUCTION

Heart failure (HF) is a leading cause of death in the United States. More than 5 million Americans are afflicted with heart failure and more than 250,000 patients die on heart failure annually (161, 182). With multiple reports of rising prevalence, recent studies showed marked increases in the numbers of patients, hospitalizations, and costs associated with HF in the near future (175). According to data from the National Hospital Discharge Survey, the total number of HF-related hospitalization has increased from 377,000 in 1979 to 1,088,349 in 1999. In 2005, the direct and indirect cost for HF equaled \$29 billion (60). The estimated direct and indirect cost of HF for 2008 is \$34.8 billion in the United States (162).

There are many underlying causes of HF, including coronary heart disease, hypertension, valvular heart disease, and myocardial disease. According to different causes, characteristics of HF are composed of various signs, such as depressed myocardial function, ventricular remodeling, altered hemodynamics, neurohormonal activation, and cytokine overexpression (73). To enhance our understanding of pathophysiology and treatment of HF, distinct experimental animal models have been established to mimic the complex human syndrome of HF (49, 73, 192). Since hypertrophy is a common sign of ventricular remodeling in HF, a number of animal models have created to simulate human cardiac hypertrophy by increasing workload of animal hearts. Pressure overload and volume overload are usually induced in animal

hearts by surgery to investigate hemodynamic and electrophysiological alterations as well as underlying molecular basis of those changes in hypertrophied ventricle (16).

Patients with heart failure typically die from either progressive deterioration of ventricular pump function or lethal cardiac arrhythmia. Among the death of patients with HF, up to 50% are sudden and unexpected (86, 180, 181). The sudden death is usually associated with cardiac arrhythmia, which is involved in alteration of cardiac electrical properties (86, 127).

Prolonged action potential duration and decreased K^+ currents are the most common electrical features in human failing hearts and animal models with experimental induced heart failure (180, 181). In pressure overload model induced by aortic banding (or constriction) action potential prolongation and downregulation of potassium currents have been reported (180). Chronic volume overload is associated with many clinical conditions, such as aortic and mitral regurgitation, surgery- and trauma-induced aortocaval shunt, anemia, and patent ductus arteriosus (85, 193). Abnormal ventricular myocyte contractility has been reported in volume overload. In a recent study reported from our group, chronic volume overload was induced by an infrarenal aortocaval fistula and functional changes in ventricular myocytes were evaluated during the progression of ventricular remodeling induced by volume overload (46). Depressed myocyte contractility was demonstrated with the development of ventricular hypertrophy and dilatation induced by chronic volume overload. Nevertheless no study has been reported on the possible alteration of electrophysiological properties following ventricular remodeling induced by chronic volume overload.

In the present study, we hypothesized that action potential in ventricular myocytes is prolonged due to downregulation of outward K^+ currents, during development of ventricular remodeling induced by chronic volume overload. We evaluated action potentials and outward K^+ currents using whole-cell patch clamp technique. We also examined the expression of voltage-gated potassium channel (Kv) α subunits underlying outward K^+ currents in ventricles following volume overload.

Proteasome and lysosome are two distinct fates of cellular proteins undergoing degradation. It was assumed that the lysosomes degrade most membrane and extracellular proteins by endocytosis as well as cytosolic proteins, whereas the proteasomes degrade cytosolic, nuclear, and myofibrillar proteins. But we now know that the ubiquitin-proteasome system (UPS) also label and degrade some integral membrane proteins (79). Many ion channels, membrane receptors and transporters have been recently reported to be ubiquitinated and degraded via the UPS (1, 53, 121). Gong et al. suggested that the degradation of the voltage-gated hERG channels, which encodes the rapidly activating delayed rectifier K^+ current (I_{Kr}), is mediated by the UPS (66). Jespersen et al. suggested that the internalization of the voltage-gated KCNQ1 channel protein, which assembles with the KCNE1 together encoding the slowly activating delayed rectifier K^+ current (I_{Ks}) in cardiomyocytes, is physiologically regulated by ubiquitin ligase (E3) dependent ubiquitination (87). These mechanisms may be important in regulating the surface density of voltage-gated potassium channels (Kv) in cardiomyocytes. However, whether the transient outward potassium channels are regulated by the UPS has not been reported.

Recently, an increasing number of evidences indicated that ubiquitin-proteasome system (UPS) altered in distinct heart diseases (44, 104, 109, 184, 197). Accumulation of

ubiquitinated proteins has been observed in cardiac myocytes obtained from human failing hearts and diseased hearts of experimental animal model (3, 109, 184). Either increased or decreased expression of UPS components is reported in affected hearts (119). In transverse aorta contraction induced cardiac hypertrophy, increased levels of UPS components and proteasome activities has been observed (44). However, so far, there is no study investigating the possible role of ubiquitin proteasome degradation in the reduced potassium channel proteins in HF. In the present study, we tested the hypothesis that the UPS alteration is involved in the downregulation of Kv α subunits in ventricular myocytes following volume overload induced ventricular remodeling. We examined the role of the UPS in alterations of both potassium currents and potassium channel protein expression by evaluating expression of ubiquitinated Kv α subunits and effects of proteasome/lysosome inhibitors on potassium currents and channel protein expression during cardiac remodeling induced by volume overload.

CHAPTER II. LITERATURE REVIEW

Heart failure (HF) is a significant public health problem with an extremely high morbidity and mortality. In developed countries, HF is one of leading causes of death. According to the latest statistics from American Heart Association, 5.3 million Americans are afflicted with heart failure in 2008 (162). Despite advances in medical therapy, the incidence and prevalence of HF have increased in Western society (189). Over 660,000 patients in the US are diagnosed with HF each year (162). For 2008, the estimated direct and indirect cost of HF is \$34.8 billion in the United States (162). Every year, more than 250,000 people die on HF. About 50% of deaths in patients with HF are sudden and unexpected. The mechanism of sudden death in patients with HF remains incompletely clear.

Heart failure

The cardiovascular system is responsible for maintaining normal systemic arterial blood pressure, normal blood flow to tissues, and normal venous and capillary pressures. Various abnormal conditions, such as neurohormonal changes, hemodynamic alteration, mechanical stress, affecting the heart and the blood vessels in the heart, lead to heart diseases. As heart disease becomes severe enough heart failure (HF) occurs.

Heart failure is a complicated clinical syndrome, in which the cardiovascular system can no longer maintain its normal functions (82). In a patient with heart failure,

the heart is unable to pump adequate blood to satisfy the demand of the metabolizing tissues. Thus low cardiac output, low blood pressure, or increased capillary or venous pressure can be signs to diagnose heart failure with severe heart disease. Patients with HF may experience distinct symptoms, such as dyspnea (difficulty in breathing), pulmonary edema, ascites (fluid in the peritoneal cavity), exercise intolerance, angina pectoris (chest pain), and fatigue (86).

Heart failure is a developing process. At the beginning, index events initially produce a decline of cardiac function. Following this initial decline of cardiac function, a variety of compensatory mechanisms are activated, inducing neurohormonal and hemodynamic changes, which are responsible to compensate those functional alterations. The stresses leading to compensation sustains continuously and triggers a cascade of maladaptive structural and electrical events, such as cardiac fibrosis, dilation or hypertrophy, abnormal electrical generation and propagation (113, 139). These maladaptive events finally result in the irreversible impairment of heart function and mortality.

Anatomic changes are discovered in human heart failure. Fibrosis and changes in membrane protein composition are two independently regulated biological modifications and play a determining role during the onset of cardiac hypertrophy (10). In addition, cytoskeleton alterations play an equally important role as structural component contributing to HF (75, 103). Both intracellular and extracellular structural alterations contribute to the deterioration of cardiac function (29, 69, 76).

In addition to anatomic changes, functional deficiencies of heart have been described. Two types of functional cardiac dysfunction are classified in heart failure:

systolic dysfunction and diastolic dysfunction. Systolic dysfunction refers to the impaired cardiac contractility and decreased force development; while diastolic dysfunction refers to deficiency of cardiac filling due to abnormal relaxation (138).

In early studies about HF, both depressed contractility and impaired relaxation were found in failing hearts, so attention was drawn to the abnormalities in the heart muscle. To alleviate those symptoms, a variety of inotropic, diuretic, and vasodilator drugs were developed and can produce clinical improvement in the vast majority of patients. Various therapies have been developed to treat HF. Based on the neurohormonal condition of HF patients, angiotensin converting enzyme (ACE) inhibitors, β -blockers, and diuretics have been developed and employed to relieve symptoms in patients. However, these drugs can not prevent HF from progression in patients. ACE inhibitors and β -blockers do not directly and/or sufficiently antagonize all of the biologically active systems that become activated in the setting of HF (113). It is likely that the therapies and drugs currently used in HF patients that improve symptoms have little effect on the underlying mechanisms of HF progression. To date, the mechanisms underlying the transition from compensation to decompensation in HF patients remain unknown.

Despite the advances in HF patient management, the mortality of patients with HF remains extremely high, and there is no therapeutic intervention sufficient to improve long-term survival (134). So far the mechanisms underlying HF still remain obscure. The current therapeutic strategies improve the symptoms rather than the causal problems leading to the symptoms. Thus there is no cure for HF before the causal mechanisms were recognized.

Sudden death in HF

Patients with HF die of two main causes: lethal arrhythmias and cardiac deterioration with pump failure. Many patients died suddenly, unexpectedly, without any evidence of hemodynamic or functional deterioration. Sudden death (SD) is often defined as death prior to a short duration (less than 1 hour) of acute symptoms (80). The first Vasodilator in Heart Failure Trial (V-HeFT I) indicated that the largest single cause of death over the first 60 months of follow-up was sudden death (180). The percentage of sudden deaths tends to be the highest early, presumably in patients with the least severe disease (67). In New York Heart Association (NYHA) functional classification, patients are grouped according to the progression of HF (Table 2.1). The higher the class, the more limitations of physical activity the patient has. Surprisingly, the percentage of patients who died suddenly was not related to the extent of HF (134). There is even a higher percentage of sudden death reported with classer I and II. In patients with classes I and II HF, 50-60% of all deaths were sudden, whereas in patients with classes IV this was only 20-30% (149).

Table 2.1. New York Heart Association functional classification

Class I	No limitation of physical activity. Ordinary physical activity does not cause undue fatigue, palpitation or dyspnea.
Class II	Slight limitation of physical activity. Comfortable at rest, but ordinary physical activity results in fatigue, palpitation or dyspnea
Class III	Marked limitation of physical activity. Comfortable at rest, but less than ordinary physical activity causes fatigue, palpitation or dyspnea
Class IV	Unable to carry out any physical activity without discomfort. Symptoms of cardiac insufficiency at rest. If physical activity is undertaken, discomfort is increased.

Patients with HF have a high incidence of ventricular arrhythmias (99). Of the patients with HF who die, 35% to 50% of the deaths are SD and unexpected (94, 135). Based on studies of heterogeneous populations of patients with out-of-hospital cardiac arrest, the mechanism of death in the majority of patients with organic heart disease who die suddenly is sustained ventricular tachyarrhythmias (159, 201). In SD of hospitalized patients with NYHA class III or IV HF who were having end-stage HF, 52% of SD was due to acute fatal arrhythmias, such as ventricular tachycardia/fibrillation (VT/VF), the others resulting from bradyarrhythmias or electromechanical dissociation (EMD) (111, 123, 134, 173).

Arrhythmias

In normal hearts, various areas have automaticity, such as the sinoatrial node (SAN), the atrioventricular node (AVN), and Purkinje fibers, while normal cardiac rhythm is controlled by the SA node, which is intrinsically the fastest pacemaker. Arrhythmia refers to an abnormal rhythm produced by hearts due to any physiological or pathological conditions. Arrhythmia is a common cause of death in patients with HF. The cellular mechanisms of arrhythmia include ectopic automaticity, afterdepolarization, and reentry (9, 97, 127).

According to clinical observations, it is suggested that arrhythmias cause sudden death of patients with advanced HF (210). The majority of patients with HF have not suffered a myocardium infarction (MI) (94), suggesting that classic reentrant ventricular tachycardia (VT) may not be the principal mechanism of SD (180). On the other hand, most fatal arrhythmias in HF initiate by a nonreentrant mechanism such as early afterdepolarization (EAD) and delayed afterdepolarization (EAD) (144, 146, 148, 180).

This is true for almost all of VTs in human nonischemic cardiomyopathy and half of VTs in ischemic cardiomyopathy (145, 149). In patients with severe HF, nonsustained ventricular tachycardia may be an independent marker of increased mortality due to SD (50).

To define the mechanisms of spontaneously occurring ventricular arrhythmias in nonischemic HF, Pogwizd (146) used three-dimensional cardiac mapping to delineate reentrant versus nonreentrant (or triggered) mechanisms of VT in a rabbit model of HF induced by combined pressure and volume overload. The rabbits exhibit moderate to severe LV dysfunction similar to pathologic alteration in human nonischemic VT. Mapping studies showed that spontaneously occurring VT was initiated and maintained by a nonreentrant mechanism without any intervening electrical activity between the termination of the preceding beat and the initiation of the subsequent VT beat. Furthermore, using three-dimensional cardiac mapping, Pogwizd et al. (149) suggested that focal mechanisms play a much greater role than reentry in ventricular arrhythmias in patients with idiopathic dilated cardiomyopathy (IDCM). The focal initiation of VT may result from triggered activity arising from either EADs or DADs (147, 149).

Afterdepolarization is a membrane potential oscillation that can reach threshold and initiate one or more cardiac responses (54, 189). When the oscillation occurs before repolarization is completed, it is called an early afterdepolarization (EAD), while delayed depolarizations (DAD) occur after completion of repolarization (54, 189) Non-uniform muscle contraction can enhance DADs by dissociating Ca^{2+} from myofilaments with the border zone between contracting and stretched regions and therefore cause triggered arrhythmias (122).

The role of EAD in HF is less clear (86). In patients with HF the plasma norepinephrine is increased (39, 64). Vermeulen et al. (190) reported that, in the presence of norepinephrine, EADs were found in isolated failing and normal rabbit trabeculae, but not in failing human trabeculae. In contrast, Veldkamp et al. (188) observed norepinephrine induced APD prolongation and EAD in ventricular myocytes from end-stage HF patients.

The duration of the AP is primarily responsible for the repolarization time of the heart; prolongation of the AP reflects delays in cardiac repolarization. Abnormal cardiac repolarization plays an important role in HF, and the mechanisms of SD have been addressed extensively (180). Cells isolated from human and animal failing hearts consistently exhibited a significant prolongation of APD compared with normal hearts, independent of the cause of HF (17, 24, 32, 40, 57, 93, 107, 156, 164, 165, 183). In hypertrophied and failing myocardium, the primary electrical abnormality is prolonged action potential duration. The longer the action potential, the more labile the repolarization process is (9). Thus the early afterdepolarization appears to be the electrical abnormality most likely to develop and could play the central role in generating arrhythmias.

APD prolongation in nonischemic HF (8, 9, 55) cause EADs and lethal arrhythmias. Prolongation of repolarization has been reported in the tachycardia-induced model of HF (106, 163). Enhanced dispersion of repolarization may render the heart vulnerable to local reexcitation (45). Evidence for a reentrant mechanism for arrhythmias in nonischemic cardiomyopathy is scarce.

It is suggested that HF represents a common, acquired form of the long QT syndrome (LQTS) (115). Polymorphic VT in patients with LVH and HF might share similar mechanisms to that observed in patients with LQTS (115). In patients with the LQTS, EADs is believed to contribute to the polymorphic ventricular tachyarrhythmias (207). Long QT syndrome can be heritable or acquired. Myocyte from failing hearts show an abnormally labile repolarization in vivo (15). Dogs with heart failure exhibit QT prolongation and prolongation of AP (136). Cells isolated from failing dogs exhibit more frequent EAD than did cells from control animals. Similarly, patients with HF have markedly enhanced QT variability relative to controls (15). In the LQTS, the risk of SD is associated not only with lengthening of the QT interval, but also with increased heterogeneity of repolarization (42, 154). In HF, dispersion of repolarization may be associated with electrical instability and SD (11). Increased dispersion of repolarization has been associated with electrical instability and/or SD in ischemic heart disease (62, 140, 141) and nonischemic heart disease (28, 51, 120).

Electrophysiology

In cardiac myocytes, precisely-timed gating and the current density of the specific ion channels determine the particular duration and morphology of the action potential. Various durations and shapes of the action potential through different regions of the heart are essential for a regular heart-beat.

Action potential (AP)

In mammalian hearts, the normal mechanical function and rhythm depend on proper electrical impulse throughout the myocardium. Myocardial electrical activity is

attributed to the action potential generation in individual cardiac cells. The generation of myocardial action potential reflects the sequential activation and inactivation of various ion channels presenting on the membrane of cardiomyocytes. These distinct ion channels conduct depolarizing and repolarizing currents (Figure 2.1). A cardiac action potential is composed of four phases. The initial upstroke (phase 0) is due to the activation of the fast inward Na^+ current. The transient repolarization (phase 1) is a consequence of the rapid inactivation of Na^+ channels and the activation of transient outward K^+ channels. The plateau (phase 2) of action potential reflects a balance between inward depolarizing current through voltage-gated Ca^{2+} channels and outward repolarizing current through delayed outward K^+ channels. The terminal phase 3 is due to Ca^{2+} channel inactivation and the predominant outward K^+ currents return the membrane voltage back to the resting potential (129, 178). There are multiple types of K^+ currents that contribute to action potential repolarization in myocardium (128, 129). Of the several types of K^+ currents carried by ion channels, the transient outward K^+ current (I_{to}) and the delayed outward rectifier K^+ current (I_{K}) are described as two primary classes of cardiac repolarizing K^+ currents, whereas the inward rectifier K^+ current (I_{K1}) is responsible for the maintenance of the resting potential. Generally, it is considered that the transient outward K^+ currents contribute to phase 1 repolarization and the delayed rectifier K^+ currents are responsible for latter membrane repolarization (7, 70, 133, 205).

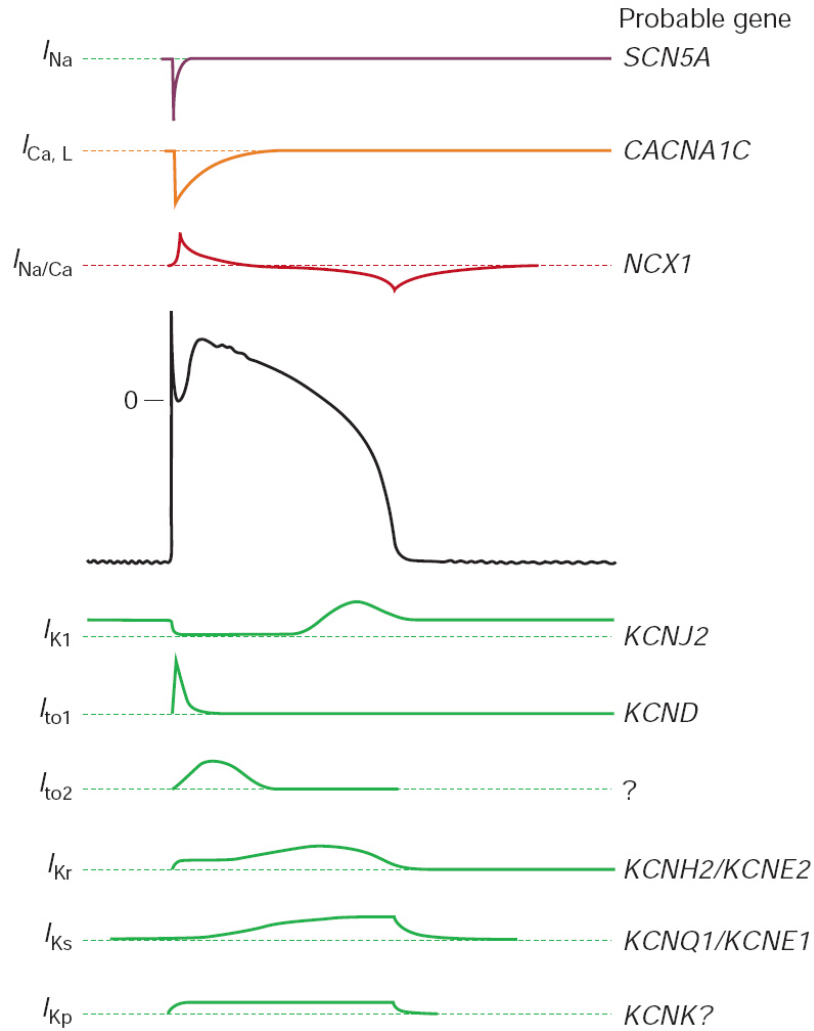


Figure 2.1. Action potential waveform and underlying ionic currents in adult human ventricular myocytes (114). Top, depolarizing currents as functions of time, and their corresponding genes; medium, action potential; bottom, repolarizing currents and their corresponding genes.

Prolonged action potential and altered ion currents

The prolonged action potential is considered to be attributed by abnormal ion currents and associated with abnormal repolarization in myocardium (8, 91, 117, 156). Abnormal cardiac repolarization plays an important role in HF, and the mechanisms of

SD have been addressed extendedly (180). Cells isolated from human and animal failing hearts consistently exhibited a significant prolongation of APD compared with normal hearts, independent of the cause of HF (8, 18, 71). Gwathmey et al. (71, 72) and Vermeulen et al. (190) have shown that a prolongation of APD can be found in ventricular muscle from patients with terminal HF or with severe cardiac hypertrophy. In single cells, duration of AP was markedly prolonged in myocytes isolated from end-stage HF patients as compared with control cells (17, 18). Keung and Aronson (98) reported prolonged AP in muscle fibers obtained from rats with myocardial hypertrophy induced by renal hypertension. Brooksby et al. (24) and Cerbai et al. (32) reported prolonged AP in myocytes from spontaneously hypertensive rat (SHR). In a cat model of pressure overload, AP prolongation was observed in hypertrophied right ventricular myocytes (100). In guinea pig model of pressure overload, APD of left ventricular myocytes was prolonged (130, 165). In ferret model of pulmonary artery constriction (151), rat model of myocardium infarction (156), and dog model of pacing induced cardiomyopathy (93, 132), APs were also prolonged in failing myocytes.

Despite the uniform observation of APD prolongation in distinct animal models, the current alteration underlying prolonged AP was nonuniform between studies. The most consistent change in ionic currents is a reduction in the transient outward current (14, 32, 40, 151, 183). Alteration of I_{to} was observed in myocytes isolated from patient with HF (124, 198). Similarly, in patients with severe HF, both the inward rectifier potassium current (I_{K1}) density and the transient outward potassium (I_{to}) density were significantly reduced (17). In addition to findings from human hearts, various animal models of HF have been reported for the alteration of I_{to} . In a dog model with pacing

induced cardiomyopathy, I_{to} density was dramatically reduced in cells from failing hearts (93). In rats with pressure overload induced cardiac hypertrophy, I_{to} density was significantly decreased in hypertrophied myocytes (14, 183). Such a decrease was also observed in rat hearts with deoxycorticosterone acetate (DOCA) salt induced hypertension (40) and cat hearts with pulmonary artery (100). In rat myocytes with post myocardium infarction (MI) remodeling, I_{to} density was decreased (156). In ferret right ventricular myocytes following pulmonary artery constriction, the I_{to} density was also reduced (151).

Despite the most consistent change in I_{to} , other current alterations were also reported. Undrovinas et al. reported an alteration of I_{Na} in human myocytes with left ventricular cardiomyopathy (185). Increased late sodium current ($I_{Na, Late}$) contribute to APD prolongation in failing human hearts and dog pacing model (186). In a guinea pig model with aortic banding causing cardiac hypertrophy, APDs were significantly prolonged in banded animals (4). No significant difference in K^+ currents was observed between the banded animals and age-matched sham-operated animals. However, a significant increase in Na^+ and Na^+-Ca^{2+} exchange (NCX) current densities were found in banded animals. There was also a significant attenuation in the Ca^{2+} -dependent inactivation of the L-type Ca^{2+} current found in banded group. Their findings suggested an alternate mechanism for APD prolongation in cardiac hypertrophy and failure. In another guinea pig model after aortic coarctation, an increased I_{Ca} density may contribute to the prolonged APD. An increased magnitude and prolonged time course of NCX current was also observed (165). In addition, a decreased inward rectifier channel density may play a role in APD prolongation in SHR myocytes (24).

Regional diversity of APD and underlying currents distribution have been reported (27, 125, 198). In guinea pig model of cardiac hypertrophy induced by aortic constriction, action potential duration (APD) was prolonged in sub-epicardial and mid-myocardial myocytes (27). In control animals, there is a gradient of APD observed (APD₉₀: sub-endocardial > mid-myocardial > sub-epicardial). However, this gradient disappears in hypertrophied hearts. Causally, increased I_{Ca} was observed in sub-epicardial and mid-myocardial myocytes in hypertrophied hearts. The factor that APDs were similar in all regions may favor the propagation of reentry arrhythmias in hypertrophied hearts.

Downregulation of the outward K^+ currents is associated with prolonged action potential duration in myocardium and myocytes from both human patients and experimental models of cardiac hypertrophy and failure (95, 126, 199). A reduction in the I_{to} density is the most consistent ionic current change in cardiac hypertrophy and failure (86, 127). Beuckelmann and colleagues (17) reported that in ventricular myocytes isolated from heart of patients with terminal heart failure, the average current density of I_{to} was significantly reduced. In rabbits with HF induced by aortic constriction (150), I_{to} and I_{K1} were reduced significantly, as reported in human HF (17). I_{to} density is differently expressed in subepicardium and subendocardium and in human myocytes isolated from hearts in terminal heart failure, I_{to} densities were reduced differentially (125, 198). The effect of HF-induced I_{to} downregulation on APD varies across species. Downregulation of the I_{to} is unlikely to produce effects on APD in the ventricles of large mammals with long APDs such as human and dog (181). Nonetheless, I_{to} does influence phase 1 action potential and the level of the plateau (phase 2), subsequently affecting all currents active later in action potential (181). However I_{to} is the major repolarizing current that

determines the APD in rats (90). In rat model of cardiac diseases, the prolonged APD can be attributed to the significantly depressed I_{to} density in ventricular myocytes (32, 40).

Potassium channel

At the molecular level, K^+ channels are transmembrane proteins that selectively conduct K^+ ions across the cell membrane down its electrochemical gradient (168). Voltage-gated K^+ channels (Kv) are such selective channels for K^+ ions conduction that membrane depolarization causes conformational change to lead to channel opening and allow potassium ions to flow. In addition, a functional Kv channel comprises four α -subunits (Figure 2.2) (21, 129, 143). Furthermore, the formation of homo- and/or heteromultimeric channels from two or more types of Kv α -subunits contributes to functional Kv channel diversity in cardiac myocytes (21, 128).

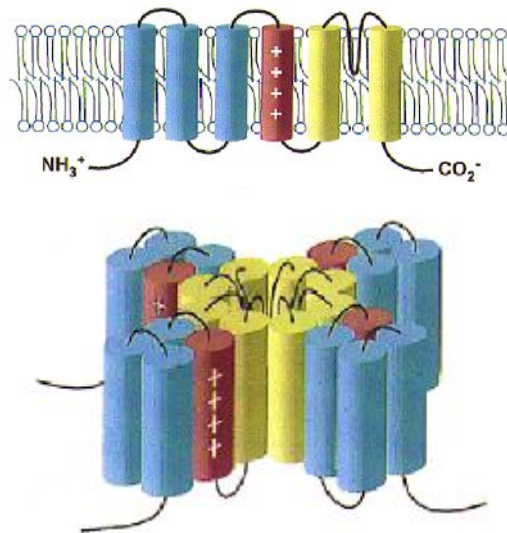


Figure 2.2. Structure and assembly of voltage-gated potassium channel (Kv) α subunits (128). Top, Kv α subunits are integral membrane proteins with six transmembrane domains; bottom, schematic diagram illustrating the assembly of four Kv α subunits to form a functional K^+ selective pore.

Voltage-gated K^+ channels (Kv) are the primary determinants of action potential repolarization in the mammalian myocardium. Two broad classes of repolarizing cardiac Kv currents have been distinguished based primarily on differences in time- and voltage-dependent properties: transient outward K^+ currents (I_{to}) and delayed rectifier K^+ currents (I_K) (129). The I_{to} activates and inactivates rapidly as membrane depolarized to potentials positive to approximately -30 mV and underlies the phase 1 of action potential in both ventricular and atrial cells. I_K activates at similar membrane potentials and determines the phase 3 of repolarization back to the resting potential. Despite the marked electrophysiological diversity of repolarizing K^+ currents, the detailed pharmacological, time- and voltage-dependent properties of I_{to} and I_K currents in different cardiac cell types and species are quite similar.

Transient outward currents I_{to}

There are two transient outward current components with distinct properties and referred to as I_{to1} and I_{to2} . I_{to1} is blocked by 4-aminopyridine (4-AP) and is Ca^{2+} -independent K^+ current, whereas I_{to2} is not blocked by 4-AP and is Ca^{2+} dependent Cl^- current. Furthermore, two distinct transient outward K^+ currents $I_{to,fast}$ ($I_{to,f}$) and $I_{to,slow}$ ($I_{to,s}$) have been distinguished (205). A great number of evidence suggested that $I_{to,f}$ is a prominent repolarizing current in atrial and ventricular myocytes in most species, including human (129).

Studies indicated that channel proteins Kv4.2 and Kv4.3 serve as pore-forming subunits for the native I_{to} in cardiac myocytes (23, 48, 206). There is no Kv4.2 detected in canine and human ventricle, but mRNA encoding Kv4.3 is present (48). It is believed that Kv4.3 is the prominent candidate subunit underlying I_{to} in human myocardium (48,

91, 128). Kv4.2 and Kv4.3 form heteromultimeric channels to generate I_{to} in rodent left ventricular myocytes (167). In rat myocytes, both Kv4.2 and Kv4.3 contribute to I_{to} (47, 48). Kv4.2 and Kv4.3 antisense oligonucleotides significantly reduced I_{to} by similar levels in rat ventricular myocytes (approximately 55-60%) (56). A dominant negative Kv4.3 construct suppressed I_{to} and significantly prolonged action potential duration in rat ventricular myocytes (81). Likewise, expression of dominant negative Kv4.2 produced a depression of I_{to} and prolonged action potential (13, 89). In human cardiac myocytes, three components of the delayed outward rectifier current have been identified, including ultra rapid current (I_{Kur}), rapid current (I_{Kr}), and slow current (I_{Ks}), which are encoded by Kv1.5, ERG1, and KvLQT1, respectively (129). In rat cardiomyocytes, only one type of delayed K^+ current (I_K) is detected, which is encoded by Kv1.5 and Kv2.1 (7, 204).

Molecular basis of I_{to} downregulation in HF

Although there are extended observation of I_{to} downregulation in various studies using different animal models of HF, the underlying molecular basis of I_{to} changes in HF was rarely studied to date.

For studies of human heart samples, the ventricular myocardium was obtained from explanted failing hearts and donor hearts unsuitable for transplantation. The failing hearts usually have various etiologies, such as dilated cardiomyopathy (DCM), ischemia cardiomyopathy (ICM). Kaab et al. (91) reported their study of I_{to} and mRNA level in tissue and isolated ventricular myocytes from failing human hearts with DCM and ICM. The level of Kv4.3 mRNA is reduced by 30% in failing cells. This reduction of transcript was correlated with the reduction in peak I_{to} density. In addition, there was no significant change observed in the mRNA level of any other studied channel subunits (HERG,

Kv1.4, Kir2.1, Kv β 1.3, Cav1.2). Thus the downregulation of I_{to} in human heart failure may be transcriptionally regulated.

Furthermore, two Kv4.3 isoforms, Kv4.3-S and Kv4.3-L, have been described in human (102). In addition, the function of Kv4.3 channels can be modulated by several accessory subunits such as potassium channel interaction protein (KChIP) 2 and KCNE1-KCNE5 (6). Recently, it was shown that compared to non-failing tissue, failing hearts from NYHA IV patients with DCM exhibited higher expression of Kv4.3-L and KCNE1 and lower expression of Kv4.3-S, KChIP2, KCNE4, and KCNE5 (157). In the same report, the heterologous coexpression of KCNE proteins in CHO cells provided evidence that KCNE2 and possibly KCNE4 have functional interaction with Kv4.3.

Akar et al. (5) reported their study about the molecular basis for APD prolongation and K^+ current downregulation in a canine model of tachycardia-induced HF. Marked reductions of mRNA and protein levels of canine Kv4.3 in left ventricle were observed in HF. Canine Kv1.4 and KChIP2 protein level had no significant change in HF. Thus the downregulation of I_{to} is associated with decreased Kv4.3 and not Kv1.4 or KChIP2 in this model. Interestingly, the Kir2.1 mRNA and protein levels was unaffected by HF, whereas the I_{K1} density was significantly reduced in failing heart, suggesting possible posttranslational modification of the current in HF.

In a transgenic mice model (199), a dominant-negative Kv4.2 was overexpressed in the hearts. Young transgenic mice showed heterogeneous reductions in I_{to} and APD prolongation. Between 8 and 16 weeks of age, these mice developed a dilated cardiomyopathy, thereafter culminated in congestive heart failure and death. This transgenic model suggested that, at least in rodent, reduction in I_{to} and consequent APD

prolongation lead to the development of cardiac hypertrophy and HF. It is also reported that a reduction of Kv4.2 occurred in mRNA and protein levels in post-MI remodeled rat LV (61). Similarly, the mRNA and/or protein levels of Kv4.2 and Kv4.3 were decreased to a varying extent in different regions of LV of another post-MI rat heart (83). In renovascular hypertension rats, expression of Kv4.2 and Kv4.3 mRNA was diminished (177). However, to date no study has reported the potential alterations in electrophysiological properties in cardiac myocytes following volume overload.

Ubiquitin-proteasome system

Discovery of ubiquitin

In 1974, a polypeptide was isolated and purified from bovine thymus (65). Besides thymus, this polypeptide was also presented in many other tissues and was able to induce immunocyte differentiation, thus named ubiquitous immunopoietic polypeptide (UBIP). This small peptide was detected in animal cells, yeast, bacteria, and higher plants. The high degree of evolutionary conservation suggests that UBIP performs a pivotal function in living organisms. Later, this new polypeptide was called ubiquitin and discovered to be ATP-dependent proteolytic factor-1 (APF-1), a small, heat-stable polypeptide (36). APF-1, the first component isolated for the ATP-dependent proteolytic system, has no protease activity per se but stimulates protein breakdown in the presence of the other components and ATP.

The ubiquitin-proteasome system

The ubiquitin-proteasome system (UPS) plays a major role in intracellular protein degradation (38, 63, 77). Degradation of a protein via the UPS involves two successive

steps: enzymes catalyzed ubiquitination and proteasome dependent degradation. In ubiquitination, multiple ubiquitin molecules are covalently attached to the protein substrate. In the process of degradation, the ubiquitinated protein are recognized and degraded by the 26S proteasome with release of free and reusable ubiquitin. The ubiquitination is catalyzed by three types of enzyme(s). The ubiquitin-activating enzyme (E1), the ubiquitin-conjugating enzymes (E2s) and the ubiquitin ligases (E3s) activate ubiquitin molecules and catalyze the formation of an isopeptide bond between the ubiquitin and the target protein. There are one E1 enzyme, hundreds of E2 enzymes and thousands of E3 enzymes. E3s are believed to be responsible for the specificity of ubiquitination of substrate proteins.

Ubiquitin (Ub) is a highly conserved protein of 76 amino acids in all eukaryotic cells. The last residue at the C-terminal end, Gly76, can be conjugated to the ϵ -amino group of a lysine residue in a target protein. There are seven Lysine (K) residues in an Ub molecule. Theoretically, each Lysine can be attached by the C-terminal Gly76 of another ubiquitin to form polyubiquitin chain. Now it is clear that monoubiquitin and polyubiquitin chain signal different fates for their target proteins (78, 79, 142) It is believed that monoubiquitin attached to integral plasma membrane proteins or transport modifiers to serves as a regulated signal for internalization of the membrane proteins into the endocytotic pathway (79). Furthermore, different polyubiquitin chain may have distinct function, for instance K48 chains usually signal proteasomal degradation, whereas K63 chains act as non-proteolytic signals in several intracellular pathways (142).

The proteasome, or 26S proteasome, is an intracellular proteolytic complex, which composed of catalytic 20S core and one or two regulatory 19S cap (2). 20S core

consisted two inner β rings and two outer α rings. Ubiquitinated proteins bind to 19S, are then cut off the ubiquitin chain and denatured and feed into the 20S core. There are three type of hydrolytic activities, trypsin-like, chymotrypsin-like, and post-glutamyl peptide hydrolase (PGPH) activity in the proteasome.

The UPS alteration in the heart

Depre et al. (44) reported significantly increased gene and protein expression of proteasome subunits and increased proteasome activity accompanied with compensated hypertrophy induced by transverse aortic constriction. In this model, the proteasome inhibitor epoxomicin not only blocked proteasome activation but prevented left ventricular hypertrophy as well. However, the activities of the proteasome reported in different studies are inconsistent. In various studies, either electrophysiological changes or alteration of the UPS was reported independently in different cardiac diseases (119, 127, 152). However, whether both changes are concomitant has not been reported.

Growing evidence indicates alterations of the ubiquitin-proteasome system in both human and experimental failing hearts. Accumulation of ubiquitinated proteins has been reported in human failing heart (20, 74, 184, 197).

Tsukamoto et al. (184) found an increase of ubiquitin-positive cardiomyocytes in patients with HF. They proposed that depression of proteasome activities may shift the balance between antiapoptotic and proapoptotic proteins, resulting in cardiomyocyte apoptosis in the progression of heart failure. Importantly, since the presence of cardiac dysfunction was preceded by both the depression of proteasome activities and accumulation of ubiquitinated proteins, it is likely that the depression of proteasome activities was not a consequence of heart failure but one of the causes for heart failure.

Since it has been also reported that three different proteasome activities may be regulated independently (192), multiple mechanisms may be involved in the depression of proteasome activities in pressure-overloaded hearts such as altered gene expression, modifications of the proteasome subunits (oxidation, glycation, glycooxidation, and conjugation with lipid peroxidation products), and presence of inhibitory damaged proteins that inhibit proteasome function (112, 166). Thus, further investigations are required to elucidate the cellular mechanisms of the depression of proteasome activities during the development of heart failure.

MG-132 is a potent proteasomal inhibitor (137, 160). This compound is a peptide aldehyde inhibitor that can enter mammalian cell to inhibit major peptidase activities of the 20S and 26S proteasome. MG-132 can inhibit not only abnormal and short-lived polypeptides but long-lived proteins in intact cells.

Various membrane transporters, receptors and ion channels have been reported to undergo ubiquitin-mediated internalization and degradation (1, 121). Staub et al. (169) reported that the stability of epithelial sodium channel (ENaC) at the plasma membrane is regulated by ubiquitination. Chapman et al. (34) reported that the surface expression of HERG potassium channel is strictly regulated by ubiquitination.

Kv1.5 has been demonstrated to be degraded by the proteasome (96). In COS cells, Kv1.5 half-life time was prolonged by the proteasome inhibitors, but not by a lysosomal inhibitor chloroquine. MG132 increased the protein level of both Kv1.5 and its ubiquitinated form. Similarly, in cultured rat atrial cells, MG132 increased endogenous Kv1.5. Furthermore, MG132 also increased $I_{K_{ur}}$ currents through the cell-surface Kv1.5. This study suggested that the inhibition of the proteasome increased $I_{K_{ur}}$ currents

secondary to the increased cell-surface-expression of mature Kv1.5. Similarly, inhibition of proteasome activity by MG132 and other proteasome inhibitors not only prolonged half-life time of Kir6.2 in COS cells, but also augmented K_{ATP} currents in both COS cells expressing SUR2A and Kir6.2 and neonatal rat cardiomyocytes (179). However, so far, whether the cardiac Kv4 channels are regulated by the UPS has not been reported.

Animal model for HF

In mammals, after birth, most cardiac myocytes lose their ability to proliferate and growth occurs primarily by means of increasing myocyte size (118). As functional load changes, the heart triggers an adaptive hypertrophy to counterbalance the increase in wall stress. Cardiac hypertrophy can be classified as either physiological or pathological. Physiological hypertrophy can result from exercise or pregnancy. Pathological hypertrophy occurs due to mechanical overload, ischemia, or genetic abnormalities. Based on difference of initial stimulus, physiological and pathological hypertrophy can be subclassified as concentric or eccentric (68). Pressure overload (PO), induced by stresses such as hypertension and aortic stenosis, produces concentric hypertrophy characterized by relatively small cavities of ventricles with thick walls. In contrast, volume overload (VO), such as aortic regurgitation and arteriovenous fistula, produces eccentric hypertrophy with large dilated cavities and relatively thin walls. Whatever the cause is, prolonged pathological hypertrophy leads finally to heart failure.

Several animal models of heart diseases have been created to study ventricular remodeling. For instance, pressure overload can be induced by coronary artery ligation, aortic or pulmonary artery banding, or spontaneous hypertension. Volume overload is

induced by aortocaval fistula, mitral regurgitation, aortic regurgitation, tricuspid regurgitation. Other animal models include combined volume and pressure overload, rapid pacing and genetically determined cardiomyopathy (49, 73, 192).

Chronic volume overload is one of the risk factors that induce ventricular remodeling and heart failure. Chronic volume overload is associated with many clinical conditions, such as surgical induced trauma, patent ductus arteriosus, aortic and mitral regurgitation (52, 85). Ventricular morphological remodeling following chronic volume overload has been studied.

HF can be triggered when the heart is subjected to sustained periods of pathological pressure overload or volume overload. Pressure overload and volume overload induced different changes in cardiac structure and function (30, 31). In a comparative study of PO and VO in rats (16), PO was induced by abdominal aortic banding, while VO was induced by aortocaval shunt procedures. PO rats showed progressive ventricular wall thickening consistent with concentric hypertrophy, while VO rats showed marked left ventricular dilatation consistent with eccentric hypertrophy. PO led to low cardiac output and general systolic dysfunction. Diastolic dysfunction was also observed as indicated by poor compliance and reduced myocardial relaxation capabilities. VO led to high CO and systolic dysfunction, while diastolic dysfunction and compliance of the ventricle was unchanged or enhanced.

Wang et al. reported that HF-related remodeling of outward K^+ currents in murine left ventricle (LV) (195). Using thoracic aortic constriction (TAC)-induced pressure overload, they evaluated the transmural gradient of outward K^+ currents in murine failing LV. Outward K^+ current density in sham-operated LV was significantly larger in

subepicardial (SEP) myocytes compared with subendocardial (SEN) myocytes. There is no difference in voltage dependence of current activation and inactivation between SEP and SEN myocytes. However, outward K^+ current density was significantly decreased in SEP but not in SEN cells in failing LV, leading to loss of the transmural gradient. With the abolishment of I_{to} density gradient, the gradient in Kv4.2 protein expression was similarly absent in HF. Abundance of K channel interacting protein (KChIP) 2 is also decreased in failing ventricle. Partial ligation of the abdominal aorta was performed to induce pressure overload in rats (183). APD was prolonged with diminished I_{to} in hypertrophied ventricular myocytes. There were no differences in kinetics and single channel properties of I_{to} between normal and hypertrophied cells.

Increased cardiac workload is responsible to activation of protein turnover, which refers to protein synthesis and degradation (44). Ventricular structure remodeling following volume overload has been reported using rat model of AV fistula. In a rat model of myocardial hypertrophy induced by infrarenal arteriovenous fistula, volume overload induced ventricular remodeling leads to myocardial systolic and diastolic dysfunction (172). The development of progressive hypertrophy with ventricular dilation occurred as early as two weeks post-fistula, and sustained volume overload resulted in a significant reduction in myocardial contractility (25, 26). Wang et al. reported that compensated hypertrophy occurred between two weeks and eight weeks after fistula with normal or mildly depressed hemodynamic function (193). HF occurred subsequently between eight weeks and sixteen weeks after fistula with LV contractile dysfunction (193). To date, this animal model has been employed as a rapidly developing VO model characterized by cardiac hypertrophy and neurohormonal consequences that resemble

those of HF patients (33, 43, 59, 84, 174, 176). This model is a useful platform for defining the role of specific pathways and mechanisms in the pathogenesis of load-induced heart disease (16). More recently, using this model, our lab demonstrated that myocytes contractility is depressed during the progression of ventricular remodeling secondary to volume overload (46). However, albeit SD observed consistently in this model (25, 26), there is no study that addressed the electrophysiological alterations following volume overload.

CHAPTER III. EXPERIMENTAL DESIGN

Aim 1. Determine the temporal alteration of electrical properties of ventricular myocytes isolated from rats following chronic volume overload. The temporal changes of electrical parameters, including action potential duration (APD) and outward potassium currents, I_{to} and I_K , as well as L-type calcium current (I_{CaL}), were measured in ventricular myocytes during volume overload induced ventricular remodeling. The hypothesis is that action potential durations are prolonged and outward potassium currents are decreased in fistula ventricular myocytes compared with those in age-matched control ventricular myocytes.

Aim 2. Assess expression of outward potassium channels during volume overload induced ventricular remodeling. Expression of voltage-gated potassium channel (Kv) α subunits in ventricular myocytes was evaluated using western blot technique. mRNA level of Kv α subunits was also determined to analyze the possible alteration in channel protein synthesis. The hypothesis is that the expression of Kv α subunits underlying outward potassium currents is decreased in fistula ventricular myocytes during the progression of ventricular remodeling following volume overload.

Aim 3. Examine the role of the ubiquitin-proteasome system in altered potassium currents and potassium channel degradation during development of volume overload induced ventricular remodeling. Expression of ubiquitinated Kv α subunits was evaluated using immunoprecipitation. Ventricular myocytes isolated from control and fistula

animals were treated with proteasomal inhibitor or lysosomal inhibitor, respectively, to determine the place where the ubiquitinated Kv α subunits undergo degradation. The hypothesis is that at least one of the inhibitors affects the expression of Kv α subunits.

**CHAPTER IV. ELECTROPHYSIOLOGICAL REMODELING IN RAT
VENTRICULAR MYOCYTES DURING VENTRICULAR REMODELING
FOLLOWING CHRONIC VOLUME OVERLOAD**

ABSTRACT

Congestive heart failure (CHF) is the leading cause of death in the United States. CHF patients typically die from deterioration of ventricular pump function or cardiac arrhythmias. The electrical remodeling of cardiac myocytes during ventricular remodeling induced by volume overload has not been elucidated. In the present study, we investigated the electrophysiological properties of ventricular myocytes following volume overload. Volume overload was induced by creation of aortocaval (AV) fistula in rats. Action potential and outward K^+ currents were recorded using whole-cell patch clamp technique in isolated ventricular myocytes at 5-, 10-, and 13-week following AV fistula. Prolonged action potential duration (APD) and decreased transient outward K^+ current (I_{to}) densities were observed in myocytes from fistula rats at different times compared with age-matched control rats. Activation and inactivation of I_{to} were similar between fistula and control groups. Ca^{2+} current densities were comparable between fistula and control myocytes. Western blotting analysis revealed that the expression of Kv4.3 and Kv4.2 in myocytes from fistula group at 13-week was significantly decreased when compared with control. However, mRNA level of Kv4.2 and Kv4.3 was not changed. We conclude that action potential prolongation and decrease of outward K^+

current density are associated with downregulation of Kv4 α subunits following chronic volume overload.

INTRODUCTION

Heart failure (HF) is a leading cause of death in the U.S. More than 5 million Americans have heart failure and more than 250,000 patients die on heart failure annually (161, 182). Patients with HF typically die from either progressive deterioration of ventricular pump function or cardiac arrhythmias. Among the deaths of patients with HF, up to 50% are sudden and unexpected (86, 180, 181). The sudden death is usually associated with cardiac arrhythmia, which is involved in alteration of cardiac electrical properties (86, 127).

Cardiac hypertrophy is a compensatory response to a sustained hemodynamic overload during the development of heart failure. In patients with HF, cardiac hypertrophy may be induced by pressure overload, volume overload or the combination of both. Although both pressure and volume overload lead to the development of heart failure, the structural remodeling and molecular events are quite distinct (30, 31). Prolonged action potential (AP) and decreased K^+ currents are the most common phenomenon in failing human hearts and experimental animal models of heart failure (180, 181). In pressure overload model induced by aortic banding/constriction, alteration in both ventricular contractility and electrophysiological properties have been reported (180). On the other hand, less attention has been paid to volume overload induced cardiac deterioration. Chronic volume overload is associated with many clinical conditions, such as aortic and mitral regurgitation, surgery- and trauma-induced AV shunt,

hyperthyroidism, anemia, and patent ductus arteriosus (85, 193). Ventricular hypertrophy and contractile dysfunction have been reported experimentally (58, 85, 193) using a well-established model of aortocaval (AV) fistula. Using this same rat model of fistula, a recent study from our laboratory demonstrated a decrease of intrinsic contractility of isolated ventricular myocytes that was associated with altered intracellular Ca^{2+} handling following volume overload (46). However, no study has been reported on the possible alteration of electrophysiological properties following ventricular remodeling induced by chronic volume overload.

In the present study, we tested the hypothesis that electrophysiological properties are altered during pathologic ventricular remodeling induced by chronic volume overload. We recorded the action potentials and outward K^+ currents using whole-cell patch clamp technique and also examined the expression of voltage-gated potassium channel (Kv) α subunits in rat ventricular myocytes. The pore-forming α subunit, Kv4.3, is the candidate that is thought to underlie the transient outward potassium current (I_{to}) in human heart. In rat, both Kv4.2 and Kv4.3 are responsible for I_{to} (48, 128). Thus, our experiments focused on the possible alteration of Kv4.2 and Kv4.3 in the volume overload model.

MATERIALS AND METHODS

Animal model of heart failure. The animal model of volume overload was induced by aortocaval (AV) fistula using a previously described method (46). Briefly, male Sprague-Dawley rats (250-300g) were anesthetized with isoflurane inhalation, and a ventral abdominal laparotomy was performed to expose the aorta and caudal vena cava below the renal arteries. After the vessels were exposed, both vessels were occluded

proximal and distal to the intended puncture site. A fistula were created by inserting an 18-gauge needle into the exposed abdominal aorta and advanced through the medial wall into the vena cava. After the needle was withdrawn, the aortic puncture site was sealed with cyanoacrylate glue. Creation of a successful AV fistula was visualized by the pulsatile flow of oxygenated blood into the vena cava from the abdominal aorta. The abdominal musculature and skin incisions were closed by standard techniques with absorbable suture and autoclips. For age-matched control rats, sham operation was performed without creation of AV fistula. All animal handling procedures were approved by the Auburn University Institutional Animal Care and Use Committee.

Preparation of isolated ventricular myocytes. At 5-, 10- and 13-week after the AV fistula surgery, ventricular myocytes were isolated from fistula and age-matched control rats. The time course of fistula duration was chosen based on the previous reports of the temporal ventricular remodeling in this model (25, 193). Body weight and heart weight were measured before the myocyte isolation. Rats were anesthetized with sodium pentobarbital and killed by decapitation. Hearts were rapidly removed and hung on a retrograde perfusion apparatus. The hearts were perfused with oxygenated Ca^{2+} -free Tyrode's solution for 3-5 minutes. The heart was then perfused with 0.45 mg/ml Type 2 collagenase (305U/mg, Worthington) in Ca^{2+} -free Tyrode's solution for 17-18 minutes. After perfusion, the ventricles were minced into small pieces in storage solution (100 mg bovine serum albumin in 100 ml low Ca^{2+} Tyrode's solution) and screened to collect individual myocytes. Isolated myocytes were centrifuged at low speed and resuspended in storage solution followed by the addition of increasing concentrations of Ca^{2+} until the final concentration of Ca^{2+} reached 1 mM to yield Ca^{2+} -tolerant cardiomyocytes. Half of

the isolated myocytes were quick-frozen in liquid nitrogen and stored in -80°C for later analysis of protein and mRNA expression and half of the isolated myocytes were used for electrophysiology experiments within 8 hours.

Action potential and current measurement. Action potentials and currents were studied using the whole-cell patch clamp technique. Patch pipettes were prepared from borosilicate glass (Sutter instrument, CA) with a pipette puller (PP-830, Narishige, Japan) and fire-polished with a micro forge (MF-830, Narishige, Japan). After the whole-cell configuration was established, the cell membrane capacitance was measured and recorded. Membrane potentials and currents of myocytes were elicited and measured through an AXOPATCH 200B patch clamp amplifier (Axon Instruments, CA) and the data acquisition package pClamp 8 or 9 (Axon Instruments, CA). All experiments were performed at room temperature.

For action potential measurements, myocytes were perfused with bath solution (flow rate ~ 2 ml/minute). After establishment of the whole-cell configuration, the amplifier was switched to current-clamp mode. Action potentials were elicited by a 6 ms current pulse (30% above threshold) at a 20-second interval. Resting membrane potential, amplitude of action potential, and time to 50% (APD50) and 90% repolarization (APD90) were recorded and analyzed.

Outward K^+ currents were recorded in the voltage clamp mode. Myocytes were perfused with bath solution (flow rate ~ 2 ml/minute). I_{to} was recorded in the presence of external tetraethylammonium chloride (TEA-Cl, 50 mM), which is used to block I_{K} . I_{K} was recorded in the presence of external 4-aminopyridine (4-AP, 5 mM), which is used to block I_{to} . I_{Na} was eliminated by applying a 30-ms prepulse from holding potential to -40

mV. Current was elicited by test pulse between -30 and +50 mV applied in 10 mV increments at a frequency of 0.1 Hz. Currents were normalized to myocyte capacitance and expressed as current density (pA/pF). The steady-state activation and inactivation of K^+ channels were estimated using a double-pulse protocol.

L-type Ca^{2+} current (I_{CaL}) was recorded using whole-cell voltage clamp mode in ventricular myocytes. I_{CaL} was elicited by stepping voltage to 0 mV from the holding potential of -40 mV at 30-second intervals. Current density was determined by dividing the measured peak current amplitude by cell capacitance.

Solutions for electrophysiological experiments. Tyrode's solution was composed of (in mM) 130 NaCl, 5.4 KCl, 1.2 $MgSO_4$, 6 HEPES, 1.8 $CaCl_2$, 1.2 KH_2PO_4 , and 10 glucose (pH adjusted to 7.4 with NaOH).

For action potential measurements, bath solution contained (in mM) 137 NaCl, 5.4 KCl, 1 $MgCl_2$, 1.8 $CaCl_2$, 10 HEPES, 0.33 NaH_2PO_4 , and 10 glucose (pH adjusted to 7.4 with NaOH). The pipette solution contained (in mM) 100 KCl, 10 NaCl, 5 ATP-Mg, 10 EGTA, 2 $MgCl_2$, 10 HEPES, 5.5 glucose and 0.5 GTP-Mg (pH adjusted to 7.2 with KOH).

For outward K^+ currents measurements, bath solution contained (in mM) 137 NaCl, 4 KCl, 1 $MgCl_2$, 0.5 $CaCl_2$, 10 HEPES, 1 $CoCl_2 \cdot 6H_2O$, and 10 glucose (pH adjusted to 7.4 with NaOH). The pipette solution was composed of (in mM) 80 L-aspartic acid, 50 KCl, 10 KH_2PO_4 , 10 EGTA, 5 HEPES, 3 ATP-Mg, 1 $MgSO_4$ (pH adjusted to 7.2 with KOH).

The bath solution used to record I_{CaL} was composed of (in mM) 137 NaCl, 5.4 CsCl, 1 $MgCl_2$, 1.8 $CaCl_2$, 10 HEPES, and 10 glucose (pH adjusted to 7.4 with NaOH).

CsCl are used to block K⁺ currents. Na⁺ channels and T-type Ca²⁺ channels were inactivated by holding the resting membrane potential at -40 mV. Pipette solution for I_{CaL} contained (in mM) 85 CsCl, 20 TEA-Cl, 5 ATP-Mg, 10 EGTA, 2 MgCl₂, 10 HEPES, 5.5 glucose, and 0.5 GTP-Mg (pH adjusted to 7.2 with CsOH).

Cell membrane preparation. Cardiac cell membrane preparation was performed as described previously (12, 155). The tube containing frozen ventricular myocyte preparations were put on ice. Buffer A (in mM: 50 Tris-HCl, 250 Sucrose, 10 EGTA, 4 EDTA, 1 PMSF, and 0.004 Leupeptin) and buffer B (buffer A with 1% Triton X-100) were prepared and chilled on ice. For each sample, 1.5 ml of buffer A was added into the tube. The myocytes were suspended in buffer A and transferred to a glass homogenizer (Wheaton Science Products, NJ) by pipetting and homogenized for 30 strokes. The myocytes were then transferred to a 2 ml ultracentrifuge tube and centrifuged at 100,000 x g for one hour at 4 °C. The supernatant was removed and represented cytosol proteins. Pellets were resuspended in 1 ml of pre-chilled buffer B and incubated on ice for one hour to allow complete lysis of membrane proteins. Samples were centrifuged at 40,000 x g for one hour at 4°C and the supernatants were used as the membrane fraction and stored at -80°C for later analysis.

Western blot. Cytoplasmic and membrane protein concentrations were determined by Bio-Rad protein assay. Equal amount of proteins of ventricular myocyte lysates prepared from fistula and sham rats were loaded onto the same gel to quantitatively compare expression of potassium channels at various time intervals. Protein lysates obtained from isolated ventricular myocytes were boiled in Laemmli buffer containing 5% β-Mercaptoethanol. Proteins were separated by 10% SDS

polyacrylamide gels and electrophoretically transferred to nitrocellulose membranes. The membranes were stained by Ponceau S dye to determine the total amount of proteins loaded onto the gels. The membranes were then blocked in phosphated-buffered saline with 0.1% Tween-20 (PBST) containing 5% nonfat dry milk for 1 hour at room temperature, and incubated with primary antibodies against Cav1.2, Kv4.3 (Santa Cruz, CA) and Kv4.2 (alomone, Israel), overnight at 4°C. Nitrocellulose membranes were washed in PBST and then incubated with horseradish peroxidase (HRP)-conjugated secondary antibodies against particular primary antibodies. After wash with PBST, enhanced chemiluminescence (ECL) was used to detect the protein bands. Experiments were repeated three times and the optical densities of the specific bands were determined by UN-SCAN-IT Gel & Graph Digitizing Software (Silk Scientific Corporation, UT). All western blots were normalized with Ponceau S images of total proteins to demonstrate equal protein loading.

mRNA level of outward K⁺ channel α subunits. Gene expression of Kv4.2 (accession number NM_031730) and Kv4.3 (accession number NM_031739) were measured in rat myocytes from sham operated and volume overload rats using real-time PCR. Primers for Kv4.2 were: forward 5'- AGCAACCAACTGCAGTCCTC and reverse 5'-GGTTTTCTCCAGGCAGTGAA and for Kv4.3 were: forward 5'-CATGGCCATCATCATCTTTG and reverse 5'- AGGCACCATGTCTCCATAACC. Total RNA was extracted from frozen cells using the RNeasy Mini kit (Qiagen, CA) according to the manufacturers' instructions. Sample RNA was analyzed spectrophotometrically for concentration and the integrity of sample RNA was determined using denaturing-formaldehyde agarose gel electrophoresis. In all samples,

the 28S band was twice as dense as the 18S band. First strand cDNA was synthesized from pooled RNA for control and fistula rats. Each pooled cDNA was synthesized using 200 µg RNA from each rat and reverse transcribed to cDNA using the iScript cDNA Synthesis Kit (Bio-Rad, CA). Real-time PCR was carried out using a iCycler My iQ Real-Time PCR Detection System and iQ SYBR Green Supermix (Bio-Rad, CA). Three house keeping genes, glucuronidase beta (accession number NM_017015), phosphoglycerate kinase 1 (accession number NM_053291) and ribosomal protein L13A (accession number NM_173340) were used as internal controls. The first strand synthesis and real time PCR was performed three times in triplicate. Gene expression in fistula myocytes was calculated relative to the gene expression in control hearts according to the modified $\Delta\Delta C_t$ method (187).

Statistical analysis. Electrophysiological experiments were performed on at least 4 myocytes that were randomly chosen from each heart and data were averaged to represent that animal. For each protocol, the number of myocytes recorded from a heart was further expanded if the standard deviation of the values of measurement obtained from the animal myocytes was large. Values of data were presented as mean \pm SE and n as the number of animals used. Data from different groups were compared using two-tailed unpaired Student's t-test and two way analysis of variation (ANOVA) with a Student-Newman-Kuels post test whenever appropriate. Differences were considered statistically significant at $P < 0.05$.

RESULTS

General characteristics of control and fistula rats. To evaluate ventricular remodeling in the animal model following volume overload, the body weight and heart weight were obtained from both fistula and age-matched control rats and the ratio of heart weight/body weight were calculated as an index for cardiac remodeling. Figure 4.1 presents the general characteristics of control and fistula rats at various time intervals. The heart weight/body weight ratio was significantly increased at all three time intervals in the fistula group (Figure 4.1C). Furthermore, the capacitance of individual myocytes isolated from the fistula group was 128.8%, 139.7%, and 154.9% of control at 5-, 10-, and 13-week, respectively. The increased heart weight/body weight ratio and higher myocyte capacitance indicated development of cardiac hypertrophy in the fistula group following volume overload. This observation of cardiac hypertrophy after fistula surgery is similar to the findings in our previous and other studies (14, 46, 110, 193).

Action potential durations. To determine the electrical properties of cardiac myocytes during development of volume overload induced heart failure, the action potential profiles were measured and analyzed. The resting membrane potentials (E_m) and amplitudes of action potentials were not different between fistula and control groups at three time intervals (Table 4.1). However, the action potential duration (APD) was increased in the fistula group as compared with control group (Figure 4.2). The times to 50% and 90% repolarization were 119.1% and 125.1%, respectively, in fistula myocytes at 5-week, 140.8% and 131.9%, at 10-week and 149% and 148.7% at 13-week, respectively, relative to age-matched control values. These results indicated that the action potential duration was significantly prolonged in fistula myocytes at 10- and 13-

week following fistula induced volume overload. The prolongation of APD observed in fistula myocytes was consistent with findings in other animal model (127, 182).

L-type Ca^{2+} current density and Cav 1.2 expression. To determine the possible contribution of L-type Ca^{2+} channels to the prolonged APD, we compared L-type Ca^{2+} currents (I_{CaL}) in both groups of myocytes (Figure 4.3A). Peak I_{CaL} densities were similar in ventricular myocytes isolated from fistula and age-matched control groups. Expression of Cav 1.2 underlying I_{CaL} was comparable between control and fistula myocytes (Figure 4.3B). These data indicate that cardiac Ca^{2+} channel activity was not affected by chronic volume overload.

Outward K^+ currents. To determine the possible contribution of K^+ currents in the prolonged APD, transient and delayed outward K^+ currents (I_{to} and I_K) were measured. Peak I_{to} density was progressively reduced by 22.7%, 37.7%, and 44.3% at 5-, 10-, and 13-week, respectively, in fistula myocytes when compared with age-matched control myocytes at the test potential of +50 mV (Figure 4.4). Similarly, peak I_K density in fistula group was reduced by 17.3%, 18.8%, and 28.0% at 5-, 10-, and 13-week, respectively, at the test potential of +50 mV (Figure 4.5). Thus the depressed outward potassium currents contributed, at least in part, to the action potential prolongation in fistula myocytes during development of heart failure induced by volume overload. These data also present a temporal and progressive downregulation of potassium currents during ventricular remodeling induced by chronic volume overload.

Voltage dependent activation and inactivation of I_{to} . Since changes in ion channel kinetics can alter the conduction activity of channels under pathophysiological conditions, we also analyzed the voltage dependent activation and inactivation of I_{to} . The voltage

dependent I_{to} activation in fistula myocytes was not significantly different when compared with that in control myocytes at all three time intervals (Figure 4.6A-C). The voltage dependent I_{to} inactivation was also not significantly different between fistula and control myocytes (Figure 4.6D, E). Therefore the depressed I_{to} in fistula myocytes unlikely resulted from the altered kinetics of I_{to} .

Expression of Kv α subunits. To determine whether the depression of potassium currents was due to a change in Kv α subunit expression, Kv 4.3 and Kv4.2 expression were examined by western blot technique (Figure 4.7). The expression of Kv4.3 and Kv4.2 in ventricular myocyte lysates was significantly decreased in the fistula group when compared with age-matched control at 13-week. The expression of Kv4.3 was decreased by 17.6%, 24.8%, and 36.7% compared with control myocytes at 5-, 10-, and 13-week, respectively (Figure 4.7D). Similarly, the expression of Kv4.2 was decreased by 11.1%, 25.6%, and 33.4% at 5-, 10-, and 13-week, respectively (Figure 4.7E). These data indicate that the downregulation of K^+ currents is associated with a temporal change of K^+ channel protein expression following volume overload-induced ventricular remodeling. Furthermore, the surface expression of Kv4.2 and Kv4.3 was compared between fistula and control groups (Figure 4.8). The Kv4.3 expression on sarcolemma in fistula myocytes was significantly decreased by 43.0% and 30.1% compared with control myocytes at 10- and 13-week, respectively (Figure 4.8C). The Kv4.2 expression on sarcolemma in fistula myocytes was decreased by 28.7% and 42.8% at 10- and 13-week, respectively (Figure 4.8D). These observations indicated that the depressed I_{to} density may be attributed to the decrease of Kv4 α subunits expression on cell membrane.

mRNA of Kv α subunits. To determine if the depressed protein expression of Kv4 subunits in fistula myocytes was associated with reduced gene expression, mRNA levels of Kv4.2 and Kv4.3 in fistula were compared with age-matched control rat myocytes. mRNA expression of Kv4.2 and Kv4.3 in myocytes from 13-week fistula rats were 1.34 ± 0.39 and 1.43 ± 0.36 fold, compared with sham-operated myocytes, respectively (Figure 4.9).

DISCUSSION

In the present study, higher heart weight/body weight ratio and larger myocyte capacitances were observed in fistula ventricular myocytes compared with sham-operated control group, indicating ventricular remodeling and hypertrophy had occurred in the fistula group following volume overload. These observations are similar with findings from previous studies using fistula-induced volume overload (25, 193) and aortic constriction-induced pressure overload (194, 196). These findings demonstrate that ventricular remodeling is a common pathway leading to the development of heart failure despite the distinct etiological conditions. This also validates our animal model of heart failure used in this study.

In the present study, the action potential duration was significantly prolonged in fistula ventricular myocytes following volume overload. There was no change in the resting membrane potential and the amplitudes of action potentials in fistula myocytes when compared to the values in control group. These findings are consistent with reports from other animal models of heart failure (181, 182). In addition, depressed I_{to} density was observed and associated with the prolonged action potential duration following

volume overload. These data indicate a pathological alteration in electrophysiological properties following ventricular remodeling induced by chronic volume overload. These data are consistent to the findings of altered electrophysiological properties in ventricular myocytes from other animal models of heart failure (183, 194, 195). For example, in a ventricular tachypaced animal model, a decrease in I_{to} was a consistent finding (127). In pressure overload animal models, an increase (107), no change (24, 191) or a decrease (14, 183) of I_{to} density was reported, while action potential durations were prolonged in these animals. The discrepancy between our study and others is likely due to the different animal models that were used to induce heart failure, while the discrepancies between other studies, especially in the pressure overload studies, seem to be due to the differences in either methods inducing pressure overload, or the specific regions of ventricles from which the myocytes were isolated.

Downregulation of I_{to} is the most consistent ionic current change in heart failure (127, 182). Although downregulation of I_{to} is unlikely to produce large effects on APD in the ventricles of large mammals such as dog and human (181), I_{to} is a major factor for determining APD in murine cardiomyocytes (90, 100). A reduction in I_{to} alone is able to contribute to APD prolongation. Cerbai et al. (32) reported that I_{to} density in hypertrophied myocytes isolated from spontaneously hypertensive rats (SHR) was significantly reduced as compared with normal control myocytes. I_{CaL} density was not significantly modified in hypertrophied myocytes. Thus, prolongation of APD observed in SHR is mainly due to a reduction in I_{to} density. Barry et al. (13) reported that I_{to} was functionally eliminated in myocytes isolated from Kv4.2 knockout mice. The functional knockout of I_{to} also led to increased action potential duration in ventricular myocytes.

Based on our observations, we proposed that suppressed outward current I_{to} is a predominant alteration in electrical properties that contributes to the APD prolongation following volume overload. Thus our study was focused on the alteration of I_{to} and corresponding molecular mechanisms.

Alteration of K^+ currents may be due to changes in channel kinetics. However, this seems not to be true in our study. Both voltage dependent activation and inactivation of I_{to} were comparable in ventricular myocytes between control and fistula groups at three time intervals. These results are consistent with other reports using pressure overload animal models. Benitah et al. (14) reported a decrease in I_{to} density with normal activation and inactivation kinetics in myocytes isolated from hypertrophied rat hearts induced by abdominal aorta constriction. Similarly, Wang et al. (194) reported a decreased I_{to} density without changes in voltage dependent activation and inactivation in a pressure-overload mouse model induced by thoracic aortic constriction. In addition, there was no hypertrophy-induced change in voltage-dependent activation and inactivation of I_{to} . However, there was a slowed recovery from inactivation of I_{to} .

Duration of the cardiac action potential is controlled by a balance between depolarizing currents and repolarizing currents that are active during the plateau phase of the action potential. Prolonged action potential duration may be due to either enhanced inward depolarizing currents or suppressed outward repolarizing currents. Inward L-type Ca^{2+} current (I_{CaL}) plays an important role in the plateau phase of action potential, and thus alteration in I_{CaL} may contribute to the prolongation of action potential. In the present study, I_{CaL} densities were similar in myocytes between control and fistula groups. This finding excludes the possibility that altered I_{CaL} contributes to the APD prolongation

in volume overload-induced ventricular remodeling. Other studies have reported no change, increase or decrease in I_{CaL} density in different animal models of HF (127, 131, 182). This discrepancy may be attributed to the animal model, duration of ventricular remodeling, and the region of the heart used in different studies.

Although prolongation of the action potential duration and downregulation of K^+ channels are the prominent characteristics during ventricular remodeling, the molecular mechanisms underlying these alterations remain unclear, and may differ depending on the mechanism of induction of heart failure. Kv4 α subunits are considered the pore-forming subunits that underlie I_{to} in human and animal hearts (48, 91, 128, 129). Several studies have reported that I_{to} downregulation was associated with a depressed expression of Kv4 subunits and a reduced mRNA level of Kv4 in failing ventricles (5, 91, 209). Using a pacing tachycardia-induced rabbit model of heart failure, Rose et al. (163) reported that the protein expression and mRNA level of Kv4.2 were downregulated, whereas the protein expression of a long splice variant of Kv4.3 was downregulated with no change in mRNA level. A recent study by Marionneau et al. (116) showed that although $I_{to,f}$ and I_{K1} densities were decreased in myocytes from a mouse model of pressure overload-induced ventricular hypertrophy, the amplitudes of I_{to} and I_{K1} , as well as the mRNA transcript and protein expression of Kv α subunits corresponding to these currents were not changed. These authors claimed that the functional changes in these K^+ currents resulted from cellular enlargement due to ventricular hypertrophy. Results from our study demonstrated a significant reduction in I_{to} and I_K densities that are associated with reduced current amplitudes and increased cell capacitance in fistula myocytes. In addition, total protein expression and the surface expression of Kv4.3 and Kv4.2 in fistula

myocytes were significantly reduced. Not only I_{CaL} densities had no significant difference but also the Cav1.2 expression was comparable between control and fistula myocytes. Thus, our study suggested that reduced protein expression of Kv4, especially reduced numbers of functional channels in the sarcolemma, contributes to the depressed I_{to} density in ventricular myocytes following chronic volume overload. However, reduced protein expression of Kv4 α subunits was not a result of depressed transcript in these myocytes. Real time PCR results revealed slightly higher, but not significantly different, mRNA levels of Kv4.2 and Kv4.3 in fistula myocytes at 13-week when compared to the age-matched control myocytes. It is known that the regulation of membrane ion channels involves protein synthesis, trafficking and localization to the membrane, and degradation (171, 203, 204). Our results suggest that the suppressed protein level of Kv4.2 and Kv4.3 in fistula myocytes may be associated with posttranslational modification. Further experiments are required to elucidate the exact mechanisms underlying Kv4 α subunits downregulation during ventricular remodeling following volume overload.

Although Kv4.3 and Kv4.2 are pore-forming subunits underlying transient outward K^+ channel, their function and membrane expression are regulated by auxiliary subunits (129). KCHIP2 (K^+ channel interacting proteins) regulates the trafficking and distribution of Kv α subunits (88, 105). In a recent study, a decreased KCHIP2 was associated with a slowed recovery from inactivation of I_{to} and a decreased I_{to} in ventricular myocytes following pressure overload (194). Nevertheless, we failed to detect any significant difference in KCHIP2 protein level between fistula and control group (data not shown). Thus, a possible contribution of KCHIP2 to the reduced Kv4 expression in fistula myocytes can be excluded.

In summary, results from our present study demonstrate a prolonged APD that is associated with reduced I_{to} density and depressed protein expression of Kv4 α subunits in ventricular myocytes isolated from fistula rats. Depressed protein expression of Kv4 subunits in these myocytes was not correlated with the alteration of protein synthesis, but possibly resulted from altered channel protein trafficking or protein degradation during ventricular remodeling induced by chronic volume overload. This is the first study to evaluate the temporal and progressive alteration in the electrophysiological properties of ventricular myocytes following chronic volume overload.

Table 4.1. The resting membrane potential (Em) and the action potential amplitude in control and fistula group at 5-, 10-, and 13-week.

	Em (mV)	Amplitude (mV)	APD50 (ms)	APD90 (ms)
Control				
5-week (n=5)	-70.39 ± 1.42	90.41 ± 3.56	10.68 ± 1.09	37.08 ± 2.81
10-week (n=5)	-64.11 ± 1.89	104.76 ± 3.57	10.61 ± 1.21	37.7 ± 4.53
13-week (n=5)	-70.83 ± 1.05	104.96 ± 4.45	9.35 ± 0.81	38.81 ± 2.19
Fistula				
5-week (n=6)	-70.99 ± 0.68	100.33 ± 4.35	12.72 ± 1.06	46.38 ± 3.40
10-week (n=7)	-66.00 ± 1.35	106.21 ± 4.25	14.94 ± 0.62*	49.73 ± 3.76*
13-week (n=4)	-69.74 ± 1.42	108.80 ± 6.84	13.93 ± 1.55*	57.7 ± 6.04*

Data shown are mean ± SE for control (C) and fistula (F) rats. n: the number of rats. Em: resting membrane potential. Amplitude: the peak amplitude of action potential. APD50: time to 50% repolarization. APD90: time to 90% repolarization. Three to five myocytes from each animal were tested and data were averaged to represent that animal. * represents significant difference when compared with age-matched control group, $P < 0.05$.

Figure 4.1. General characteristics in control and aortocaval (AV) fistula rats at 5-, 10-, and 13-week after the AV fistula was induced. A: body weight. B: heart weight. C: heart weight-to-body weight ratio. D: ventricular myocyte capacitance. For myocyte capacitances, three to five myocytes were examined for each animal and data were averaged to represent that animal. Data are shown as mean \pm SE for control (n=8, 11, 5 at 5-, 10-, and 13-week, respectively) and fistula rats (n=13, 9, 5 at 5-, 10-, and 13-week, respectively) where n represents the number of animals in each group. * $P < 0.05$ compared with age-matched control group.

Figure 4.1.

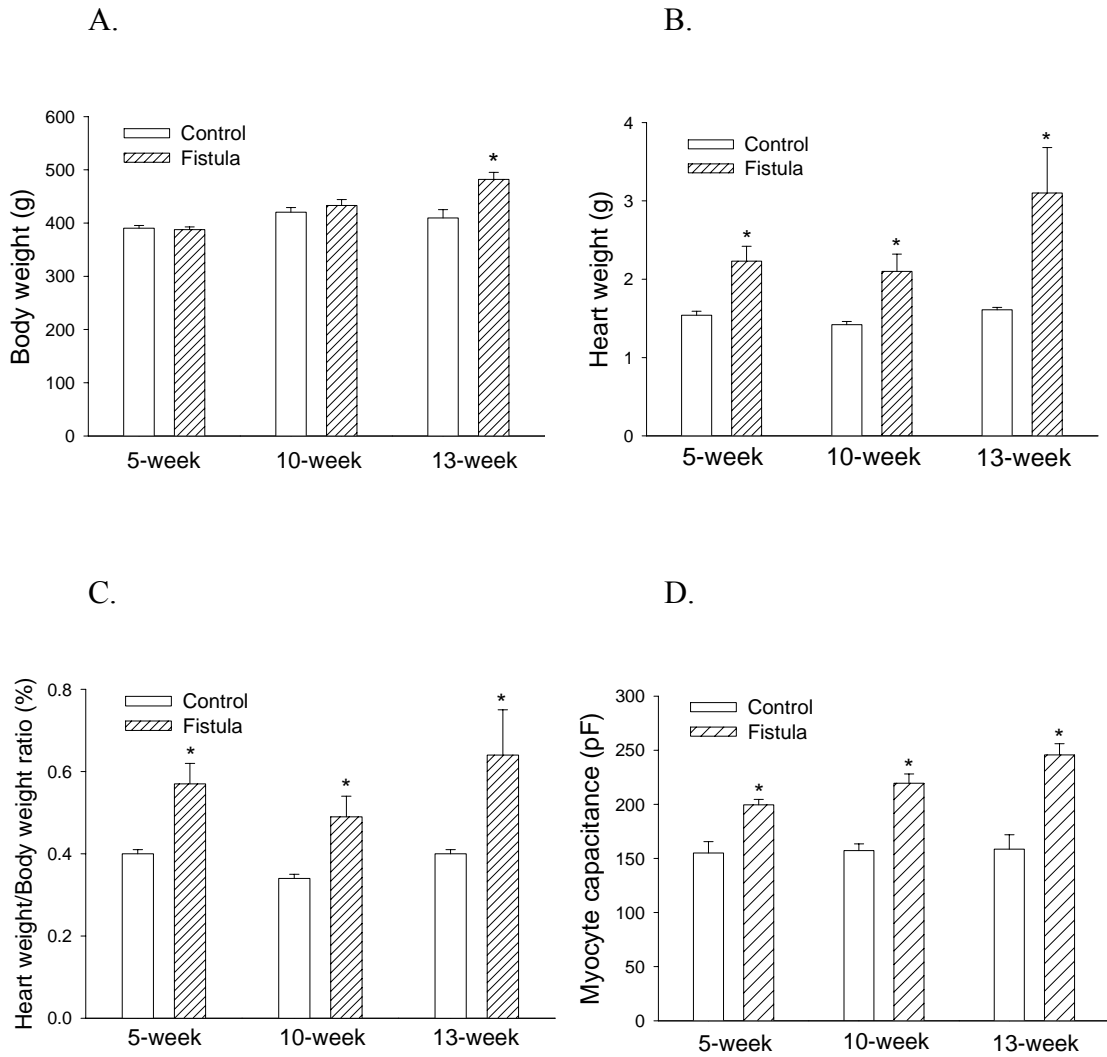


Figure 4.2. Membrane action potential (AP) in ventricular myocytes. A and B: representative AP traces recorded from a control and a fistula myocyte at 13-week after fistula.

Figure 4.2.

A.

B.

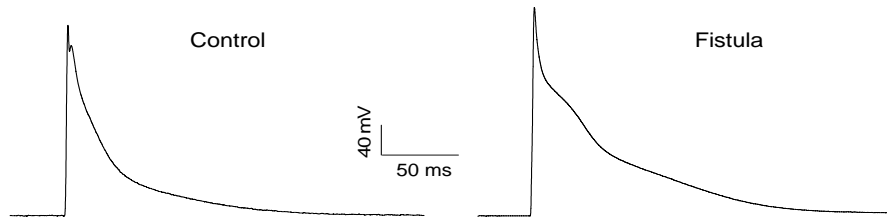
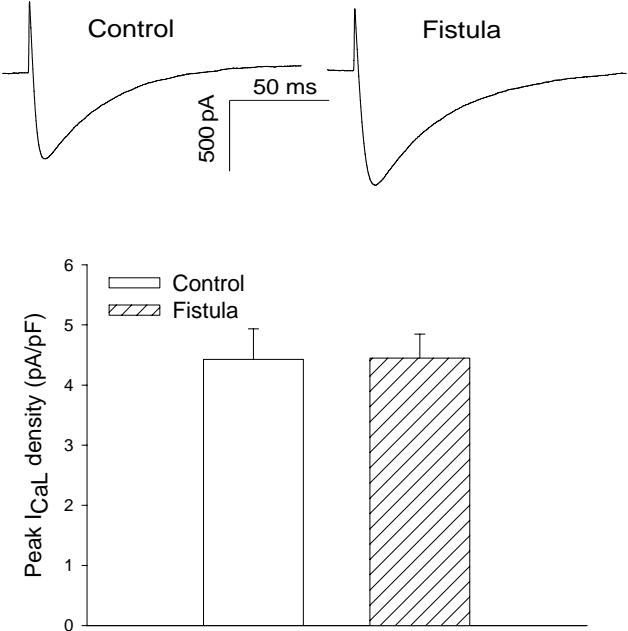


Figure 4.3. Calcium currents (I_{CaL}) and Cav1.2 expression in ventricular myocytes. A. Upper panel shows representative calcium currents recorded from control and fistula myocytes at 13-week after fistula. Lower panel shows peak I_{Ca} density of control and fistula groups at 13-week. Four myocytes were examined for each animal and values were averaged to represent that animal. Values are mean \pm SE for control (n=4) and fistula (n=7) where n represents the number of animals in each group. B. Upper panel shows representative western blots of Cav1.2 expression in lysates obtained from control and fistula myocytes at 13-week after fistula. Lower panel shows quantitative analysis of Cav1.2 expression in myocytes. Experiments were repeated three times. Proteins were separated by SDS-polyacrylamide gel electrophoresis and transferred to nitrocellulose membranes. The nitrocellulose membranes were then stained by Ponceau S. The images of both blots and Ponceau-stained membranes were subjected to densitometry. The optical density of the blot of interest was normalized to the optical density value of the Ponceau image of the line where the blot comes from. Data are presented as mean \pm SE.

Figure 4.3.

A.



B.

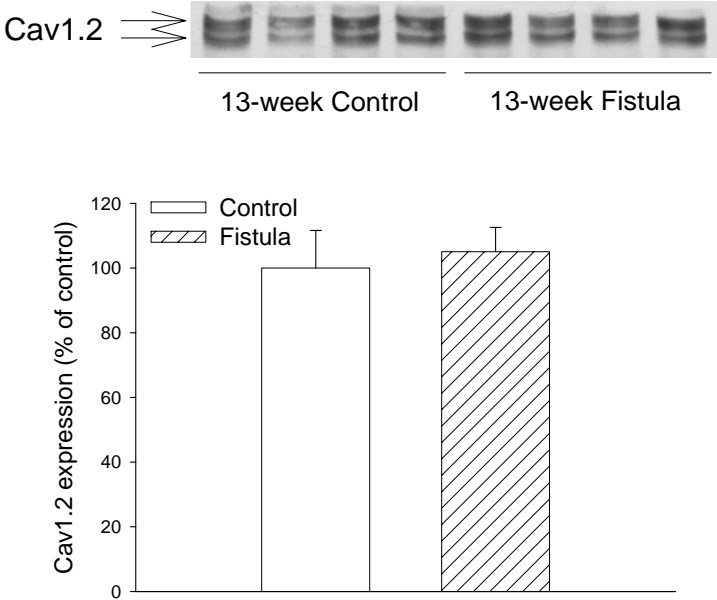
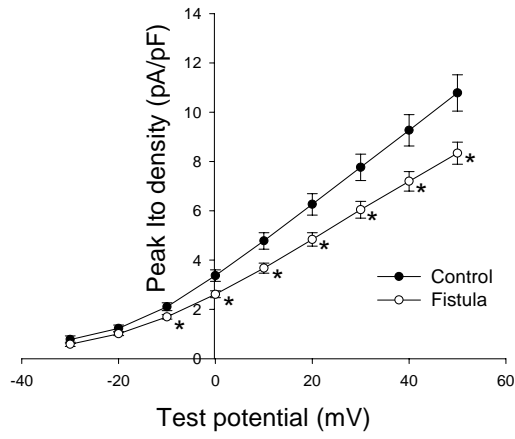


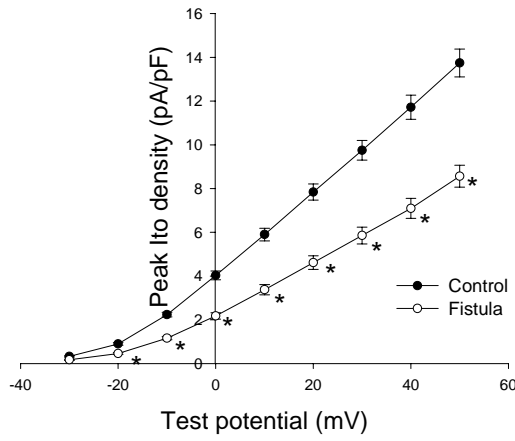
Figure 4.4. Transient outward K^+ currents (I_{to}) in ventricular myocytes. A, B, and C show the current density-voltage relations of I_{to} in myocytes recorded from control and fistula groups at 5-, 10-, and 13-week, respectively. Four to five myocytes were examined for each animal and values were averaged to represent that animal. Values shown are mean \pm SE for control (n=5, 6, 5 at 5-, 10-, and 13-week, respectively) and fistula rats (n= 6, 7, 5 at 5-, 10-, and 13-week, respectively) where n represents the number of animals in each group. * $P < 0.05$ compared with age-matched control group.

Figure 4.4.

A.



B.



C.

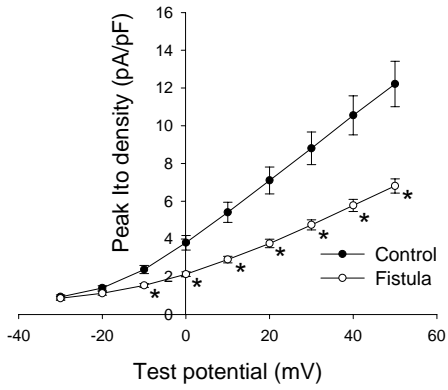
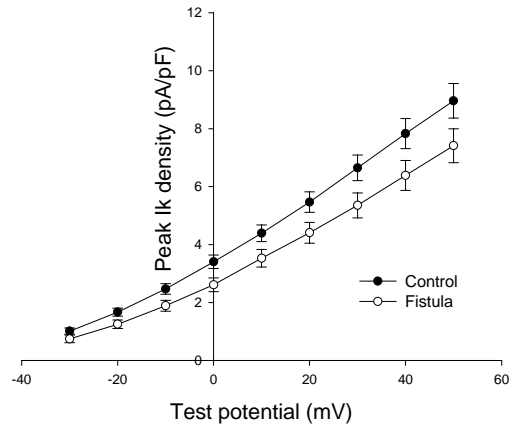


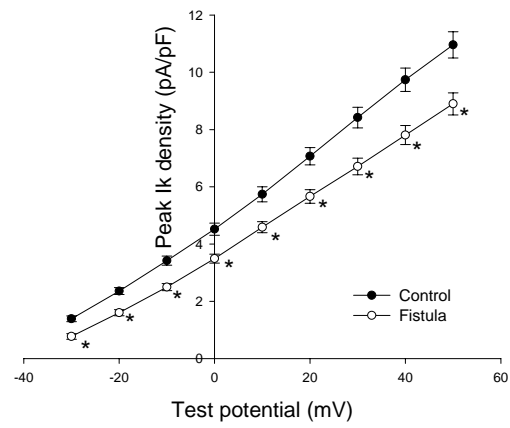
Figure 4.5. Delayed rectifier K^+ currents (I_K) in ventricular myocytes. A, B, and C show the current density-voltage relations of I_K in myocytes recorded from control and fistula groups at 5-, 10-, and 13-week, respectively. Four to five myocytes were examined for each animal and values were averaged to represent that animal. Values shown are mean \pm SE for control (n=5, 6, 5 at 5-, 10- and 13-week, respectively) and fistula rats (n= 6, 7, 5 at 5-, 10-, and 13-week, respectively) where n represents the number of animals in each group. * $P < 0.05$ compared with age-matched control group.

Figure 4.5.

A.



B.



C.

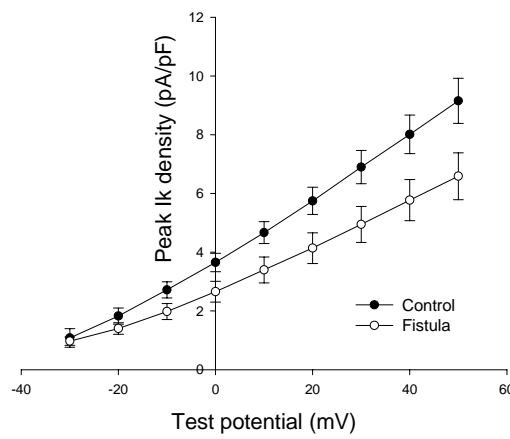


Figure 4.6. Voltage dependent I_{to} activation and inactivation. A, B, and C show the voltage dependent I_{to} activation in ventricular myocytes isolated from control and fistula rats at 5-, 10-, and 13-week, respectively. D and E show the voltage dependent I_{to} inactivation in ventricular myocytes isolated from control and fistula rats at 5- and 13-week. Inset shows the protocol for evaluation of I_{to} inactivation. Data are shown as mean \pm SE for control (n=5, 6, 5 at 5-, 10-, and 13-week, respectively) and fistula rats (n= 6, 7, 5 at 5-, 10-, and 13-week, respectively) where n represents the number of rats used.

Figure 4.6.

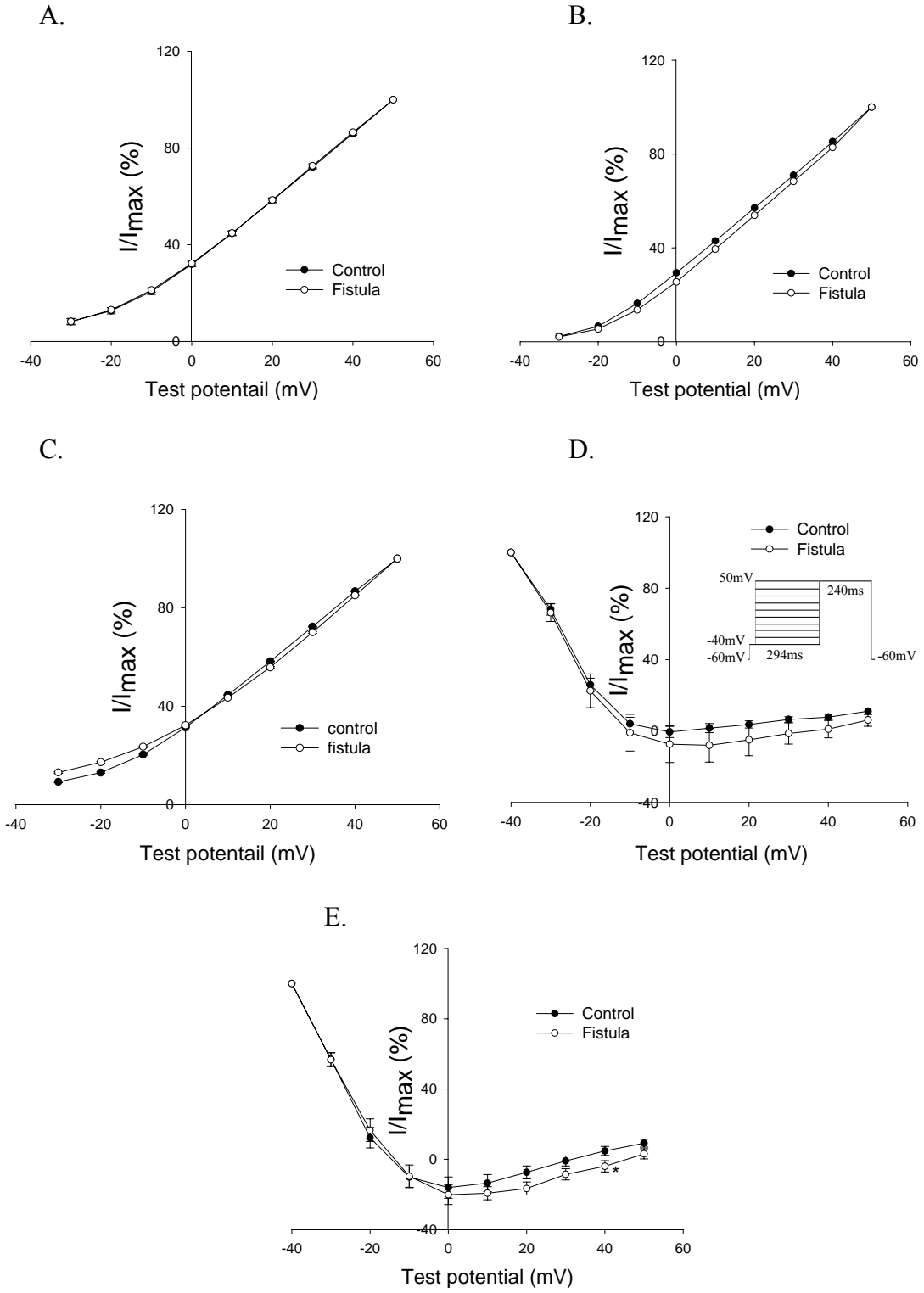


Figure 4.7. Protein expression of Kv4 α subunits of ventricular myocytes. A: representative blots of Kv4.3 and Kv4.2 at 5-week post-fistula. B: representative blots of Kv4.3 and Kv4.2 at 10-week post-fistula. C: representative blots of Kv4.3 and Kv4.2 at 13-week post-fistula. D and E are quantitative analysis for expression of Kv4.3 and Kv4.2 at different time interval, respectively. Experiments were repeated three times. Proteins were separated by SDS-polyacrylamide gel electrophoresis and transferred to nitrocellulose membranes. The nitrocellulose membranes were then stained by Ponceau S. The images of both blots and Ponceau-stained membranes were subjected to densitometry. The optical density of the blot of interest was normalized to the optical density value of the Ponceau image of the line where the blot comes from. Data are presented as mean \pm SE. * $P < 0.05$ compared with time matched control.

Figure 4.7.

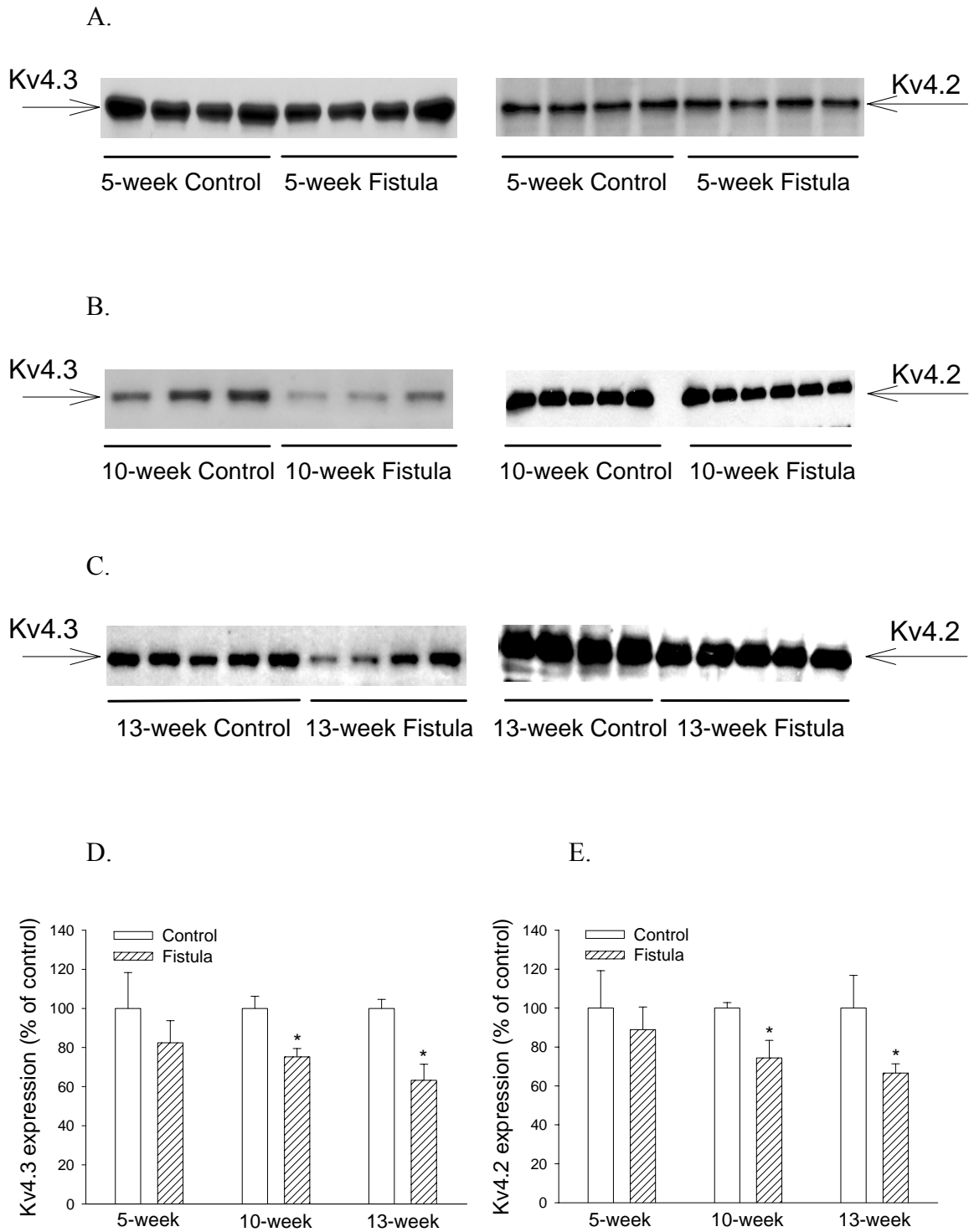


Figure 4.8. Protein expression of Kv4 α subunits in sarcolemma of ventricular myocytes. A: representative blots for expression of Kv4.3 and Kv4.2 on sarcolemma at 10-week after fistula. B: representative blots for expression of Kv4.3 and Kv4.2 on sarcolemma at 13-week after fistula. C: quantitative analysis of expression of Kv4.3 and Kv4.2 on sarcolemma at 10-week. D: quantitative analysis of expression of Kv4.3 and Kv4.2 on sarcolemma at 13-week. Experiments were repeated three times. Proteins were separated by SDS-polyacrylamide gel electrophoresis and transferred to nitrocellulose membranes. The nitrocellulose membranes were then stained by Ponceau S. The images of both blots and Ponceau-stained membranes were subjected to densitometry. The optical density of the blot of interest was normalized to the optical density value of the Ponceau image of the line where the blot comes from. Data are presented as mean \pm SE. * $P < 0.05$.

Figure 4.8.

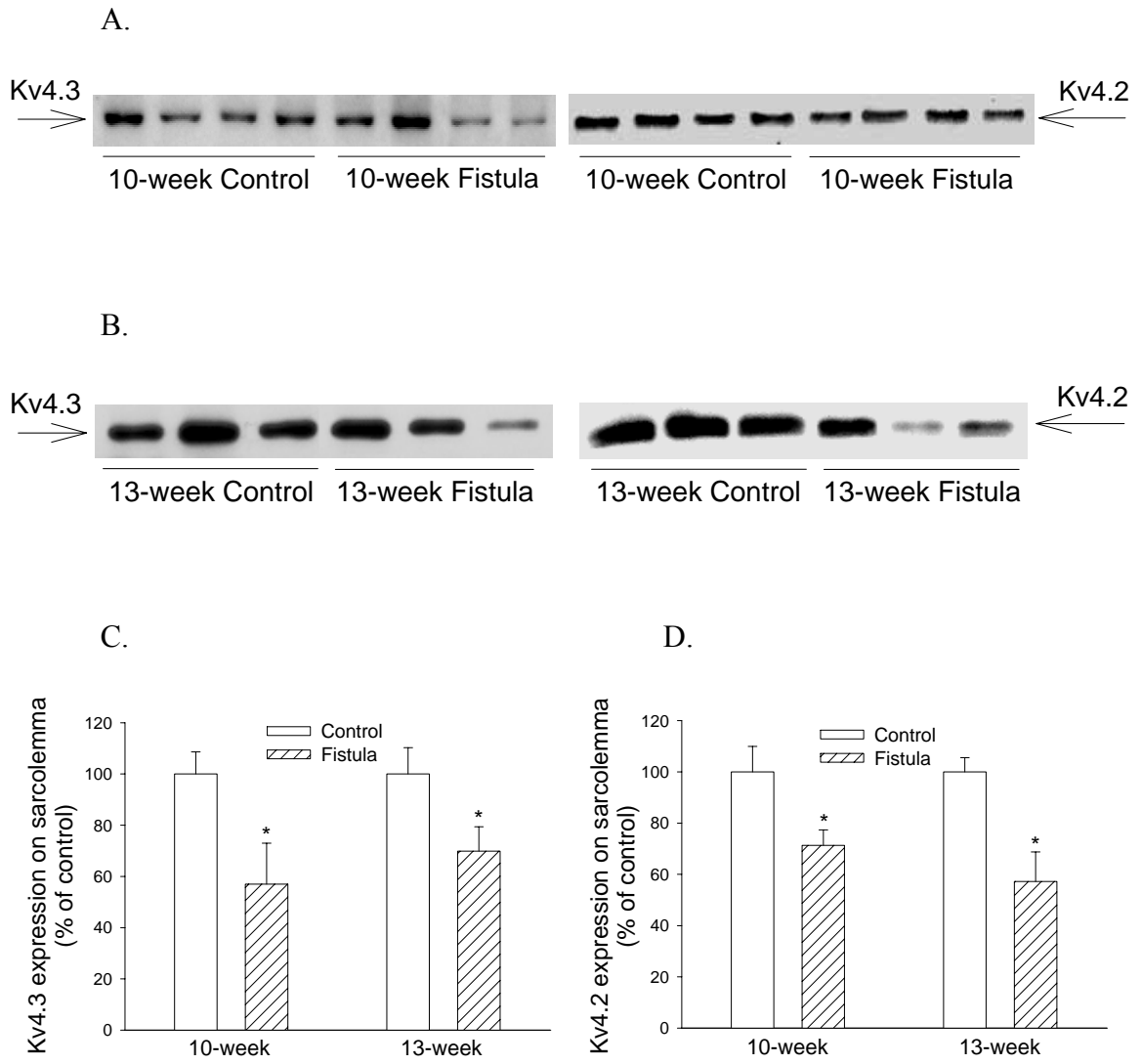
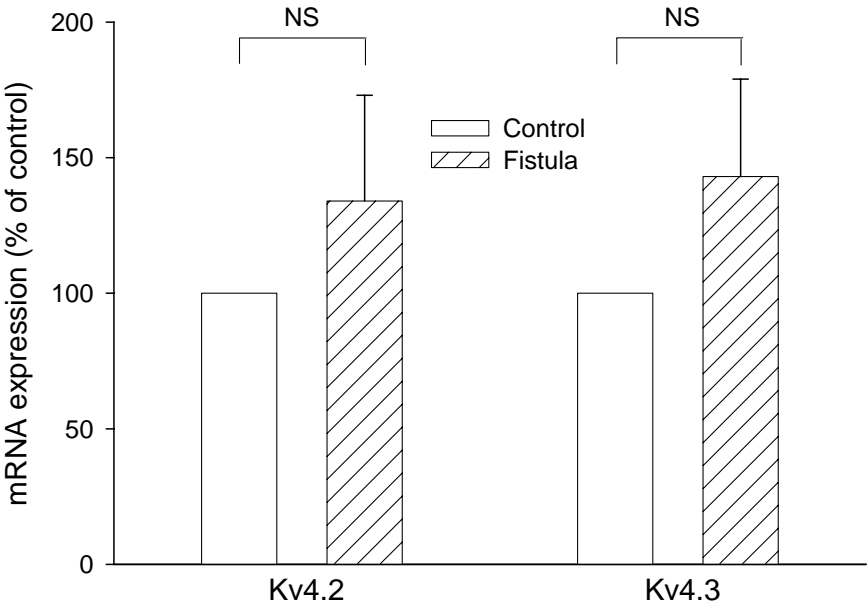


Figure 4.9. mRNA level of Kv4.2 and Kv4.3 in ventricular myocytes. The samples were normalized with the mRNA of three house keeping genes. Each real time PCR was performed three times in triplicate. There is no significant difference between control and fistula myocytes ($P>0.05$).

Figure 4.9.



**CHAPTER V. MEDIATION OF TRANSIENT OUTWARD POTASSIUM
CHANNEL BY PROTEASOME IN RAT VENTRICULAR MYOCYTES DURING
VOLUME OVERLOAD-INDUCED VENTRICULAR REMODELING**

ABSTRACT

Heart failure is a leading cause of death in America. Prolonged action potential duration (APD) and depressed transient outward potassium current (I_{to}) underlying APD prolongation are predominant features in failing ventricles. In our recent study, prolonged APD, decreased I_{to} density, and depressed potassium channel proteins were observed in ventricular myocytes following volume overload. However, molecular mechanisms underlying the depressed I_{to} remain unclear. We hypothesized that the depression of I_{to} is associated with elevated degradation of potassium channel proteins by the ubiquitin proteasome system (UPS). An infrarenal arteriovenous fistula rat model of volume overload was used. Ventricular myocytes were isolated at 13-week after fistula and treated with lysosomal inhibitor chloroquine (10 μ M) or proteasomal inhibitor MG-132 (2 μ M), respectively, for 24 hours. Myocytes cultured without inhibitor were served as sham control. Similar to our previous study, I_{to} densities in fistula myocytes were significantly decreased. MG-132 treatment, but not chloroquine, reversed the depression of I_{to} densities in fistula myocytes. Associated with the current data, protein expression of Kv4.2 and Kv4.3 that underlie I_{to} were significantly decreased, while the ubiquitinated Kv4 subunits were increased in fistula myocytes. Treatment of fistula myocytes with

MG-132 brought these values back to normal ranges. On the other hand, treatment of control myocytes with either MG-132 or chloroquine did not have effect on I_{to} and Kv4 expression. Our data suggest that elevated degradation of Kv4 α subunits by UPS is responsible for the depressed I_{to} density during ventricular remodeling induced by volume overload.

INTRODUCTION

Heart failure (HF) is a complex clinical syndrome, which cause more than 250,000 deaths annually in the US (161). Among the deaths of patients with HF, 50% were sudden and unexpected (182). Growing evidences suggested that cardiac arrhythmias play a pivotal role in sudden death, whereas the molecular mechanisms underlying lethal cardiac arrhythmias in HF patients are ambiguous.

Abnormal electrical properties have been reported in failing animal and human hearts (17, 18, 71). Prolongation of action potential duration (APD) is a hallmark of ventricular myocytes isolated from failing hearts independent of the etiology. In addition, downregulation of transient outward potassium current (I_{to}) is the most common change in currents prone to prolonged APD in various investigations. Our recent studies demonstrated APD prolongation and decreased I_{to} in rat ventricular myocytes following chronic volume overload. Parallel with decreased I_{to} , protein expression of Kv4.2 and 4.3 was reduced, whereas the mRNA levels of Kv4 α subunits were not altered, in myocytes from rat ventricles following volume overload. These data suggested an alteration in the posttranscriptional and/or posttranslational modification of the potassium channel proteins.

Functional retention of cellular proteins is balanced by protein synthesis and degradation. Most work has been focused on the abnormal protein synthesis of ion channels in failing hearts from patients and animal models (91, 92, 108, 208). On the other hand, abnormal protein degradation during ventricular remodeling has received less attention. In eukaryotic cells, protein degradation is processed by lysosome and proteasome (37, 158). The ubiquitin-proteasome system (UPS) have been demonstrated to play major roles in intracellular protein degradation and multiple basic cellular processes, including regulation of cell cycle, differentiation and development, the cellular response to extracellular effectors and stress (38). Recent studies also indicated an important role of UPS in the degradation of membrane receptors, transporters and ion channels (1, 121). Due to the miscellaneous functions of the UPS, it is not surprised to find the UPS aberration in different diseases, such as cancer and neurodegenerative diseases. Alteration of the UPS has also been observed in human cardiac diseases (119, 202). Recent studies reported an increased overall protein ubiquitination in hearts of patients with dilated cardiomyopathy (DCM) (197), an enhanced proteasome activity with elevated levels of polyubiquitinated proteins in human DCM tissues (20), an increased proteasome activity in ventricular tissue with an increase of cardiac mass in animal model of pressure overload (44), and accumulated ubiquitinated protein and depressed proteasome activity in patients with end-stage HF and mice model of pressure overload (184). However, the potential relationship between the UPS alteration and downregulation of potassium channels in HF remains to be elucidated.

In the present study, we examined the potential role of protein degradation in the downregulation of Kv4 α subunits following volume overload. Using a rat model of

volume overload induced by aortocaval (AV) fistula, we tested the hypothesis that the depressed potassium current is associated with elevated degradation of Kv4 proteins by the UPS.

MATERIALS AND METHODS

Animal model of heart failure. The animal model of heart failure was induced by aortocaval (AV) fistula using a previously described method (46). Briefly, rats were anesthetized with isoflurane inhalation and a ventral abdominal laparotomy was performed to expose the aorta and inferior vena cava. After the vessels were exposed, both vessels then were occluded proximal and distal to the intended puncture site. A fistula was created by inserting an 18-gauge needle into the exposed abdominal aorta and advanced through the medial wall into the vena cava. After the needle was withdrawn, the aortic puncture site was sealed with cyanoacrylate glue. Creation of a successful AV fistula was visualized by the pulsatile flow of oxygenated blood into the vena cava from the abdominal aorta. The abdominal musculature and skin incisions were closed by standard techniques with absorbable suture and autoclips. For control rats, sham operation was performed without creation of AV fistula. All the animal handling procedures were approved by the Institutional Animal Care and Use Committee of Auburn University.

Isolation of ventricular myocytes. At 13-week after the AV fistula surgery, ventricular myocytes were isolated described previously (46). Briefly, rats were anesthetized with sodium pentobarbital and killed by decapitation. Hearts were rapidly removed and hanged on a retrograde perfusion apparatus. The hearts were perfused with

oxygenated Ca^{2+} -free Tyrode's solution for 3-5 minutes. Tyrode's solution was composed of (in mM) 130 NaCl, 5.4 KCl, 1.2 MgSO_4 , 6 HEPES, 1.2 KH_2PO_4 , and 10 glucose (pH adjusted to 7.4 with NaOH). Then the heart was perfused by Type II collagenase (Worthington, NJ) in Ca^{2+} -free Tyrode's solution for 17-18 minutes. After perfusion, the ventricles were minced into small pieces in Kraftbrühe (KB) solution containing (in mM) 30 KCl, 70 L-Glutamic acid, 1 MgCl_2 , 10 HEPES, 10 KH_2PO_4 , 10 Taurine, 10 glucose, 2 EGTA, 10 DL- β -Hydroxybutyric acid (pH adjusted to 7.4 with KOH) and screened to collect individual myocytes. Isolated myocytes were centrifuged at low speed and resuspended in KB solution followed by the addition of increasing concentrations of Ca^{2+} until the final concentration of Ca^{2+} reaches 1 mM to yield Ca^{2+} -tolerant cardiomyocytes.

Cell culture and incubation with inhibitors. Freshly isolated myocytes was evenly divided into three Petri dishes. One was treated with the lysosomal inhibitor, chloroquine (10 μM , Sigma). Another was treated with the proteasomal inhibitor, N-benzyloxycarbonyl-leucyl-leucyl-leucinal (MG132, 2 μM , Sigma). The third one was served as vehicle treated control. All three Petri dishes were incubated at room temperature ($\sim 25^\circ\text{C}$) for 24 hours. After incubation, parts of the myocytes were used for the patch clamp experiments. The remaining was then frozen in liquid nitrogen for at least 10 minutes and then stored at -80°C for protein analysis.

Transient outward potassium current measurement. Transient outward potassium current was measured using whole-cell voltage-clamp technique. Patch pipettes were prepared from borosilicate glass (Sutter instrument, CA) with a pipette puller (PP-830, Narishige, Japan) and fire-polished with a micro forge (MF-830, Narishige, Japan).

Myocytes were perfused with bath solution (flow rate ~2 ml/minute) containing (in mM) 137 NaCl, 4 KCl, 1 MgCl₂, 0.5 CaCl₂, 10 HEPES, 50 Tetraethylammonium chloride (TEA-Cl), 2 CoCl₂·6H₂O, and 10 glucose (pH adjusted to 7.4 with NaOH). The pipette solution contains (in mM) 80 L-aspartic acid potassium salt, 50 KCl, 10 KH₂PO₄, 10 EGTA, 5 HEPES, 3 ATP-Mg, and 1.0 MgSO₄ (pH adjusted to 7.2 with KOH). After the whole-cell configuration was established, the cell membrane capacitance was measured and recorded. K⁺ currents were elicited and measured through an AXOPATCH 200B patch clamp amplifier (Axon Instruments, CA) and the data acquisition package pClamp 8 or 9 (Axon Instruments, CA). I_{to} was recorded in the presence of external TEA-Cl, which is used to block delayed rectifier potassium current (I_K). I_{Na} was eliminated by applying a 30-ms prepulse from holding potential to -40 mV. Current was elicited by test pulse between -30 and +50 mV applied in 10 mV increments at a frequency of 0.1 Hz. Currents were normalized to myocyte capacitance and expressed as current density (pA/pF). All experiments were performed at room temperature.

Western blot. Protein concentrations were determined by Bio-Rad protein assay. Equal amount of proteins of ventricular myocyte lysates prepared from fistula and sham rats were loaded onto the same gel to quantitatively compare expression of potassium channels. Protein lysates obtained from isolated ventricular myocytes were boiled in Laemmli buffer containing 5% β-Mercaptoethanol. Proteins were separated by 10% SDS polyacrylamide gels and electrophoretically transferred to nitrocellulose membranes (Bio-Rad, CA). The membranes were stained by Ponceau S dye to indicate the total amount of proteins loaded onto the gels. The membranes were then blocked in phosphated-buffered saline with Tween-20 (PBST) containing 5% nonfat dry milk for 1

hour at room temperature, and incubated with primary antibodies against ubiquitin, Kv4.3 (Santa Cruz, CA), and Kv4.2 (alomone, Israel), respectively, overnight at 4°C. Nitrocellulose membranes were washed in PBST and then incubated with horseradish peroxidase (HRP)-conjugated secondary antibodies against particular primary antibodies. After wash with PBST, enhanced chemiluminescence (ECL) was used to detect protein bands. Experiments were repeated three times and the optical densities of the specific bands were determined by UN-SCAN-IT Gel & Graph Digitizing Software (Silk Scientific Corporation, UT). All western blots were normalized with Ponceau S images of total proteins to demonstrate equal protein loading.

Immunoprecipitation. For immunoprecipitation, protein concentrations of whole cell lysates were determined via protein assay. Five hundred micrograms of total proteins were added into tubes with proper amounts of RIPA buffer with protease inhibitor to give samples final concentration of 500µg/100µl. The samples were incubated with the antibody against ubiquitin (10 µl, Santa Cruz, CA) on a rotating tube mixer for 3 hours at 4°C. The samples were then incubated with 20 µl of protein A/G-agarose beads on rotating tube mixer overnight at 4°C. Immunoprecipitates were collected by centrifugation at 550 x g for 30 seconds at 4°C. Supernatant were removed and discarded. Pellets were washed 3 times in lysis buffer. After final wash, pellets were resuspended in 2X Laemmli buffer with 5% β-Mercaptoethanol and boiled for 5 minutes. The immunoprecipitation samples were loaded on 10% polyacrylamide gel and transferred to nitrocellulose membranes. Membranes were blocked with 5% nonfat dry milk in PBST at room temperature. Following blocking, membranes were incubated with primary antibodies against Kv4.3 (Santa Cruz, CA) and Kv4.2 (alomone, Israel), respectively,

overnight at 4°C. Membranes were then incubated with Horseradish Peroxidase (HRP)-conjugated secondary antibodies (Santa Cruz, CA) against primary antibodies. After incubation with secondary antibody, membranes were washed with PBST and incubated with ECL to detect particular proteins. Experiments were performed three times and the bands of proteins of interest were analyzed using UN-SCAN-IT Gel & Graph Digitizing Software (Silk Scientific Corporation, UT).

Statistical analysis. Electrophysiological experiments were performed on at least 4 myocytes that were randomly chosen from each heart and data were averaged to represent that animal. Values of data were presented as mean \pm SE and n as the number of animals used. Data from different groups were compared using two-tailed unpaired Student's t-test and two way analysis of variation with a Student-Newman-Kuels post test whenever appropriate. Differences were considered statistically significant at $P < 0.05$.

RESULTS

Effects of inhibitors on I_{to} . To determine whether the alteration in the UPS influent the depression of Kv4 α subunits and parallel decreased transient outward potassium current (I_{to}) observed in our preliminary studies, we evaluated the effects of inhibitor treatment on the potassium current and the abundance of corresponding channel proteins. Myocytes were incubated with lysosomal inhibitor, chloroquine (10 μ M), or proteasomal inhibitor, MG-132 (2 μ M), respectively. The effect of inhibitor treatment on transient outward K⁺ current (I_{to}) was presented in Figure 5.1. Similar to our previous study, peak I_{to} densities in vehicle treated fistula myocytes were significantly reduced as compared with control group without inhibitor treatment (Figure 5.1A). Treatment of

fistula myocytes with MG-132, but not chloroquine, significantly increased the I_{to} densities in test potential range between 0 mV and +50 mV (Figure 5.1C). On the other hand, neither MG-132 nor chloroquine affected I_{to} densities in control myocytes (Figure 5.1B). As an index, the I_{to} density at 50 mV was compared between inhibitor treatment and vehicle treatment in both fistula and control myocytes (Figure 5.1D). The data revealed that the I_{to} density at 50 mV was significantly lower in vehicle treated fistula myocytes (9.8 ± 0.7 pA/pF) as compared with vehicle treated control myocytes (13.0 ± 1.0 pA/pF), whereas the I_{to} density at 50 mV was comparable between MG-132 treated fistula myocytes (13.2 ± 0.6 pA/pF) and MG-132 treated control myocytes (15.0 ± 0.7 pA/pF). In addition, there was no difference in I_{to} densities at 50 mV in control myocytes treated with or without MG-132. These observations indicate that MG-132 treatment is able to reverse the decreased I_{to} in fistula myocytes.

Presence of ubiquitinated Kv4 α subunits. To examine the possible alteration in degradation of potassium channel, the potassium channel protein ubiquitination was determined. In the present study, the expression of Kv4.3 and Kv4.2 in fistula ventricular myocytes was significantly decreased as compared with age-matched control at 13-week (Figure 5.2A). Expression of Kv4.3 and Kv4.2 was decreased by 27.4% and 37.7%, respectively (Figure 5.2C). These data are similar to our previous data. On the other hand, ubiquitinated Kv4.2 and Kv4.3 were increased by 93.7% and 71.4%, respectively, in fistula myocyte as compared with age-matched control counterpart at 13-week (Figure 5.2 B and D). These data indicate that modulation of channel protein expression by ubiquitin pathway was altered in fistula ventricular myocytes following volume overload and that the decreased expression of Kv4.2 and Kv4.3 in fistula ventricular myocytes

may be associated with the elevated degradation of Kv4 α subunits during ventricular remodeling induced by chronic volume overload.

Effects of inhibitors on the expression of Kv4 α subunits. To examine the molecular basis of the effect of proteasome inhibition on potassium current, the protein expression of Kv4 α subunits was evaluated (Figure 5.3). The protein level of Kv4.3 was significantly lower in vehicle treated fistula (76.3%) myocytes as compared with vehicle treated control myocytes. In control myocytes, the expression of Kv4.3 was not significantly changed by chloroquine treatment (115.6% vs. vehicle treatment) or MG-132 treatment (107.0% vs. vehicle treatment). The protein level of Kv4.3 in chloroquine treated fistula myocytes (87.5%) was significantly lower when compared with chloroquine treated control myocytes (115.6%). However, the expression of Kv4.3 was significantly increased in MG-132 treated fistula myocytes. The expression of Kv4.3 in MG-132 treated fistula myocytes (96.6%) was not significantly different from that in MG-132 treated control myocytes (107.0%). Similarly, the expression of Kv4.2 was depressed in vehicle treated fistula myocytes compared with vehicle treated control myocytes, whereas the expression of Kv4.2 was comparable between MG-132 treated, but not chloroquine treated, fistula myocytes and control counterparts. These observations were parallel with the effects of inhibitors on I_{to} , suggesting that the I_{to} recovery by proteasome inhibition may be secondary to the elevated expression of Kv4 α subunits in fistula myocytes by MG-132 treatment.

Ubiquitinated proteins in fistula ventricular myocytes. To determine the role of ubiquitin-proteasome system in the volume overload-induced ventricular remodeling, the protein ubiquitination in ventricular myocytes was examined using western blot. We

found that the ubiquitinated proteins in fistula ventricular myocyte were 139.7% of those in control counterpart at 13-week after fistula (Figure 5.4A), indicating an increased ubiquitination in fistula myocytes isolated from hearts following volume overload. Figure 5.4B shows the abundance of ubiquitinated proteins after inhibitor treatment. Abundance of ubiquitinated proteins was significantly higher in vehicle treated fistula ventricular myocyte as compared with control counterpart. Treatment of MG-132 significantly increased the ubiquitinated protein level in both fistula (127.9% vs. vehicle treated myocytes) and control (126.8% vs. vehicle treated myocytes) ventricular myocytes (Figure 5.4B). The level of ubiquitinated proteins were comparable in vehicle and chloroquine treated myocytes in both control and fistula group.

DISCUSSION

Prolongation of action potential duration (APD) and downregulation of potassium currents are the common features observed in the pathological ventricular remodeling. However, the molecular mechanisms responsible for these pathological alterations remain unclear. The present study evaluated the potential contribution of elevated protein degradation to the downregulation of K^+ channels induced by volume overload. The major findings of this study include that, 1) protein expression of Kv4 α subunits was decreased, whereas the ubiquitinated Kv4 α subunits were elevated in ventricular myocytes following volume overload; 2) treatment of myocytes with the proteasome inhibitor, MG-132, successfully reversed the downregulated K^+ currents; and 3) MG-132 treatment restored the protein expression of Kv4 α subunits. Taking together, these data

suggest that enhanced degradation of Kv4 channel proteins play an important role in the down regulation of K⁺ channel following volume overload.

The ubiquitin-proteasome system (UPS) plays a major role in intracellular protein degradation (38, 63, 77). Degradation of a protein via the UPS involves two successive steps: enzymes catalyzed ubiquitination and proteasome dependent degradation. In addition, various membrane proteins, including membrane transporters, receptors and ion channels, have been reported to undergo ubiquitin-mediated internalization and degradation (1, 121). Alteration in UPS has recently observed in patients with heart disease (35, 74, 109, 153, 197). Patients with dilated cardiomyopathy (DCM) tissue contained elevated levels of polyubiquitinated proteins and possessed enhanced 20S-proteasome chymotrypsin-like activities (20). In addition, elevated levels of E1 ubiquitin-activating enzymes and unchanged deubiquitinating enzyme activities were observed in DCM, suggesting that the accumulation of ubiquitinated proteins is likely due to high rates of ubiquitination (20). Previous studies from our laboratory indicated a reduced protein expression of Kv4 α subunits without any depression of Kv4 at mRNA level in ventricular myocytes from the 13-week fistula rats. In the present study, we observed that depressed protein expression of Kv4 was associated with an increased ubiquitination of these channel subunits. These data suggest that the reduced protein level of Kv4 α subunits was not resulted from the protein synthesis, but resulted from the altered protein trafficking and/or degradation by the UPS in ventricular myocytes following volume overload.

The involvement of ubiquitin in the internalization and degradation of plasma membrane proteins has been reviewed (22, 121, 170). During this process, multiple

ubiquitin molecules are covalently attached to the protein substrate. The ubiquitination is catalyzed by three types of enzyme(s). The ubiquitin-activating enzyme (E1), the ubiquitin-conjugating enzymes (E2s) and the ubiquitin ligases (E3s) activate ubiquitin molecules and catalyze the formation of an isopeptide bond between the ubiquitin and the target protein. There are one E1 enzyme, hundreds of E2 enzymes and thousands of E3 enzymes. E3s are believed to be responsible for the specificity of ubiquitination of substrate proteins. Staub et al. (169) reported that the stability of epithelial sodium channel (ENaC) at the plasma membrane is regulated by ubiquitination. Chapman et al. (34) reported that the surface expression of HERG potassium channel is strictly regulated by ubiquitination. In most cases, ubiquitination of plasma membrane proteins is followed by lysosomal/vacuolar degradation. In addition, ubiquitinated membrane proteins can also be degraded by the proteasome. Kv1.5 has been demonstrated to be degraded by the proteasome in heterogenous expression system and cultured rat atrial myocytes. In COS cells, Kv1.5 half-life time was prolonged by the proteasome inhibitors, but not by a lysosomal inhibitor chloroquine. MG-132 increased the protein level of both Kv1.5 and its ubiquitinated form. In cultured rat atria cells, MG-132 increased endogenous Kv1.5. Furthermore, MG-132 also increased I_{Kur} currents through the cell-surface Kv1.5 (96). Similarly, inhibition of proteasome activity by MG132 and other proteasome inhibitors not only prolonged half-life time of Kir6.2 in COS cells, but also augmented K_{ATP} currents in both COS cells expressing SUR2A and Kir6.2 and neonatal rat cardiomyocytes (179). In the present study, MG-132 treatment, but not chloroquine treatment, restored the protein expression of Kv4 α subunits as well as the I_{to} density in fistula myocytes. Consistently, MG-132 treatment elevated the total ubiquitinated protein

level in these cells. These observations suggested an elevated protein degradation of Kv4 and other unknown cellular proteins by the UPS during ventricular remodeling following chronic volume overload. Elevated protein degradation of Kv4 α subunits is responsible for the reduced I_{to} and prolonged APD in fistula myocytes.

The enhanced degradation of specific proteins could be caused by elevated UPS proteolytic activity, or more likely by an increased E3-ubiquitin ligases in the case that only a selected group of proteins is degraded. E3 ligases select target proteins for ubiquitination, which leads membrane protein internalization and subsequent degradation. Depre et al. (44) reported an increased gene, protein expression and activity of proteasome subunits during left ventricular hypertrophy induced by pressure overload. On the other hand, Kobayashi et al. (101) reported that the transcription factor GATA4 was reduced in cardiac myocytes by high glucose. The reduced GATA4 protein level was associated with an upregulation of an E3 ligase and unchanged proteasome activity. In the present study, we observed a reduced protein level of Kv4 α subunits and an increased level of ubiquitinated Kv4 in fistula myocytes. Treatment of cells with the proteasome inhibitor restored the protein expression of Kv4 in myocytes from fistula rats. However, our study did not distinguish the potential contribution of E3 and/or proteasome activity in the elevated degradation of K channel proteins during ventricular remodeling. Further experiments are deserved to evaluate these process.

E3s, the ubiquitin-protein ligases, recognize their specific substrates and direct the ubiquitination process. E3s have specificity for protein substrates that are ubiquitinated. Several E3s have been reported to be specific to different cellular proteins. Nedd4-2 has been demonstrated to be an E3 ligase to recognize the epithelial sodium channel (169,

200). KCNQ1 potassium channel, which have a PY motif, has also been reported to be modulated for ubiquitination by Nedd4-2 (87). However, the specific E3 enzyme that targets Kv4 α subunits in cardiac myocytes has not been identified yet. On the other hand, phosphorylation of a specific protein may play an important role in the ubiquitination of the target proteins (19, 41). In the present study, several questions remain to be addressed, such as what the E3 enzyme is for the Kv4 α subunits, whether phosphorylation or other posttranslational modification contribute to the Kv4 α subunits ubiquitination, as well as if there is any change in level of enzymes in the UPS, for instance, E1, E2s, deubiquitinating enzymes. Further experiments are required to determine the trigger events leading to the ubiquitination of Kv4 α subunits in fistula myocytes during volume overload-induced ventricular remodeling.

Figure 5.1. Transient outward K^+ current (I_{to}) density in ventricular myocytes treated with chloroquine and MG-132, respectively, at 13-week post-fistula. A shows the mean current density-voltage relationship of I_{to} in myocytes recorded from vehicle treated control and fistula group. B and C show the mean current density-voltage relationship of I_{to} in myocytes recorded from control and fistula group, respectively. Three to five myocytes were examined for each animal and data were averaged to represent that animal. Data are mean \pm SE for control (n=5, 5, 5 for vehicle, chloroquine, and MG-132, respectively) and fistula rats (n= 6, 6, 5 for vehicle, chloroquine, and MG-132, respectively) where n represents the number of animals in each group. * $P < 0.05$ compared with vehicle values. D represents I_{to} density at 50 mV recorded from myocytes treated with chloroquine and MG-132, respectively. * $P < 0.05$. NS represents no significant difference.

Figure 5.1.

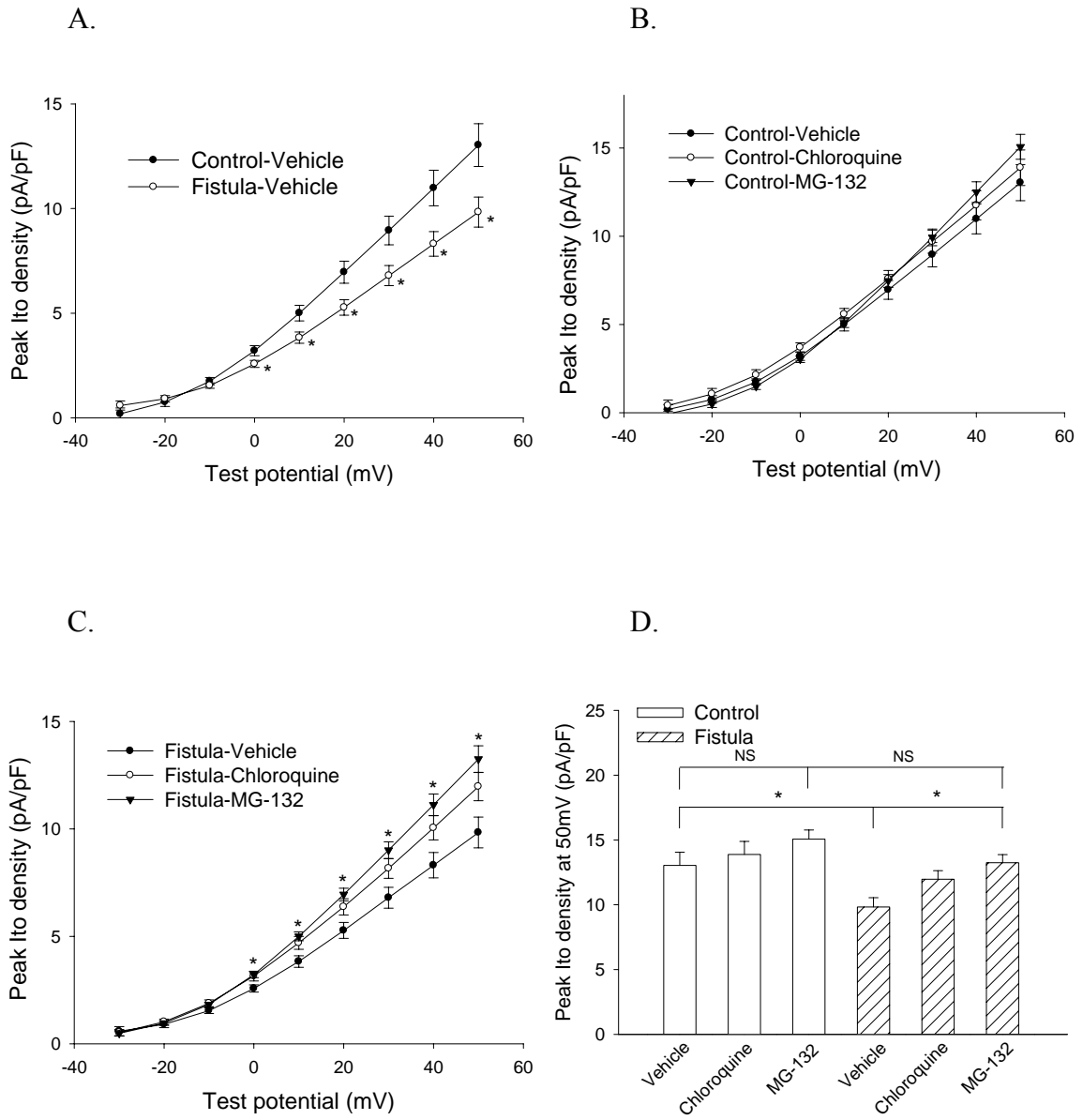


Figure 5.2. Ubiquitinated Kv4 α subunits in ventricular myocytes at 13-week post-fistula. A: representative blots of Kv4.3 and Kv4.2 at 13-week post-fistula. B: representative blots of immunoprecipitation for ubiquitinated Kv4 α subunits in myocytes obtained from control and fistula group at 13-week. C: quantitative analysis for Kv4.3 and Kv4.2 in ventricular myocytes. D: quantitative analysis for ubiquitinated Kv4.3 and Kv4.2 in ventricular myocytes. Experiments were repeated three times. Data are presented as mean \pm SE. * $P < 0.05$ compared with control values.

Figure 5.2.

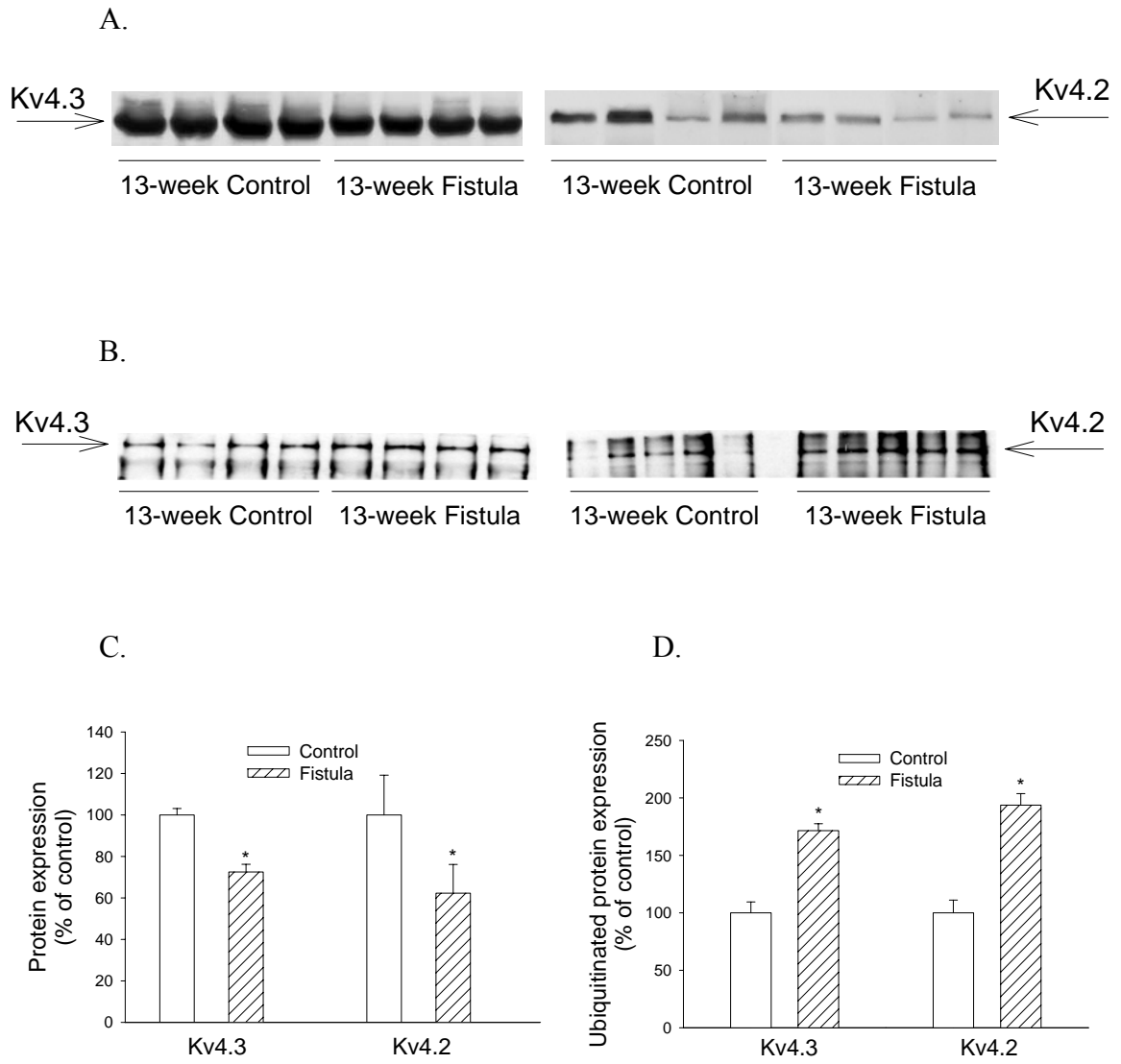


Figure 5.3. Expression of Kv4 α subunits in lysates from myocytes with treatment of inhibitors at 13-week after fistula. A shows representative blots of Kv4.3 expression in lysates obtained from control (C) and fistula (F) myocytes treated with chloroquine or MG-132, respectively. B shows representative blots of Kv4.2 expression in lysates obtained from control (C) and fistula (F) myocytes treated with chloroquine or MG-132, respectively. C shows quantitative analysis of Kv4.3 expression in myocyte lysates obtained from control and fistula group. D shows quantitative analysis of Kv4.2 expression in myocyte lysates obtained from control and fistula group. Experiments were repeated three times. Proteins were separated by SDS-polyacrylamide gel electrophoresis and transferred to nitrocellulose membranes. The membranes were then stained by Ponceau S. The images of both blots and Ponceau-stained membranes were subjected to densitometry. The optical density of the blot of interest was normalized to the optical density value of the Ponceau image of the line where the blot comes from. Data are mean \pm SE. * $P < 0.05$ compared with control values.

Figure 5.3.

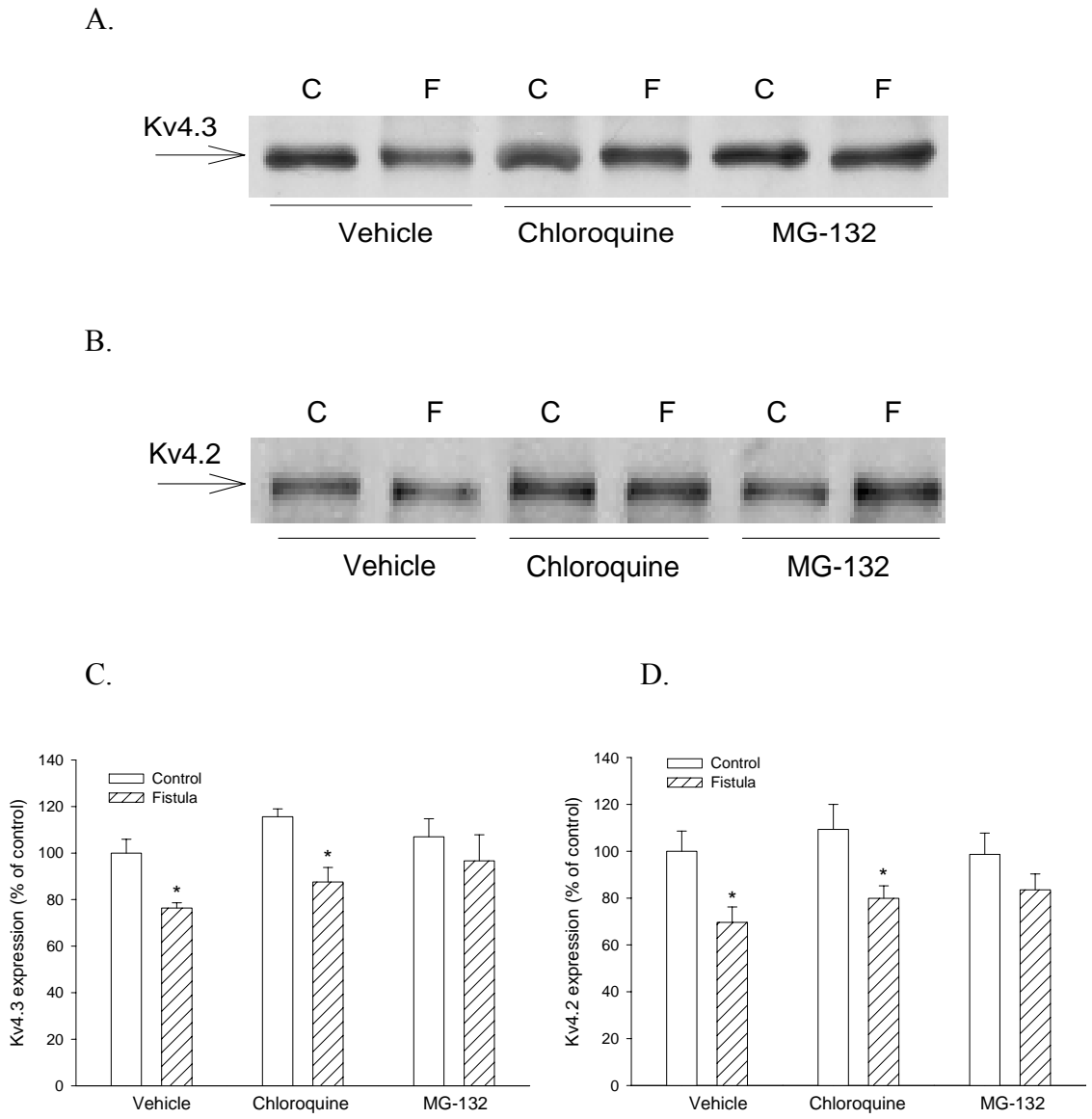
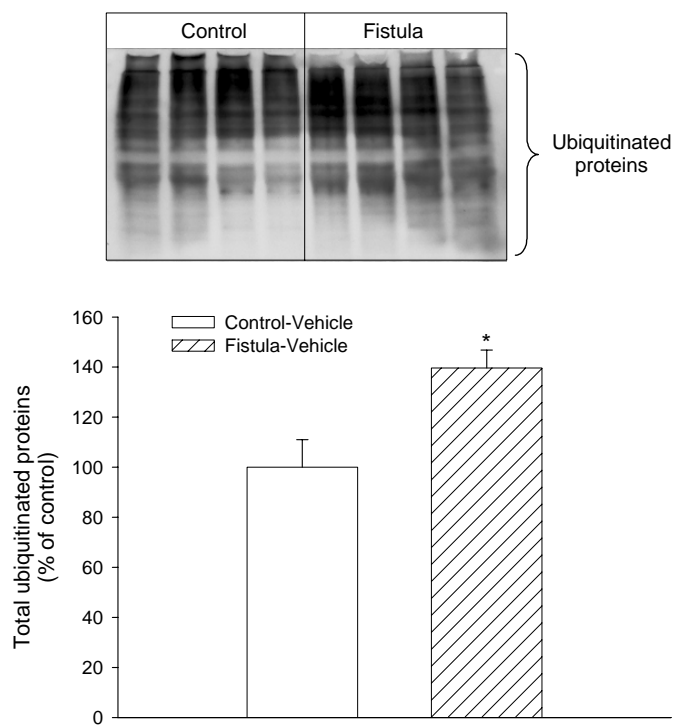


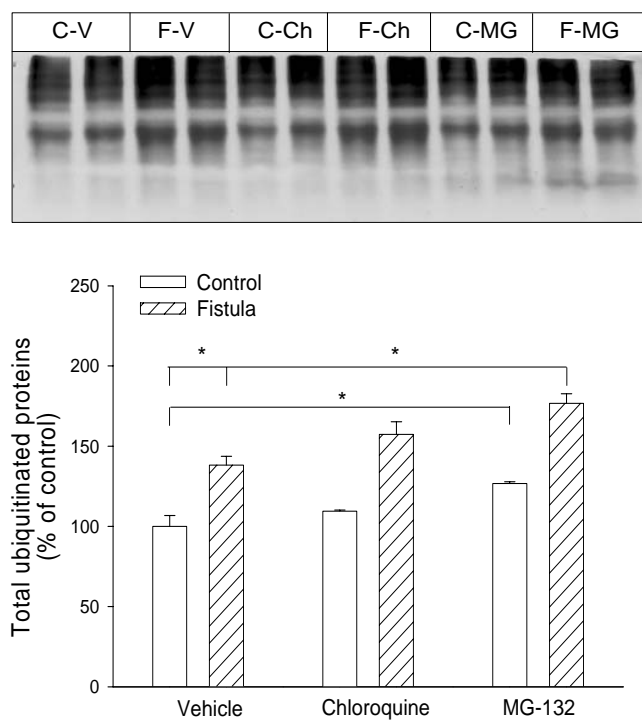
Figure 5.4. Accumulation of ubiquitinated proteins in protein lysates of ventricular myocytes. A. Upper panel shows the representative western blots of ubiquitinated proteins in lysates of myocytes isolated from control and fistula rat hearts at 13-week post-fistula. Lower panel presents quantitative comparison of ubiquitinated proteins between control and fistula myocytes. B. Effect of lysosomal inhibitor and proteasomal inhibitor on ubiquitinated proteins in control (C) and fistula (F) ventricular myocytes at 13-week post-fistula. Upper panel shows representative blots. Lower panel shows quantitative analysis. “V” indicated vehicle treated with no any inhibitor, “Ch” indicated incubation with 10 μ M Chloroquine, “MG” indicated incubation with 2 μ M MG-132. Experiments were repeated three times. Proteins were separated by SDS-polyacrylamide gel electrophoresis and transferred to nitrocellulose membranes. The membranes were then stained by Ponceau S. The images of both blots and corresponding Ponceau-stained membranes were subjected to densitometry. The optical density of the blot of interest was normalized to the optical density value of the Ponceau image of the line where the blot comes from. Data are presented as mean \pm SE for control (n=5) and fistula (n=5) rats where n is the number of rats used in each group. * $P < 0.05$ compared with control values.

Figure 5.4.

A.



B.



CHAPTER VI. SUMMARY

In the present study, we assessed the alterations of electrophysiological properties and underlying molecular mechanisms in the rat model of volume overload induced by aortocaval (AV) fistula. During volume overload induced ventricular remodeling, action potential duration (APD) was prolonged with decreased transient outward potassium current (I_{to}). L-type calcium current density was not changed in fistula myocytes compared with age-matched control group. Thus, the prolonged APD was mainly attributed to the decreased I_{to} . Voltage-dependent activation and inactivation had no difference between fistula and control group. The surface expression of Kv4 α subunits encoding I_{to} , Kv4.2 and Kv4.3, were depressed in fistula myocytes as compared with control group. Thus, the decrease of I_{to} may be resulted from the decreased number of potassium channels expressed on cell membrane. The mRNA level of Kv4 α subunits was comparable between fistula and control group. Therefore, the depression of Kv4 α subunits in fistula myocytes was unlikely due to the protein synthesis. The abundance of ubiquitinated proteins was higher in fistula myocytes as compared with control group. The expression of ubiquitinated Kv4 α subunits was also increased in fistula myocytes, suggesting the elevated degradation of potassium channel. The treatment of proteasome inhibitor, but not lysosome inhibitor, recovered the depressed I_{to} densities and increased the expression of Kv4 α subunits in fistula myocytes. In addition, neither proteasome inhibitor treatment nor lysosome inhibitor treatment affected potassium channel

expression and I_{to} density in control myocytes. These data suggest that elevated degradation of potassium channel is responsible for the depression of I_{to} and subsequent APD prolongation in rat ventricular myocytes following volume overload.

REFERENCES

1. **Abriel H and Staub O.** Ubiquitylation of ion channels. *Physiology* 20: 398-407, 2005.
2. **Adams J.** The proteasome: structure, function, and role in the cell. *Cancer Treat Rev* 29: 3-9, 2003.
3. **Adams V, Linke A, Wisloff U, Doring C, Erbs S, Krankel N, Witt CC, Labeit S, Muller-Werdan U, Schuler G and Hambrecht R.** Myocardial expression of Murf-1 and MAFbx after induction of chronic heart failure: effect on myocardial contractility. *Cardiovasc Res* 73: 120-129, 2007.
4. **Ahmed GU, Dong PH, Song G, Ball NA, Xu Y, Walsh RA and Chiamvimonvat N.** Changes in Ca^{2+} cycling proteins underlie cardiac action potential prolongation in a pressure-overloaded guinea pig model with cardiac hypertrophy and failure. *Circ Res* 86: 558-570, 2000.
5. **Akar FG, Wu RC, Juang GJ, Tian Y, Burysek M, DiSilvestre D, Xiong W, Armoundas AA and Tomaselli GF.** Molecular mechanisms underlying K^+ current downregulation in canine tachycardia-induced heart failure. *Am J Physiol Heart Circ Physiol* 288: H2887-H2896, 2005.
6. **An WF, Bowlby MR, Betty M, Cao J, Ling HP, Mendoza G, Hinson JW, Mattsson KI, Strassle BW, Trimmer JS and Rhodes KJ.** Modulation of A-type potassium channels by a family of calcium sensors. *Nature* 403: 553-556, 2000.
7. **Apkon M and Nerbonne JM.** Characterization of two distinct depolarization-activated K^+ currents in isolated adult rat ventricular myocytes. *J Gen Physiol* 97: 973-1011, 1991.
8. **Aronson RS.** Characteristics of action potentials of hypertrophied myocardium from rats with renal hypertension. *Circ Res* 47: 443-453, 1980.

9. **Aronson RS and Ming Z.** Adaptive and maladaptive processes: cellular mechanisms of arrhythmias in hypertrophied and failing myocardium. *Circulation* 87: VII76-VII83, 1993.
10. **Assayag P, Carre F, Chevalier B, Delcayre C, Mansier P and Swynghedauw B.** Compensated cardiac hypertrophy: arrhythmogenicity and the new myocardial phenotype. I. Fibrosis. *Cardiovasc Res* 34: 439-444, 1997.
11. **Barr CS and Naas A.** QT dispersion and sudden unexpected death in chronic heart failure. *Lancet* 343: 327, 1994.
12. **Barry DM, Trimmer JS, Merlie JP and Nerbonne JM.** Differential expression of voltage-gated K⁺ channel subunits in adult rat heart: relation to functional K⁺ channels? *Circ Res* 77: 361-369, 1995.
13. **Barry DM, Xu H, Schuessler RB and Nerbonne JM.** Functional knockout of the transient outward current, long-QT syndrome, and cardiac remodeling in mice expressing a dominant-negative Kv4 α subunit. *Circ Res* 83: 560-567, 1998.
14. **Benitah JP, Gomez AM, Bailly P, Da Ponte JP, Berson G, Delgado C and Lorente P.** Heterogeneity of the early outward current in ventricular cells isolated from normal and hypertrophied rat hearts. *J Physiol (Lond)* 469: 111-138, 1993.
15. **Berger RD, Kasper EK, Baughman KL, Marban E, Calkins H and Tomaselli GF.** Beat-to-beat QT interval variability: novel evidence for repolarization lability in ischemic and nonischemic dilated cardiomyopathy. *Circulation* 96: 1557-1565, 1997.
16. **Berry JM, Naseem RH, Rothermel BA and Hill JA.** Models of cardiac hypertrophy and transition to heart failure. *Drug Discov Today Dis Models* 4: 197-206, 2007.
17. **Beuckelmann DJ, Nabauer M and Erdmann E.** Alterations of K⁺ currents in isolated human ventricular myocytes from patients with terminal heart failure. *Circ Res* 73: 379-385, 1993.
18. **Beuckelmann DJ, Nabauer M and Erdmann E.** Intracellular calcium handling in isolated ventricular myocytes from patients with terminal heart failure. *Circulation* 85: 1046-1055, 1992.

19. **Bhalla V, Oyster NM, Fitch AC, Wijngaarden MA, Neumann D, Schlattner U, Pearce D and Hallows KR.** AMP-activated kinase inhibits the epithelial Na⁺ channel through functional regulation of the ubiquitin ligase Nedd4-2. *J Biol Chem* 281: 26159-26169, 2006.
20. **Birks EJ, Latif N, Enesa K, Folkvang T, Luong LA, Sarathchandra P, Khan M, Ovaas H, Terracciano CM, Barton PJR, Yacoub MH and Evans PC.** Elevated p53 expression is associated with dysregulation of the ubiquitin-proteasome system in dilated cardiomyopathy. *Cardiovasc Res* 79: 472-480, 2008.
21. **Birnbaum SG, Varga AW, Yuan LL, Anderson AE, Sweatt JD and Schrader LA.** Structure and function of Kv4-family transient potassium channels. *Physiol Rev* 84: 803-833, 2004.
22. **Bonifacino JS and Weissman AM.** Ubiquitin and the control of protein fate in the secretory and endocytic pathways. *Annu Rev Cell Dev Biol* 14: 19-57, 1998.
23. **Brahmajothi MV, Campbell DL, Rasmusson RL, Morales MJ, Trimmer JS, Nerbonne JM and Strauss HC.** Distinct transient outward potassium current (I_{to}) phenotypes and distribution of fast-inactivating potassium channel alpha subunits in ferret left ventricular myocytes. *J Gen Physiol* 113: 581-600, 1999.
24. **Brooksby P, Levi AJ and Jones JV.** The electrophysiological characteristics of hypertrophied ventricular myocytes from the spontaneously hypertensive rat. *J Hypertens* 11: 611-622, 1993.
25. **Brower GL, Henegar JR and Janicki JS.** Temporal evaluation of left ventricular remodeling and function in rats with chronic volume overload. *Am J Physiol Heart Circ Physiol* 271: H2071-H2078, 1996.
26. **Brower GL and Janicki JS.** Contribution of ventricular remodeling to pathogenesis of heart failure in rats. *Am J Physiol Heart Circ Physiol* 280: H674-H683, 2001.
27. **Bryant SM, Shipsey SJ and Hart G.** Regional differences in electrical and mechanical properties of myocytes from guinea-pig hearts with mild left ventricular hypertrophy. *Cardiovasc Res* 35: 315-323, 1997.
28. **Buja G, Miorelli M, Turrini P, Melacini P and Nava A.** Comparison of QT dispersion in hypertrophic cardiomyopathy between patients with and without ventricular arrhythmias and sudden death. *Am J Cardiol* 72: 973-976, 1993.

29. **Burlew BS and Weber KT.** Cardiac fibrosis as a cause of diastolic dysfunction. *Herz* 27: 92-98, 2002.
30. **Calderone A, Takahashi N, Izzo NJ, Jr., Thaik CM and Colucci WS.** Pressure- and volume-induced left ventricular hypertrophies are associated with distinct myocyte phenotypes and differential induction of peptide growth factor mRNAs. *Circulation* 92: 2385-2390, 1995.
31. **Cantor EJJ, Babick AP, Vasanji Z, Dhalla NS and Netticadan T.** A comparative serial echocardiographic analysis of cardiac structure and function in rats subjected to pressure or volume overload. *J Mol Cell Cardiol* 38: 777-786, 2005.
32. **Cerbai E, Barbieri M, Li Q and Mugelli A.** Ionic basis of action potential prolongation of hypertrophied cardiac myocytes isolated from hypertensive rats of different ages. *Cardiovasc Res* 28: 1180-1187, 1994.
33. **Chancey AL, Brower GL, Peterson JT and Janicki JS.** Effects of matrix metalloproteinase inhibition on ventricular remodeling due to volume overload. *Circulation* 105: 1983-1988, 2002.
34. **Chapman H, Ramstrom C, Korhonen L, Laine M, Wann KT, Lindholm D, Pasternack M and Tornquist K.** Downregulation of the HERG (KCNH2) K⁺ channel by ceramide: evidence for ubiquitin-mediated lysosomal degradation. *J Cell Sci* 118: 5325-5334, 2005.
35. **Chen Q, Liu JB, Horak KM, Zheng H, Kumarapeli ARK, Li J, Li F, Gerdes AM, Wawrousek EF and Wang X.** Intrasarcolemmal amyloidosis impairs proteolytic function of proteasomes in cardiomyocytes by compromising substrate uptake. *Circulation Res* 97: 1018-1026, 2005.
36. **Ciechanover A, Elias S, Heller H, Ferber S and Hershko A.** Characterization of the heat-stable polypeptide of the ATP-dependent proteolytic system from reticulocytes. *J Biol Chem* 255: 7525-7528, 1980.
37. **Ciechanover A.** Proteolysis: from the lysosome to ubiquitin and the proteasome. *Nat Rev Mol Cell Biol* 6: 79-87, 2005.
38. **Ciechanover A, Orian A and Schwartz AL.** Ubiquitin-mediated proteolysis: biological regulation via destruction. *BioEssays* 22: 442-451, 2000.

39. **Cohn JN, Levine TB, Olivari MT, Garberg V, Lura D, Francis GS, Simon AB and Rector T.** Plasma norepinephrine as a guide to prognosis in patients with chronic congestive heart failure. *N Engl J Med* 311: 819-823, 1984.
40. **Coulombe A, Momtaz A, Richer P, Swynghedauw B and Coraboeuf E.** Reduction of calcium-independent transient outward potassium current density in DOCA salt hypertrophied rat ventricular myocytes. *Pflugers Arch* 427: 47-55, 1994.
41. **Dada LA, Welch LC, Zhou G, Ben Saadon R, Ciechanover A and Sznajder JI.** Phosphorylation and ubiquitination are necessary for Na,K-ATPase endocytosis during hypoxia. *Cell Signal* 19: 1893-1898, 2007.
42. **Day CP, McComb JM and Campbell RW.** QT dispersion: an indication of arrhythmia risk in patients with long QT intervals. *Br Heart J* 63: 342-344, 1990.
43. **Dent MR, Dhalla NS and Tappia PS.** Phospholipase C gene expression, protein content, and activities in cardiac hypertrophy and heart failure due to volume overload. *Am J Physiol Heart Circ Physiol* 287: H719-H727, 2004.
44. **Depre C, Wang Q, Yan L, Hedhli N, Peter P, Chen L, Hong C, Hittinger L, Ghaleh B, Sadoshima J, Vatner DE, Vatner SF and Madura K.** Activation of the cardiac proteasome during pressure overload promotes ventricular hypertrophy. *Circulation* 114: 1821-1828, 2006.
45. **Di Diego JM and Antzelevitch C.** High $[Ca^{2+}]_o$ -induced electrical heterogeneity and extrasystolic activity in isolated canine ventricular epicardium. Phase 2 reentry. *Circulation* 89: 1839-1850, 1994.
46. **Ding YF, Brower GL, Zhong Q, Murray D, Holland M, Janicki JS and Zhong J.** Defective intracellular Ca^{2+} homeostasis contributes to myocyte dysfunction during ventricular remodelling induced by chronic volume overload in rats. *Clin Exp Pharmacol Physiol* 35: 827-835, 2008.
47. **Dixon JE and McKinnon D.** Quantitative analysis of potassium channel mRNA expression in atrial and ventricular muscle of rats. *Circ Res* 75: 252-260, 1994.
48. **Dixon JE, Shi W, Wang HS, McDonald C, Yu H, Wymore RS, Cohen IS and McKinnon D.** Role of the Kv4.3 K^+ channel in ventricular muscle: a molecular correlate for the transient outward current. *Circ Res* 79: 659-668, 1996.

49. **Doggrell SA and Brown L.** Rat models of hypertension, cardiac hypertrophy and failure. *Cardiovasc Res* 39: 89-105, 1998.
50. **Doval HC, Nul DR, Grancelli HO, Varini SD, Soifer S, Corrado G, Dubner S, Scapin O and Perrone SV.** Nonsustained ventricular tachycardia in severe heart failure: independent marker of increased mortality due to sudden death. *Circulation* 94: 3198-3203, 1996.
51. **Duceschi V, Sarubbi B, D'Andrea A, Liccardo B, Briglia N, Carozza A, Marmo J, Santangelo L, Iacono A and Cotrufo M.** Increased QT dispersion and other repolarization abnormalities as a possible cause of electrical instability in isolated aortic stenosis. *Int J Cardiol* 64: 57-62, 1998.
52. **Durakoglugil ME, Kaya MG, Boyaci B and Cengel A.** High output heart failure 8 months after an acquired arteriovenous fistula. *Jpn Heart J* 44: 805-809, 2003.
53. **Ehrlich JR.** Taking ion channel degradation to heart. *Cardiovasc Res* 74: 6-7, 2007.
54. **Fang J, Mensah GA, Croft JB and Keenan NL.** Heart failure-related hospitalization in the U.S., 1979 to 2004. *J Am Coll Cardiol* 52: 428-434, 2008.
55. **Fein FSM, Capasso JMP, Aronson RSM, Cho SMD, Nordin CMD, Green BM, Sonnenblick EHM and Factor SMM.** Combined renovascular hypertension and diabetes in rats: a new preparation of congestive cardiomyopathy. *Circulation* 70: 318-330, 1984.
56. **Fiset C, Clark RB, Shimoni Y and Giles WR.** *Shal*-type channels contribute to the Ca^{2+} -independent transient outward K^{+} current in rat ventricle. *J Physiol (Lond)* 500: 51-64, 1997.
57. **Furukawa T, Bassett AL, Furukawa N, Kimura S and Myerburg RJ.** The ionic mechanism of reperfusion-induced early afterdepolarizations in feline left ventricular hypertrophy. *Journal Clin Invest* 91: 1521-1531, 1993.
58. **Garcia R and Diebold S.** Simple, rapid, and effective method of producing aortocaval shunts in the rat. *Cardiovasc Res* 24: 430-432, 1990.
59. **Gealekman O, Abassi Z, Rubinstein I, Winaver J and Binah O.** Role of myocardial inducible nitric oxide synthase in contractile dysfunction and β -

adrenergic hyporesponsiveness in rats with experimental volume-overload heart failure. *Circulation* 105: 236-243, 2002.

60. **Gibbons RJ, Jones DW, Gardner TJ, Goldstein LB, Moller JH and Yancy CW.** The American Heart Association's 2008 Statement of Principles for Healthcare Reform. *Circulation* 118: 2209-2218, 2008.
61. **Gidh-Jain M, Huang B, Jain P and El-Sherif N.** Differential expression of voltage-gated K⁺ channel genes in left ventricular remodeled myocardium after experimental myocardial infarction. *Circ Res* 79: 669-675, 1996.
62. **Glancy JM and Garratt CJ.** QT dispersion and mortality after myocardial infarction. *Lancet* 345: 945, 1995.
63. **Glickman MH and Ciechanover A.** The ubiquitin-proteasome proteolytic pathway: destruction for the sake of construction. *Physiol Rev* 82: 373-428, 2002.
64. **Goldstein DS.** Plasma norepinephrine as an indicator of sympathetic neural activity in clinical cardiology. *Am J Cardiol* 48: 1147-1154, 1981.
65. **Goldstein G, Scheid M, Hammerling U, Schlesinger DH, Niall HD and Boyse EA.** Isolation of a polypeptide that has lymphocyte-differentiating properties and is probably represented universally in living cells. *Proc Natl Acad Sci U S A* 72: 11-15, 1975.
66. **Gong Q, Keeney DR, Molinari M and Zhou Z.** Degradation of Trafficking-defective Long QT Syndrome Type II Mutant Channels by the Ubiquitin-Proteasome Pathway. *J Biol Chem* 280: 19419-19425, 2005.
67. **Gradman A, Deedwania P, Cody R, Massie B, Packer M, Pitt B and Goldstein S.** Predictors of total mortality and sudden death in mild to moderate heart failure. Captopril-Digoxin Study Group. *J Am Coll Cardiol* 14: 564-570, 1989.
68. **Grossman W, Jones D and McLaurin LP.** Wall stress and patterns of hypertrophy in the human left ventricle. *J Clin Invest* 56: 56-64, 1975.
69. **Grossman WM.** Diastolic dysfunction and congestive heart failure. *Circulation* 81: III-1-III-7, 1990.

70. **Guo W, Li H, London B and Nerbonne JM.** Functional consequences of elimination of Ito, f and Ito, s: early afterdepolarizations, atrioventricular block, and ventricular arrhythmias in mice lacking Kv1.4 and expressing a dominant-negative Kv4 α subunit. *Circ Res* 87: 73-79, 2000.
71. **Gwathmey JK, Copelas L, MacKinnon R, Schoen FJ, Feldman MD, Grossman W and Morgan JP.** Abnormal intracellular calcium handling in myocardium from patients with end-stage heart failure. *Circ Res* 61: 70-76, 1987.
72. **Gwathmey JK, Slawsky MT, Haflar RJ, Bnggs GM and Morielli AD.** Role of intracellular calcium handling in force-interval relationships of human ventricular myocardium. *J Clin Invest* 85: 1599-1613, 1990.
73. **Hasenfuss G.** Animal models of human cardiovascular disease, heart failure and hypertrophy. *Cardiovasc Res* 39: 60-76, 1998.
74. **Hein S, Arnon E, Kostin S, Schonburg M, Elsasser A, Polyakova V, Bauer EP, Klovekorn WP and Schaper J.** Progression from compensated hypertrophy to failure in the pressure-overloaded human heart: structural deterioration and compensatory mechanisms. *Circulation* 107: 984-991, 2003.
75. **Hein S, Kostin S, Heling A, Maeno Y and Schaper J.** The role of the cytoskeleton in heart failure. *Cardiovasc Res* 45: 273-278, 2000.
76. **Heling A, Zimmermann R, Kostin S, Maeno Y, Hein S, Devaux B, Bauer E, Klovekorn WP, Schlepper M, Schaper W and Schaper J.** Increased expression of cytoskeletal, linkage, and extracellular proteins in failing human myocardium. *Circ Res* 86: 846-853, 2000.
77. **Hershko A and Ciechanover A.** The ubiquitin system. *Annu Rev Biochem* 67: 425-479, 1998.
78. **Hicke L.** Protein regulation by monoubiquitin. *Nat Rev Mol Cell Biol* 2: 195-201, 2001.
79. **Hicke L and Dunn R.** Regulation of membrane protein transport by ubiquitin and ubiquitin-binding proteins. *Annu Rev Cell Dev Biol* 19: 141-172, 2003.

80. **Hinkle LE, Jr. and Thaler HT.** Clinical classification of cardiac deaths. *Circulation* 65: 457-464, 1982.
81. **Hoppe UC, Marban E and Johns DC.** Molecular dissection of cardiac repolarization by *in vivo* Kv4.3 gene transfer. *J Clin Invest* 105: 1077-1084, 2000.
82. **Houser SR and Margulies KB.** Is depressed myocyte contractility centrally involved in heart failure? *Circ Res* 92: 350-358, 2003.
83. **Huang B, Qin D and El-Sherif N.** Spatial alterations of Kv channels expression and K⁺ currents in post-MI remodeled rat heart. *Cardiovasc Res* 52: 246-254, 2001.
84. **Huang M, Hester RL and Guyton AC.** Hemodynamic changes in rats after opening an arteriovenous fistula. *Am J Physiol Heart Circ Physiol* 262: H846-H851, 1992.
85. **Huang M, LeBlanc MH and Hester RL.** Evaluation of the needle technique for producing an arteriovenous fistula. *J Appl Physiol* 77: 2907-2911, 1994.
86. **Janse MJ.** Electrophysiological changes in heart failure and their relationship to arrhythmogenesis. *Cardiovasc Res* 61: 208-217, 2004.
87. **Jespersen T, Membrez M, Nicolas CS, Pitard B, Staub O, Olesen SP, Baro I and Abriel H.** The KCNQ1 potassium channel is down-regulated by ubiquitylating enzymes of the Nedd4/Nedd4-like family. *Cardiovasc Res* 74: 64-74, 2007.
88. **Jia Y and Takimoto K.** Mitogen-activated protein kinases control cardiac KChIP2 gene expression. *Circ Res* 98: 386-393, 2006.
89. **Johns DC, Nuss HB and Marban E.** Suppression of neuronal and cardiac transient outward currents by viral gene transfer of dominant-negative Kv4.2 constructs. *J Biol Chem* 272: 31598-31603, 1997.
90. **Josephson IR, Sanchez-Chapula J and Brown AM.** Early outward current in rat single ventricular cells. *Circ Res* 54: 157-162, 1984.
91. **Kaab S, Dixon J, Duc J, Ashen D, Nabauer M, Beuckelmann DJ, Steinbeck G, McKinnon D and Tomaselli GF.** Molecular basis of transient outward potassium

current downregulation in human heart failure: a decrease in Kv4.3 mRNA correlates with a reduction in current density. *Circulation* 98: 1383-1393, 1998.

92. **Kaab S and Nabauer M.** Diversity of ion channel expression in health and disease. *Eur Heart J Suppl* 3: K31-K40, 2001.
93. **Kaab S, Nuss HB, Chiamvimonvat N, O'Rourke B, Pak PH, Kass DA, Marban E and Tomaselli GF.** Ionic mechanism of action potential prolongation in ventricular myocytes from dogs with pacing-induced heart failure. *Circ Res* 78: 262-273, 1996.
94. **Kannel WB, Plehn JF and Cupples LA.** Cardiac failure and sudden death in the Framingham Study. *Am Heart J* 115: 869-875, 1988.
95. **Kassiri Z, Zobel C, Nguyen T-T, Molckentin JD and Backx PH.** Reduction of Ito causes hypertrophy in neonatal rat ventricular myocytes. *Circ Res* 90: 578-585, 2002.
96. **Kato M, Ogura K, Miake J, Sasaki N, Taniguchi Si, Igawa O, Yoshida A, Hoshikawa Y, Murata M, Nanba E, Kurata Y, Kawata Y, Ninomiya H, Morisaki T, Kitakaze M and Hisatome I.** Evidence for proteasomal degradation of Kv1.5 channel protein. *Biochem Biophys Res Commun* 337: 343-348, 2005.
97. **Keating MT and Sanguinetti MC.** Molecular and cellular mechanisms of cardiac arrhythmias. *Cell* 104: 569-580, 2001.
98. **Keung EC and Aronson RS.** Non-uniform electrophysiological properties and electrotonic interaction in hypertrophied rat myocardium. *Circ Res* 49: 150-158, 1981.
99. **Kjekshus J.** Arrhythmias and mortality in congestive heart failure. *Am J Cardiol* 65: 42I-48I, 1990.
100. **Kleiman RB and Houser SR.** Outward currents in normal and hypertrophied feline ventricular myocytes. *Am J Physiol Heart Circ Physiol* 256: H1450-H1461, 1989.
101. **Kobayashi S, Mao K, Zheng H, Wang X, Patterson C, O'Connell TD and Liang Q.** Diminished GATA4 protein levels contribute to hyperglycemia-induced cardiomyocyte injury. *J Biol Chem* 282: 21945-21952, 2007.

102. **Kong W, Po S, Yamagishi T, Ashen MD, Stetten G and Tomaselli GF.** Isolation and characterization of the human gene encoding Ito: further diversity by alternative mRNA splicing. *Am J Physiol Heart Circ Physiol* 275: H1963-H1970, 1998.
103. **Kostin S, Hein S, Arnon E, Scholz D and Schaper J.** The cytoskeleton and related proteins in the human failing heart. *Heart Failure Rev* 5: 271-280, 2000.
104. **Kostin S, Pool L, Elsasser A, Hein S, Drexler HCA, Arnon E, Hayakawa Y, Zimmermann R, Bauer E, Klovekorn WP and Schaper J.** Myocytes die by multiple mechanisms in failing human hearts. *Circ Res* 92: 715-724, 2003.
105. **Kuo HC, Cheng CF, Clark RB, Lin JJ, Lin JL, Hoshijima M, Nguyen-Tran VTB, Gu Y, Ikeda Y, Chu PH, Ross J, Giles WR and Chien KR.** A defect in the Kv channel-interacting protein 2 (KCHIP2) gene leads to a complete loss of Ito and confers susceptibility to ventricular tachycardia. *Cell* 107: 801-813, 2001.
106. **Li HG, Jones DL, Yee R and Klein GJ.** Electrophysiologic substrate associated with pacing-induced heart failure in dogs: potential value of programmed stimulation in predicting sudden death. *J Am Coll Cardiol* 19: 444-449, 1992.
107. **Li Q and Keung EC.** Effects of myocardial hypertrophy on transient outward current. *Am J Physiol Heart Circ Physiol* 266: H1738-H1745, 1994.
108. **Li X, Tang K, Xie B, Li S and Rozanski GJ.** Regulation of Kv4 channel expression in failing rat heart by the thioredoxin system. *Am J Physiol Heart Circ Physiol* 295: H416-H424, 2008.
109. **Liu J, Chen Q, Huang W, Horak KM, Zheng H, Mestril R and Wang X.** Impairment of the ubiquitin-proteasome system in desminopathy mouse hearts. *FASEB J* 20: 362-364, 2005.
110. **Liu Z, Hilbelink DR, Crockett WB and Gerdes AM.** Regional changes in hemodynamics and cardiac myocyte size in rats with aortocaval fistulas. 1. Developing and established hypertrophy. *Circ Res* 69: 52-58, 1991.
111. **Luu M, Stevenson WG, Stevenson LW, Baron K and Walden J.** Diverse mechanisms of unexpected cardiac arrest in advanced heart failure. *Circulation* 80: 1675-1680, 1989.

112. **Malik B, Price SR, Mitch WE, Yue Q and Eaton DC.** Regulation of epithelial sodium channels by the ubiquitin-proteasome proteolytic pathway. *Am J Physiol Renal Physiol* 290: F1285-F1294, 2006.
113. **Mann DL.** Mechanisms and models in heart failure: a combinatorial approach. *Circulation* 100: 999-1008, 1999.
114. **Marban E.** Cardiac channelopathies. *Nature* 415: 213-218, 2002.
115. **Marban E.** Heart failure: the electrophysiologic connection. *J Cardiovasc Electrophysiol* 10: 1425-1428, 1999.
116. **Marionneau CI, Brunet S, Flagg TP, Pilgram TK, Demolombe S and Nerbonne JM.** Distinct cellular and molecular mechanisms underlie functional remodeling of repolarizing K⁺ currents with left ventricular hypertrophy. *Circ Res* 102: 1406-1415, 2008.
117. **McIntosh MA, Cobbe SM, Kane KA and Rankin AC.** Action potential prolongation and potassium currents in left-ventricular myocytes isolated from hypertrophied rabbit hearts. *J Mol Cell Cardiol* 30: 43-53, 1998.
118. **McMullen JR and Jennings GL.** Differences between pathological and physiological cardiac hypertrophy: novel therapeutic strategies to treat heart failure. *Clin Exp Pharmacol Physiol* 34: 255-262, 2007.
119. **Mearini G, Schlossarek S, Willis MS and Carrier L.** Ubiquitin-proteasome system in cardiac dysfunction. *Biochim Biophys Acta* 1782: 749-763, 2008.
120. **Miorelli M, Buja G, Melacini P, Fasoli G and Nava A.** QT-interval variability in hypertrophic cardiomyopathy patients with cardiac arrest. *Int J Cardiol* 45: 121-127, 1994.
121. **Miranda M and Sorkin A.** Regulation of receptors and transporters by ubiquitination: new insights into surprisingly similar mechanisms. *Mol Interv* 7: 157-167, 2007.
122. **Miura M, Wakayama Y, Endoh H, Nakano M, Sugai Y, Hirose M, ter Keurs HEDJ and Shimokawa H.** Spatial non-uniformity of excitation-contraction

coupling can enhance arrhythmogenic-delayed afterdepolarizations in rat cardiac muscle. *Cardiovasc Res* 80: 55-61, 2008.

123. **Myerburg RJ, Interian A, Mitrani, Kessler MD and Castellanos MD.** Frequency of sudden cardiac death and profiles of risk. *Am J Cardiol* 80: 10F-19F, 1997.
124. **Nabauer M, Beuckelmann DJ and Erdmann E.** Characteristics of transient outward current in human ventricular myocytes from patients with terminal heart failure. *Circ Res* 73: 386-394, 1993.
125. **Nabauer M, Beuckelmann DJ, Uberfuhr P and Steinbeck G.** Regional differences in current density and rate-dependent properties of the transient outward current in subepicardial and subendocardial myocytes of human left ventricle. *Circulation* 93: 168-177, 1996.
126. **Nabauer M and Kaab S.** Potassium channel down-regulation in heart failure. *Cardiovasc Res* 37: 324-334, 1998.
127. **Nattel S, Maguy A, Le Bouter S and Yeh YH.** Arrhythmogenic ion-channel remodeling in the heart: heart failure, myocardial infarction, and atrial fibrillation. *Physiol Rev* 87: 425-456, 2007.
128. **Nerbonne JM.** Molecular basis of functional voltage-gated K⁺ channel diversity in the mammalian myocardium. *J Physiol (Lond)* 525: 285-298, 2000.
129. **Nerbonne JM and Kass RS.** Molecular physiology of cardiac repolarization. *Physiol Rev* 85: 1205-1253, 2005.
130. **Nordin C, Siri F and Aronson RS.** Electrophysiologic characteristics of single myocytes isolated from hypertrophied guinea-pig hearts. *J Mol Cell Cardiol* 21: 729-739, 1989.
131. **Nuss HB, Kaab S, Kass DA, Tomaselli GF and Marban E.** Cellular basis of ventricular arrhythmias and abnormal automaticity in heart failure. *Am J Physiol Heart Circ Physiol* 277: H80-H91, 1999.
132. **O'Rourke B, Kass DA, Tomaselli GF, Kaab S, Tunin R and Marban E.** Mechanisms of altered excitation-contraction coupling in canine tachycardia-induced heart failure, I: experimental studies. *Circ Res* 84: 562-570, 1999.

133. **Oudit GY, Kassiri Z, Sah R, Ramirez RJ, Zobel C and Backx PH.** The molecular physiology of the cardiac transient outward potassium current (I_{to}) in normal and diseased myocardium. *J Mol Cell Cardiol* 33: 851-872, 2001.
134. **Packer M.** Sudden unexpected death in patients with congestive heart failure: a second frontier. *Circulation* 72: 681-685, 1985.
135. **Packer MM.** Lack of relation between ventricular arrhythmias and sudden death in patients with chronic heart failure. *Circulation* 85: I-50-I-56, 1992.
136. **Pak PH, Nuss HB, Tunin RS, Kaab S, Tomaselli GF, Marban E and Kass DA.** Repolarization abnormalities, arrhythmia and sudden death in canine tachycardia-induced cardiomyopathy. *J Am Coll Cardiol* 30: 576-584, 1997.
137. **Palombella VJ, Rando OJ, Goldberg AL and Maniatis T.** The ubiquitinproteasome pathway is required for processing the NF- κ B1 precursor protein and the activation of NF- κ B. *Cell* 78: 773-785, 1994.
138. **Paul S.** Diastolic dysfunction. *Crit Care Nurs Clin North Am* 15: 495-500, 2003.
139. **Paul S.** Ventricular remodeling. *Crit Care Nurs Clin North Am* 15: 407-411, 2003.
140. **Perkiomaki JS, Huikuri HV, Koistinen JM, Makikallio T, Castellanos A and Myerburg RJ.** Heart rate variability and dispersion of QT interval in patients with vulnerability to ventricular tachycardia and ventricular fibrillation after previous myocardial infarction. *J Am Coll Cardiol* 30: 1331-1338, 1997.
141. **Perkiomaki JS, Koistinen MJ, Yli-mayry S and Huikuri HV.** Dispersion of QT interval in patients with and without susceptibility to ventricular tachyarrhythmias after previous myocardial infarction. *J Am Coll Cardiol* 26: 174-179, 1995.
142. **Pickart CM and Fushman D.** Polyubiquitin chains: polymeric protein signals. *Curr Opin Chem Biol* 8: 610-616, 2004.
143. **Po S, Roberds S, Snyders DJ, Tamkun MM and Bennett PB.** Heteromultimeric assembly of human potassium channels molecular basis of a transient outward current? *Circ Res* 72: 1326-1336, 1993.

144. **Pogwizd SM.** Focal mechanisms underlying ventricular tachycardia during prolonged ischemic cardiomyopathy. *Circulation* 90: 1441-1458, 1994.
145. **Pogwizd SM, Hoyt RH, Saffitz JE, Corr PB, Cox JL and Cain ME.** Reentrant and focal mechanisms underlying ventricular tachycardia in the human heart. *Circulation* 86: 1872-1887, 1992.
146. **Pogwizd SM.** Nonreentrant mechanisms underlying spontaneous ventricular arrhythmias in a model of nonischemic heart failure in rabbits. *Circulation* 92: 1034-1048, 1995.
147. **Pogwizd SM and Bers DM.** Cellular basis of triggered arrhythmias in heart failure. *Trends Cardiovasc Med* 14: 61-66, 2004.
148. **Pogwizd SM, Chung MK and Cain ME.** Termination of ventricular tachycardia in the human heart: insights from three-dimensional mapping of nonsustained and sustained ventricular tachycardias. *Circulation* 95: 2528-2540, 1997.
149. **Pogwizd SM, McKenzie JP and Cain ME.** Mechanisms underlying spontaneous and induced ventricular arrhythmias in patients with idiopathic dilated cardiomyopathy. *Circulation* 98: 2404-2414, 1998.
150. **Pogwizd SM, Schlotthauer K, Li L, Yuan W and Bers DM.** Arrhythmogenesis and contractile dysfunction in heart failure: roles of sodium-calcium exchange, inward rectifier potassium current, and residual b-adrenergic responsiveness. *Circ Res* 88: 1159-1167, 2001.
151. **Potreau D, Gomez JP and Fares N.** Depressed transient outward current in single hypertrophied cardiomyocytes isolated from the right ventricle of ferret heart. *Cardiovasc Res* 30: 440-448, 1995.
152. **Powell SR.** The ubiquitin-proteasome system in cardiac physiology and pathology. *Am J Physiol Heart Circ Physiol* 291: H1-19, 2006.
153. **Powell SR, Samuel SM, Wang P, Divald A, Thirunavukkarasu M, Koneru S, Wang X and Maulik N.** Upregulation of myocardial 11S-activated proteasome in experimental hyperglycemia. *J Mol Cell Cardiol* 44: 618-621, 2008.

154. **Priori SG, Napolitano C, Diehl L and Schwartz PJ.** Arrhythmias/innervation/pacing: dispersion of the QT interval: a marker of therapeutic efficacy in the idiopathic long QT syndrome. *Circulation* 89: 1681-1689, 1994.
155. **Qin D, Huang B, Deng L, El-Adawi H, Ganguly K, Sowers JR and El-Sherif N.** Downregulation of K⁺ channel genes expression in Type I diabetic cardiomyopathy. *Biochem Biophys Res Commun* 283: 549-553, 2001.
156. **Qin D, Zhang ZH, Caref EB, Boutjdir M, Jain P and El Sherif N.** Cellular and ionic basis of arrhythmias in postinfarction remodeled ventricular myocardium. *Circ Res* 79: 461-473, 1996.
157. **Radicke S, Cotella D, Graf EM, Banse U, Jost N, Varro A, Tseng GN, Ravens U and Wettwer E.** Functional modulation of the transient outward current I_{to} by KCNE β-subunits and regional distribution in human non-failing and failing hearts. *Cardiovasc Res* 71: 695-703, 2006.
158. **Reinstein E and Ciechanover A.** Narrative review: protein degradation and human diseases: the ubiquitin connection. *Ann Intern Med* 145: 676-684, 2006.
159. **Roberts WC.** Sudden cardiac death: definitions and causes. *Am J Cardiol* 57: 1410-1413, 1986.
160. **Rock KL, Gramm C, Rothstein L, Clark K, Stein R, Dick L, Hwang D and Goldberg AL.** Inhibitors of the proteasome block the degradation of most cell proteins and the generation of peptides presented on MHC class I molecules. *Cell* 78: 761-771, 1994.
161. **Rosamond W, Flegal K, Friday G, Furie K, Go A, Greenlund K, Haase N, Ho M, Howard V, Kissela B, Kittner S, Lloyd-Jones D, McDermott M, Meigs J, Moy C, Nichol G, O'Donnell CJ, Roger V, Rumsfeld J, Sorlie P, Steinberger J, Thom T, Wasserthiel-Smoller S, Hong Y and for the American Heart Association Statistics Committee and Stroke Statistics Subcommittee.** Heart disease and stroke statistics--2007 update: a report from the American heart association statistics committee and stroke statistics subcommittee. *Circulation* 115: e69-171, 2007.
162. **Rosamond W, Flegal K, Furie K, Go A, Greenlund K, Haase N, Hailpern SM, Ho M, Howard V, Kissela B, Kittner S, Lloyd-Jones D, McDermott M, Meigs**

- J, Moy C, Nichol G, O'Donnell C, Roger V, Sorlie P, Steinberger J, Thom T, Wilson M, Hong Y and for the American Heart Association Statistics Committee and Stroke Statistics Subcommittee.** Heart disease and stroke statistics--2008 update: a report from the American Heart Association statistics committee and stroke statistics subcommittee. *Circulation* 117: e25-146, 2008.
163. **Rose J, Aroundas AA, Tian Y, DiSilvestre D, Burysek M, Halperin V, O'Rourke B, Kass DA, Marban E and Tomaselli GF.** Molecular correlates of altered expression of potassium currents in failing rabbit myocardium. *Am J Physiol Heart Circ Physiol* 288: H2077-H2087, 2005.
164. **Rozanski GJ, Xu Z, Whitney RT, Murakami H and Zucker IH.** Electrophysiology of rabbit ventricular myocytes following sustained rapid ventricular pacing. *J Mol Cell Cardiol* 29: 721-732, 1997.
165. **Ryder KO, Bryant SM and Hart G.** Membrane current changes in left ventricular myocytes isolated from guinea pigs after abdominal aortic coarctation. *Cardiovasc Res* 27: 1278-1287, 1993.
166. **Scheuermann-Freestone M, Simon Freestone N, Langenickel T, Hohnel K, Dietz R and Willenbrock R.** A new model of congestive heart failure in the mouse due to chronic volume overload. *Eur J Heart Fail* 3: 535-543, 2001.
167. **Schultz JH, Janzen C, Volk T and Ehmke H.** Kv4.2 and KChIP2 transcription in individual cardiomyocytes from the rat left ventricular free wall. *J Mol Cell Cardiol* 39: 269-275, 2005.
168. **Shieh CC, Coghlan M, Sullivan JP and Gopalakrishnan M.** Potassium channels: molecular defects, diseases, and therapeutic opportunities. *Pharmacol Rev* 52: 557-594, 2000.
169. **Staub O, Gautschi I, Ishikawa T, Breitschopf K, Ciechanover A, Schild L and Rotin D.** Regulation of stability and function of the epithelial Na⁺ channel (ENaC) by ubiquitination. *EMBO J* 16: 6325-6336, 1997.
170. **Staub O and Rotin D.** Role of ubiquitylation in cellular membrane transport. *Physiol Rev* 86: 669-707, 2006.
171. **Steele DF, Eldstrom J and Fedida D.** Mechanisms of cardiac potassium channel trafficking. *J Physiol (Lond)* 582: 17-26, 2007.

172. **Stefano LMD, Matsubara LS and Matsubara BB.** Myocardial dysfunction with increased ventricular compliance in volume overload hypertrophy. *Eur J Heart Fail* 8: 784-789, 2006.
173. **Stevenson WG, Stevenson LW, Middlekauff HR and Saxon LA.** Sudden death prevention in patients with advanced ventricular dysfunction. *Circulation* 88: 2953-2961, 1993.
174. **Stewart JA, Wei CC, Brower GL, Rynders PE, Hanks GH, Dillon AR, Lucchesi PA, Janicki JS and Dell'Italia LJ.** Cardiac mast cell- and chymase-mediated matrix metalloproteinase activity and left ventricular remodeling in mitral regurgitation in the dog. *J Mol Cell Cardiol* 35: 311-319, 2003.
175. **Stewart S, MacIntyre K, Capewell S and McMurray JJV.** Heart failure and the aging population: an increasing burden in the 21st century? *Heart* 89: 49-53, 2003.
176. **Su X, Brower G, Janicki JS, Chen YF, Oparil S and Dell'Italia LJ.** Differential expression of natriuretic peptides and their receptors in volume overload cardiac hypertrophy in the rat. *J Mol Cell Cardiol* 31: 1927-1936, 1999.
177. **Takimoto K, Li D, Hershman KM, Li P, Jackson EK and Levitan ES.** Decreased expression of Kv4.2 and novel Kv4.3 K⁺ channel subunit mRNAs in ventricles of renovascular hypertensive rats. *Circ Res* 81: 533-539, 1997.
178. **Tamargo J, Caballero R, Gomez R, Valenzuela C and Delpon E.** Pharmacology of cardiac potassium channels. *Cardiovasc Res* 62: 9-33, 2004.
179. **Tanaka H, Miake J, Notsu T, Sonyama K, Sasaki N, Iitsuka K, Kato M, Taniguchi Si, Igawa O, Yoshida A, Shigemasa C, Hoshikawa Y, Kurata Y, Kuniyasu A, Nakayama H, Inagaki N, Nanba E, Shiota G, Morisaki T, Ninomiya H, Kitakaze M and Hisatome I.** Proteasomal degradation of Kir6.2 channel protein and its inhibition by a Na⁺ channel blocker aprindine. *Biochem Biophys Res Commun* 331: 1001-1006, 2005.
180. **Tomaselli GF, Beuckelmann DJ, Calkins HG, Berger RD, Kessler PD, Lawrence JH, Kass D, Feldman AM and Marban E.** Sudden cardiac death in heart failure: the role of abnormal repolarization. *Circulation* 90: 2534-2539, 1994.

181. **Tomaselli GF and Marban E.** Electrophysiological remodeling in hypertrophy and heart failure. *Cardiovasc Res* 42: 270-283, 1999.
182. **Tomaselli GF and Zipes DP.** What causes sudden death in heart failure? *Circ Res* 95: 754-763, 2004.
183. **Tomita F, Bassett AL, Myerburg RJ and Kimura S.** Diminished transient outward currents in rat hypertrophied ventricular myocytes. *Circ Res* 75: 296-303, 1994.
184. **Tsukamoto O, Minamino T, Okada Ki, Shintani Y, Takashima S, Kato H, Liao Y, Okazaki H, Asai M, Hirata A, Fujita M, Asano Y, Yamazaki S, Asanuma H, Hori M and Kitakaze M.** Depression of proteasome activities during the progression of cardiac dysfunction in pressure-overloaded heart of mice. *Biochem Biophys Res Commun* 340: 1125-1133, 2006.
185. **Undrovinas AI, Maltsev VA, Kyle JW, Silverman N and Sabbah HN.** Gating of the late Na⁺ channel in normal and failing human myocardium. *J Mol Cell Cardiol* 34: 1477-1489, 2002.
186. **Valdivia CR, Chu WW, Pu J, Foell JD, Haworth RA, Wolff MR, Kamp TJ and Makielski JC.** Increased late sodium current in myocytes from a canine heart failure model and from failing human heart. *J Mol Cell Cardiol* 38: 475-483, 2005.
187. **Vandesompele J, De Preter K, Pattyn F, Poppe B, Van Roy N, De Paepe A and Speleman F.** Accurate normalization of real-time quantitative RT-PCR data by geometric averaging of multiple internal control genes. *Genome Biol* 3: research0034.1-research0034.11, 2002.
188. **Veldkamp MW, Verkerk AO, van Ginneken ACG, Baartscheer A, Schumacher C, de Jonge N, de Bakker JMT and Opthof T.** Norepinephrine induces action potential prolongation and early afterdepolarizations in ventricular myocytes isolated from human end-stage failing hearts. *Eur Heart J* 22: 955-963, 2001.
189. **Vermeulen JT.** Mechanisms of arrhythmias in heart failure. *J Cardiovasc Electrophysiol* 9: 208-221, 1998.

190. **Vermeulen JT, Mcguire MA, Opthof T, Coronel R, De Bakker JMT, Klopping C and Janse MJ.** Triggered activity and automaticity in ventricular trabeculae of failing human and rabbit hearts. *Cardiovasc Res* 28: 1547-1554, 1994.
191. **Volders PGA, Sipido KR, Vos MA, Spatjens RLHM, Leunissen JDM, Carmeliet E and Wellens HJJ.** Downregulation of delayed rectifier K⁺ currents in dogs with chronic complete atrioventricular block and acquired Torsades de Pointes. *Circulation* 100: 2455-2461, 1999.
192. **Wang QD, Bohlooly M and Sjoquist PO.** Murine models for the study of congestive heart failure: implications for understanding molecular mechanisms and for drug discovery. *J Pharmacol Toxicol Methods* 50: 163-174, 2004.
193. **Wang X, Ren B, Liu S, Sentex E, Tappia PS and Dhalla NS.** Characterization of cardiac hypertrophy and heart failure due to volume overload in the rat. *J Appl Physiol* 94: 752-763, 2003.
194. **Wang Y, Cheng J, Chen G, Rob F, Naseem R, Nguyen L, Johnstone J and Hill J.** Remodeling of outward K⁺ currents in pressure-overload heart failure. *J Cardiovasc Electrophysiol* 18: 869-875, 2007.
195. **Wang Y, Cheng J, Joyner RW, Wagner MB and Hill JA.** Remodeling of early-phase repolarization: a mechanism of abnormal impulse conduction in heart failure. *Circulation* 113: 1849-1856, 2006.
196. **Wang Z, Nolan B, Kutschke W and Hill JA.** Na⁺-Ca²⁺ exchanger remodeling in pressure overload cardiac hypertrophy. *J Biol Chem* 276: 17706-17711, 2001.
197. **Weekes J, Morrison K, Mullen A, Wait R, Barton P and Dunn MJ.** Hyperubiquitination of proteins in dilated cardiomyopathy. *Proteomics* 3: 208-216, 2003.
198. **Wettwer E, Amos GJ, Posival H and Ravens U.** Transient outward current in human ventricular myocytes of subepicardial and subendocardial origin. *Circ Res* 75: 473-482, 1994.
199. **Wickenden AD, Lee P, Sah R, Huang Q, Fishman GI and Backx PH.** Targeted expression of a dominant-negative Kv4.2 K⁺ channel subunit in the mouse heart. *Circ Res* 85: 1067-1076, 1999.

200. **Wiemuth D, Ke Y, Rohlf s M and McDonald FJ.** Epithelial sodium channel (ENaC) is multi-ubiquitinated at the cell surface. *Biochem J* 405: 147-155, 2007.
201. **Wilber DJ, Garan H, Finkelstein D, Kelly E, Newell J, McGovern B and Ruskin JN.** Out-of-hospital cardiac arrest. Use of electrophysiologic testing in the prediction of long-term outcome. *N Engl J Med* 318: 19-24, 1988.
202. **Willis MS and Patterson C.** Into the heart: the emerging role of the ubiquitin-proteasome system. *J Mol Cell Cardiol* 41: 567-579, 2006.
203. **Xiao J, Luo X, Lin H, Zhang Y, Lu Y, Wang N, Zhang Y, Yang B and Wang Z.** MicroRNA miR-133 represses HERG K⁺ channel expression contributing to QT prolongation in diabetic hearts. *J Biol Chem* 282: 12363-12367, 2007.
204. **Xu H, Dixon JE, Barry DM, Trimmer JS, Merlie JP, McKinnon D and Nerbonne JM.** Developmental analysis reveals mismatches in the expression of K⁺ channel alpha subunits and voltage-gated K⁺ channel currents in rat ventricular myocytes. *J Gen Physiol* 108: 405-419, 1996.
205. **Xu H, Guo W and Nerbonne JM.** Four kinetically distinct depolarization-activated K⁺ currents in adult mouse ventricular myocytes. *J Gen Physiol* 113: 661-678, 1999.
206. **Yeola SW and Snyders DJ.** Electrophysiological and pharmacological correspondence between Kv4.2 current and rat cardiac transient outward current. *Cardiovasc Res* 33: 540-547, 1997.
207. **Zeng J and Rudy Y.** Early afterdepolarizations in cardiac myocytes: mechanism and rate dependence. *Biophys J* 68: 949-964, 1995.
208. **Zhang TT, Dai DZ and Cui B.** Downregulation of Kv4.2 and Kv4.3 channel gene expression in right ventricular hypertrophy induced by monocrotaline in rat. *Acta Pharmacol Sin* 25: 226-230, 2004.
209. **Zicha S, Xiao L, Stafford S, Cha TJ, Han W, Varro A and Nattel S.** Transmural expression of transient outward potassium current subunits in normal and failing canine and human hearts. *J Physiol (Lond)* 561: 735-748, 2004.

210. **Zipes DP and Wellens HJJ.** Sudden cardiac death. *Circulation* 98: 2334-2351, 1998.